INTEGRATED LOWPASS AMPLIFIERS

by

A. J. Brodersen

ELECTRONICS RESEARCH LABORATORY

College of Engineering
University of California, Berkeley
94720

ABSTRACT

Design techniques for integrated broadband lowpass amplifiers are presented in this report. Existing designs of discrete-component amplifiers are used as vehicles to determine practical integrated realizations of broadband lowpass amplifiers. Different amplifiers are compared on the basis of broadband effectiveness and temperature sensitivity using a new scalar measure.

This new scalar measure, a gain-frequency integral, is introduced to facilitate the comparison of different amplifier configurations. For the comparison of broadband effectiveness, the results using this new scalar measure agrees with the results obtained using existing scalar measures, such as the gain-bandwidth product. This gain-frequency integral is particularly useful as a measure of the temperature sensitivity of an amplifier.

Feedback amplifier stages are shown to be useful as integrated broadband lowpass amplifiers. The low-frequency gain of these amplifiers can be temperature insensitive since the gain may be designed to be approximately the ratio of diffused resistors with identical temperature coefficients. The sensitivity of the bandwidth was shown to be sufficiently small such that the usefulness of the amplifier is not impaired for many applications.

Temperature insensitive bias points of the transistors are shown to be necessary to achieve a temperature insensitive response of

a broadband lowpass amplifier. The choice of local or overall feedback stages, which are shown to have identical broadband performance, can be dictated by the requirements of invariant bias points. Experimental studies are made to verify these predictions.

This report also investigates the use of composite-transistor stages as integrated broadband lowpass amplifier stages. These stages, which are particularly suited for integrated circuits, are shown to provide the attractive possibility of obtaining a wideband temperature-insensitive response from relatively simple broadbanding techniques.

ACKNOWLEDGEMENTS

TABLE OF CONTENTS

1. BROADBAND LOWPASS INTEGRATED AMPLIFIERS

1.1 Introduction

Broadband, lowpass, discrete-component amplifiers have been extensively studied in the past.[1,2,3] The results of these studies show that feedback is useful in obtaining a broadband, lowpass response. If the critical feedback elements are precision components, the response of the amplifier can be desensitized with respect to environmental conditions, aging and manufacturing tolerances.

At present, there is considerable interest in monolithic, integrated realizations[+] of broadband, lowpass amplifiers. The design of the integrated amplifiers can be done using the design procedures which were developed for discrete-component amplifiers. However, a one-to-one correspondence between the integrated amplifier and its discrete-component counterpart does not adequately describe the behavior of the integrated amplifier.[4] The use of feedback does not necessarily ensure a desensitized response since precison feedback elements are not obtainable in a monolithic integrated circuit.[5] Therefore, an objective of this report is to determine the effectiveness of the existing design procedures in achieving a broadband, lowpass, desensitized, integrated amplifier.

[+]A monolithic, integrated circuit is one in which all circuit components are fabricated on or within a single semiconductor crystal. Silicon is the semiconductor crystal typically used.

There are many inherent advantages of monolithic integrated circuits: the ease of fabricating additional active devices is comparable to the ease of fabricating passive components; the active devices have closely matched electrical characteristics over a wide temperature range; the geometries of the active devices can be chosen to optimize circuit performance; the components of the amplifier are thermally coupled.[6] These characteristics or properties can often be considered to be new degrees of freedom which provide the possibility of new design procedures which are unique to monolithic, integrated amplifiers. Consequently, the second objective of this report is to determine if improved broadband performance can accrue from the unique properties of monolithic, integrated circuits.

1.2 Monolithic integrated circuit components

The components commonly used in the realization of monolithic, integrated amplifiers are bipolar junction transistors, (BJT),[+] resistors, and capacitors. Typical cross-sectional views of these components are shown in Fig. 1.1(a), Fig. 1.2(a), and Fig. 1.3(a) respectively. Each of these components is fabricated on n-type epitaxial silicon grown on a p-type silicon substrate. Areas of n-type epitaxial silicon are electrically isolated by a p-type diffusion through the epitaxial layer. Two additional

---

[+]Field-effect transistors (FET) are not considered in this report. BJT's have gain at higher frequencies than FET's; thus, wideband amplifiers are easily realized using BJT's.

diffusions are required to fabricate a npn transistor. Either of these diffusions can be used to realize a resistor as shown in Fig. 1.2(a).[7] Capacitors can be realized either as a metal-oxide-semiconductor (MOS) capacitor or as a junction capacitor as shown in the two views of Fig. 1.3(a).[8]

The electrical behavior of an integrated BJT differs slightly from its discrete-component counterpart. The collector contact is made on the top of the transistor instead of the bottom as in discrete-transistors. This top contact increases the collector saturation resistance of the integrated BJT.[9] An additional capacitance is introduced by the isolation junction. If the substrate is grounded, an integrated transistor can be represented by a discrete transistor and a capacitor C_s, representing the capacitance of the isolation junction, as shown in Fig. 1.1(b). The capacitor C_s can limit the high-frequency response of the transistor.[10]

The integrated resistors, shown in Fig. 1.2(a), have circuit models as shown in Fig. 1.2(b) for a base-diffused resistor and Fig. 1.2(c) for an emitter-diffused resistor. The capacitor C_s models the capacitance of the isolation junction. An additional distributed capacitance is included in the models of Fig. 1.2(b) and 1.2(c). This distributed capacitance is contributed by the normally reversed biased junction which is formed by the resistor and the adjacent region. The distributed capacitance and the isolation junction capacitance can cause the performance of the integrated resistor to deviate markedly from the performance of a discrete

resistor. In addition, diffused resistors have a practical limit in value
of 10 kΩ and a large temperature coefficient.[11]

The circuit model of an integrated capacitor is shown in Fig. 1.3(b).
This model is applicable for either the MOS or junction capacitance. The
resistor R_s represents the finite contact resistance, while the resistor
R_p represents the dielectric leakage of the MOS capacitor or the leakage
current of a junction capacitor. The isolation junction is represented by
the capacitor C_s. The maximum practical value of capacitance is 400
pF.[11]

The limited values of integrated resistors and capacitors introduce
difficulties in the design of the biasing and coupling circuitry of inte-
grated amplifiers. Conventional methods of biasing and coupling discrete-
component amplifiers generally require the use of large values of capaci-
tance to reduce the effect of the biasing and coupling circuitry for low
frequencies; for integrated circuits, the required values of these capaci-
tances are too large to be reliably fabricated. As will be seen, additional
transistors, easily obtained in an integrated circuit, can be used to bias
and couple transistor amplifier stages.[4,6]

1.3 The design of integrated amplifiers

In the design of broadband, lowpass, integrated amplifiers, the
relative performance of the various amplifier configurations must be
compared to determine the best amplifier for a particular application.
Three measures of the performance are used in this report: (1) the

broadband effectiveness which measures the success that an amplifier achieves in producing a wideband response; (2) the temperature sensitivity which is the temperature variation of the response of the amplifier; (3) the response shape. To facilitate the comparison of different amplifier configurations, the design response shape is to be restricted so that the magnitude of the response is a monotonically decreasing function of the frequency. In particular, the limiting case of such a response, the maximally flat magnitude (MFM) response,[12] is specified as a standard and reasonable design goal for the amplifiers considered in this report.

To evaluate the broadband effectiveness and temperature sensitivity, is is convenient to use a scalar measure. The gain-bandwidth (GBW) product is typically used as a scalar measure of the broadband effectiveness.[13] As will be seen, there is no equivalent scalar measure of the temperature sensitivity. Chapter 2 develops a scalar measure suitable for the evaluation of the temperature sensitivity. This same scalar measure also will be shown to be useful in the evaluation of the broadband effectiveness.

To establish the usefulness of the scalar measure of broadband performance, which is developed in Chapter 2, single-transistor amplifier stages are evaluated for their use as broadband, lowpass, integrated amplifiers in Chapter 3. Two particular stages, the series-feedback stage and the shunt-feedback stage are found to be particularly useful as

broadband amplifier stages. These stages are compared in detail for both broadband effectiveness and temperature sensitivity. Experimental studies of these stages are made and a monolithic, integrated realization of the series-feedback stage is given.

The important class of two-transistor amplifier stages is studied in Chapter 4. Two particular, common-emitter pairs, the shunt-series cascade and the shunt-series feedback pair are used to evaluate the relative performance of local or overall feedback stages. Monolithic, integrated realizations confirm the results of the evaluation of these stages. Other pair configurations, e. g., a common-emitter transistor driving a common-base transistor, are compared to a single common-emitter transistor to determine if any advantages in broadband performance accrue from the use of an additional transistor, which is easily obtained in integrated circuits.

The results of these studies of one and two-transistor stages are summarized in Chapter 5. Several examples of industrial integrated amplifiers are presented to show the applicability of the design techniques which result from the previous studies. An additional design example indicates the method of applying these techniques.

EMITTER   SiO$_2$

BASE   COLLECTOR

n$^+$

P

n-TYPE EPITAXIAL

p-TYPE SUBSTRATE

ISOLATION JUNCTION

(a)

C_s

(b)
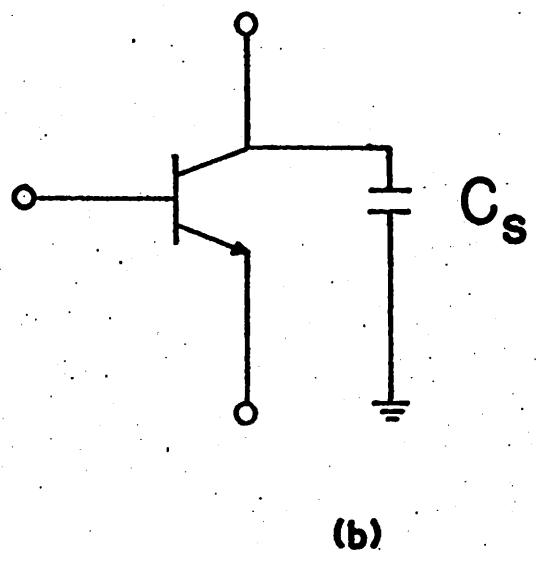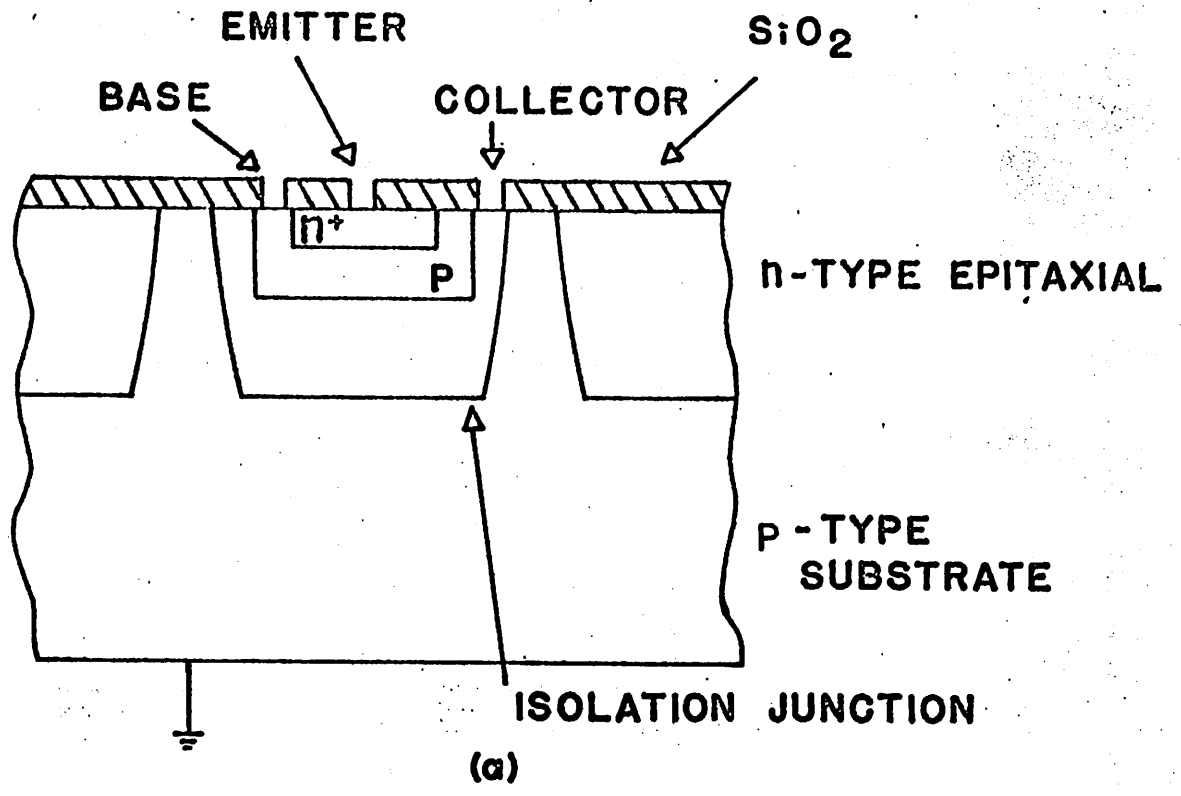
Figure 1.1 (a) Integrated circuit transistor; (b) its discrete-component model.
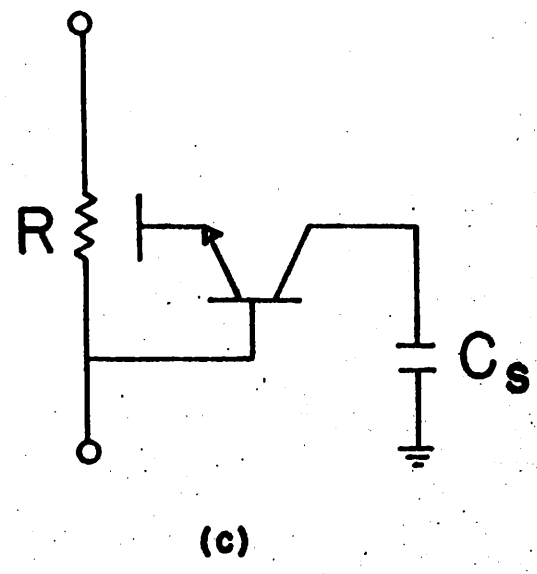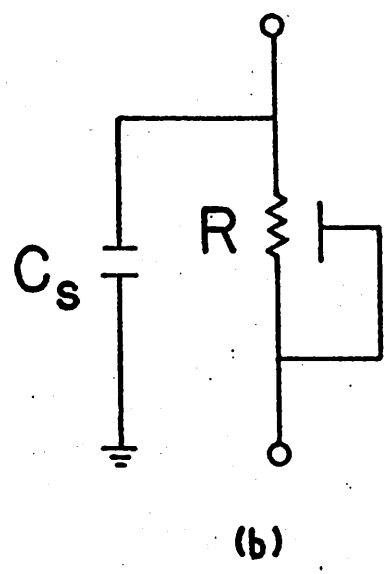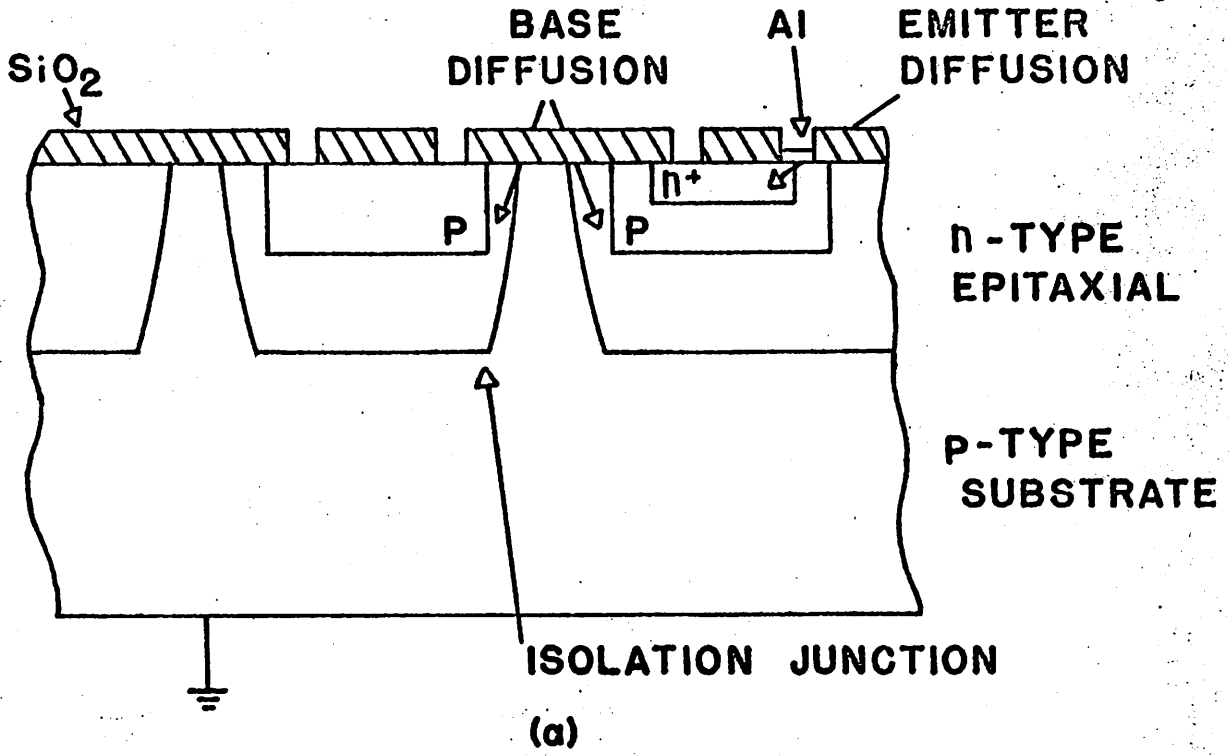
Figure 1.2 (a) Integrated circuit resistors; (b) and (c) their discrete-component model.
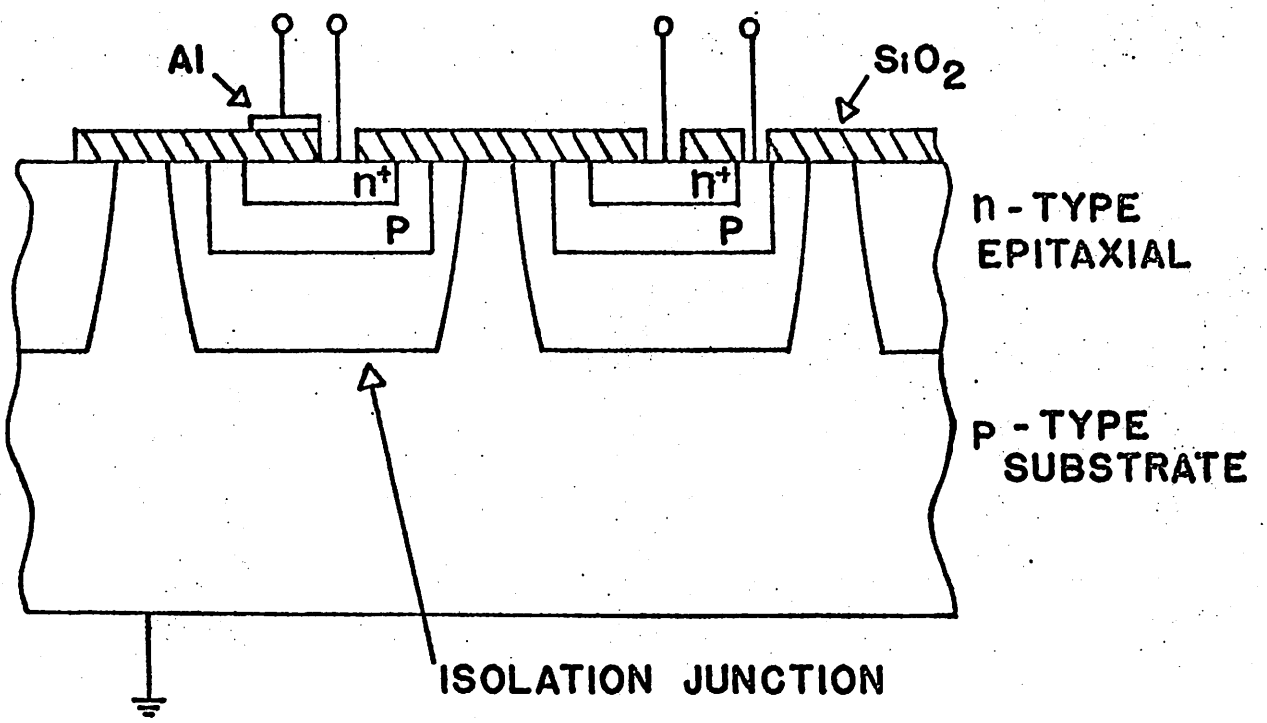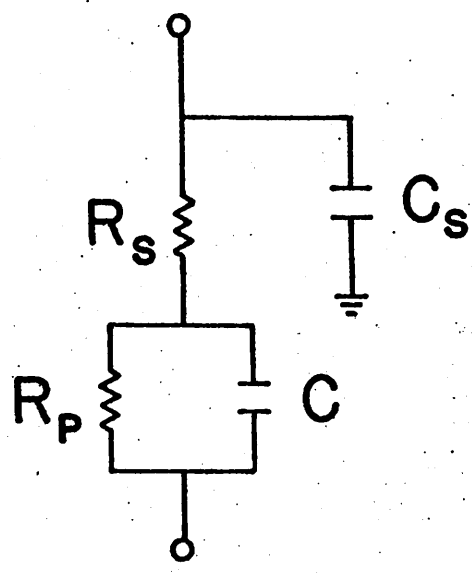
Figure 1.3 (a) Integrated circuit capacitors; (b) their discrete-component model.

2. THE GAIN-SQUARED FREQUENCY INTEGRAL

2.1 Introduction

The gain-magnitude, frequency response of a typical lowpass, broadband amplifier is shown in Fig. 2.1. A general transfer function of the amplifier is to be denoted by $T(j\omega)$. As mentioned previously, the performance of an amplifier may be evaluated by determining the broadband effectiveness, the temperature sensitivity and the response shape. If additional gain-magnitude, frequency curves which represent the response of the amplifier at different ambient temperatures are given, plots, such as the one of Fig. 2.1, certainly convey the necessary information to evaluate the performance of a broadband, lowpass amplifier. However, it is convenient to have a gross scalar measure of the broadband effectiveness and temperature sensitivity since different amplifiers can then be easily compared. The response shape of the amplifier is not critical in the preliminary stages of the investigation, since shape may be adjusted by appropriately choosing the values of the passive components.

Integral measures have been used to give a scalar measure suitable for the evaluation of the broadband effectiveness of lowpass amplifiers.[1] Integral measures provide an averaged assessment of the broadband behavior. The gain frequency integral is one such integral and is given by

$$I = \int_0^{\omega_0} |T(j\omega)| \, d\omega \qquad\qquad (2.1)$$

The computation of this integral is difficult even for simple transfer functions; the gain frequency integral is typically approximated by the GBW product which is the product of the low-frequency gain $T(0)$ and the -3 dB bandedge ω_0. If the scalar measure (2.1) is to be used to evaluate the temperature sensitivity, the altered transfer function $T_A(j\omega)$ can be used in (2.1) and the resulting scalar measure can be compared to the original value of (2.1).

Another possible scalar measure, which is more mathematically tractable, is given by the gain-squared frequency integral

$$J = \int_0^{\omega_0} |T(j\omega)|^2 \, d\omega \qquad\qquad (2.2)$$

It is not difficult to see the changes in the scalar measure due to the squaring of the integrand of (2.1). Eqn. (2.2) can be also written as

$$J = \frac{1}{2} \int_{-\omega_0}^{\omega_0} |T(j\omega)|^2 \, d\omega \qquad\qquad (2.3)$$

since the integrand is an even function of the frequency ω. As will be seen, the infinite integral

$$J = \frac{1}{2}\int_{-\infty}^{\infty} |T(j\omega)|^2 \, d\omega \qquad (2.4)$$

is easily evaluated by the Cauchy integral formula. Both (2.3) and (2.4) measure the broadband effectiveness of the amplifier. The computational ease of evaluating (2.4) justifies its use as a scalar measure of the broadband effectiveness.

As is to be brought out shortly, the change of the scalar measure J, due to changes in the transfer function of the amplifier, is also easily evaluated by the Cauchy integral formula. Hence, (2.4) can be used to evaluate both the broadband performance and temperature sensitivity of an amplifier.

2.2 The gain-squared frequency integral[†]

The linear, time invariant, two-port amplifier including the source and load resistances of Fig. 2.2 is characterized by the rational, voltage-transfer function

$$T(j\omega) = \frac{V_L(j\omega)}{V_s(j\omega)} \qquad (2.5)$$

where ω is the frequency in rad/s. The two-port network could as well be characterized by a current transfer function, a transadmittance

---

[†]This section deals only with the infinite integral. For an evaluation of the finite integral, see App. A.

function, or a transimpedance function. The voltage-transfer function is used in this section as a representative transfer function. The gain-squared frequency integral J is given by (2.4) as

$$J = \frac{1}{2} \int_{-\infty}^{\infty} |T(j\omega)|^2 \, d\omega \qquad (2.6)$$

Upon normalization by the frequency independent constant $\frac{1}{4R_s R_L}$, J becomes the available power gain-bandwidth integral, which is of fundamental importance in many network applications.[14,15] For real networks,

$$\overline{T}(j\omega) = T(-j\omega) \qquad (2.7)$$

Then, (2.5) may be rewritten as

$$J = \frac{1}{2} \int_{-\infty}^{\infty} T(-j\omega) \, T(j\omega) \, d\omega \qquad (2.8)$$

For practical amplifiers (and for the discrete-component prototypes of integrated, broadband, amplifiers in particular)[16]

$$\lim_{\omega \to \infty} [T(j\omega)] = 0 \qquad (2.9)$$

Consequently (2.8) is also given by

$$J = \frac{1}{2j} \oint_C T(-p) \, T(p) \, dp \qquad (2.10)$$

where the meromorphic function $T(p)$ is the analytical continuation of the transfer function $T(j\omega)$ into the entire complex frequency plane (p-plane) and the contour of integration C (for infinitely large R) is shown in Fig. 2. 3. In any practical application the network must be stable (bounded-input, bounded-output), thus necessitating that the poles of the transfer function $T(p)$ all occur in the open left half, complex frequency plane. Hence, (2. 10) and therefore (2. 6), can be evaluated by means of the Cauchy integral formula, the result being

$$J = -\pi \sum_{k=1}^{m} T(p_k) \, \text{Res} \, [T(-p), \, p_k] \qquad (2.11)$$

where $\text{Res} \, [T(-p), \, p_k]$ is the residue of $T(-p)$ at the kth pole p_k of the m poles of $T(-p)$ which occur in the open right half complex frequency p-plane.

In the present study, the gain-squared frequency integral is not nearly so important as are changes in it which are brought about by changes in the network. In general, any change in the two-port amplifier of Fig. 2. 2 yields a new two-port imbedding network which corresponds to a new transfer function $T_A(j\omega)$; the change[+] can be characterized by

$$T_\Delta(j\omega) = T_A(j\omega) - T(j\omega) \qquad (2.12)$$

[+]Other definitions, such as the mean-squared change of $T(j\omega)$ could be used. This particular definition, as will be seen, leads to an easily evaluated J_Δ.

The corresponding change in the gain-squared frequency integral is

$$J_\Delta = J_A - J = \frac{1}{2} \int_{-\infty}^{\infty} [\,|T_A(j\omega)|^2 - |T(j\omega)|^2\,]\, d\omega \qquad (2.13)$$

Under the assumption that both the original and the altered networks are real, this expression for the deviation in the gain-squared frequency integral may be written as

$$J_\Delta = \frac{1}{2} \int_{-\infty}^{\infty} [\,T(-j\omega)\, T_\Delta(j\omega) + T_A(j\omega)\, T_\Delta(-j\omega)\,]\, d\omega \qquad (2.14)$$

or, equivalently

$$J_\Delta = \frac{1}{2} \int_{-\infty}^{\infty} [\,T(-j\omega)\, T_\Delta(j\omega) + T_A(-j\omega)\, T_\Delta(j\omega)\,]\, d\omega \qquad (2.15)$$

since the transformation of ω to $-\omega$ of the variable of integration in the second term does not alter the value of the integral. Finally, it is convenient to separate the first-order effects and the second-order effects

$$J_\Delta = \frac{1}{2} \int_{-\infty}^{\infty} [\,2T(-j\omega)\, T_\Delta(j\omega) + T_\Delta(-j\omega)\, T_\Delta(j\omega)\,]\, d\omega \qquad (2.16)$$

The result of arguments identical to those used for the computation of (2.6) is that the deviation in the gain-squared frequency integral may be written more conveniently as the contour integral.

$$J_\Delta = +\frac{1}{2j} \oint_C [2T(-p) \, T_\Delta (p) + T_\Delta (-p) \, T_\Delta (p)] \, dp \qquad (2.17)$$

where the contour C is again that given in Fig. 2.4. Now (2.17), and therefore (2.13), can be calculated by the Cauchy integral formula; the result being

$$J_\Delta = 2\pi \sum_{k=1}^m T_\Delta (p_k) \, \mathrm{Res} \, [T(-p), \, p_k] + \frac{1}{2} \int_{-\infty}^\infty |T_\Delta (j\omega)|^2 \, d\omega \qquad (2.18)$$

In a first-order theory the positive second term on the right hand side of (2.18) may be neglected under the assumption that

$$\left| \frac{T_\Delta (j\omega)}{T(j\omega)} \right| << 1 \qquad (2.19)$$

The first order term is then given by

$$J_\delta = -2\pi \sum_{k=1}^m T_\Delta (p_k) \, \mathrm{Res} \, [T(-p), \, p_k] \qquad (2.20)$$

An alternate expression which is valid for large deviations is

$$J_\Delta = -\pi \sum_{k=1}^m T_\Delta (p_k) \, \mathrm{Res} \, [T(-p), \, p_k] - \pi \sum_{k=1}^n T_\Delta (q_k) \, \mathrm{Res} \, [T_A(-q_k), \, q_k]$$

$$(2.21)$$

where the q_k, $k = 1, 2, \ldots$, n are the n poles of the altered transfer function $T_A(-p)$. Only the first term on the right hand side of (2.21) -- which

is one-half of the first term on the right hand side of (2.18)--need be

retained in a first-order theory when

$$\left| \frac{T_A(j\omega)}{T(j\omega)} \right| << 1 \qquad (2.22)$$

almost everywhere. This is frequently true in practical broadband

amplifiers. In what follows, (2.20) and (2.21) are used to evaluate the

sensitivity of a broadband, lowpass, integrated circuit with regard to

various changes.

2.3 The use of the gain-squared frequency integral in the evaluation of integrated circuits

The class of circuits which are suitable for integrated, broadband,

lowpass amplifiers is symbolically shown in Fig. 2.4(a). (The sources

and the bias and coupling circuitry are omitted for simplicity.) This

diagram represents an amplifier consisting of m transistors imbedded

in a 3(m+1) terminal RC network which is connected between a specified

source and load resistance. The variation of the gain-squared frequency

integral (2.21) can be used to evaluate the effectiveness of a specified

RC network in achieving broadband performance. In particular, different

RC imbedding networks can be compared to some reference amplifier,

such as the very basic one of Fig. 2.4(b), or one which has been chosen

by experience or by intuition. The procedure is as follows:

1. A reference amplifier, such as the amplifier of Fig. 2.4(b),

is chosen. The transfer function of this amplifier defines the reference transfer function $T(p)$.

2. The reference amplifier is imbedded in the desired RC network to give the amplifier of Fig. 2.4(b). The transfer function of this amplifier defines the altered transfer function $T_A(p)$.

3. Eqn. (2.12) can now be used to calculate $T_\Delta(p)$.

4. Residue formula (2.21) is then used to calculate the change of the gain-squared frequency integral J_Δ.

This procedure can be repeated for different RC imbedding networks; and in this manner, comparisons of the broadband capabilities of different imbedding networks can be made.

The temperature sensitivity of an amplifier can be calculated using the above procedure for effecting a broadband capability comparison. For computing the temperature sensitivity, the reference amplifier is the amplifier of Fig. 2.4(a) at the reference temperature. The altered amplifier is then the amplifier of Fig. 2.4(a) at some new temperature. The deviation of the gain-squared frequency integral can be calculated using residue formula (2.20) since the expected changes are usually small.

2.4 Conclusions

This chapter has developed a scalar measure, the gain-squared

frequency integral, which is potentially useful in the evaluation of broad-band, lowpass amplifiers. In the next chapter, the implementation of the gain-squared frequency integral is demonstrated by evaluating the performance of single-transistor amplifier stages.
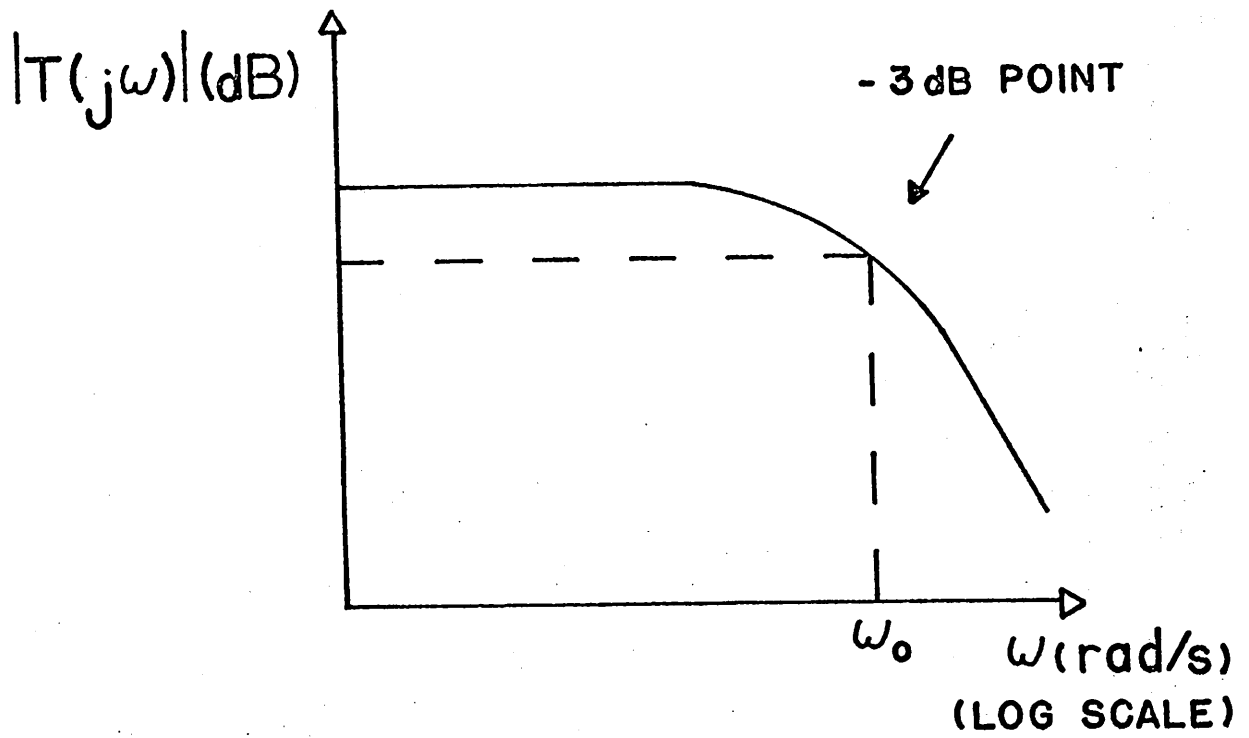
Figure 2. 1 The gain-magnitude, frequency response of a typical broadband, lowpass amplifier.
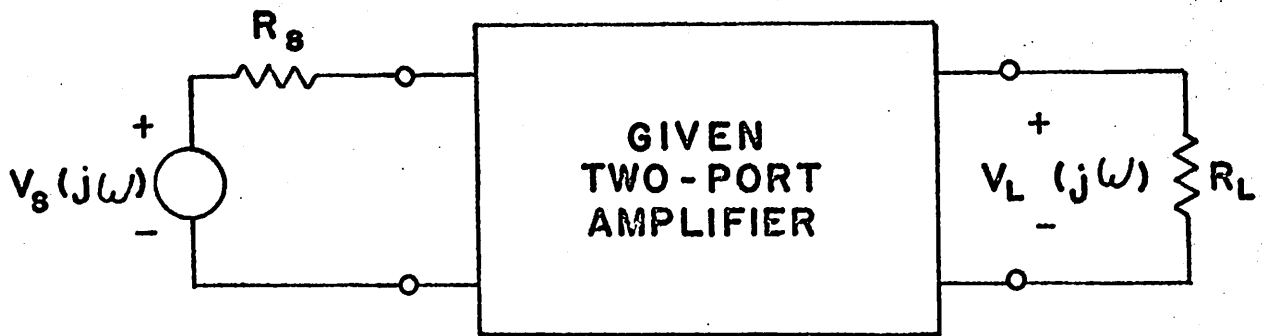
Figure 2.2 The two-port network with resistive source and load defines the transfer function $T(j\omega)$.
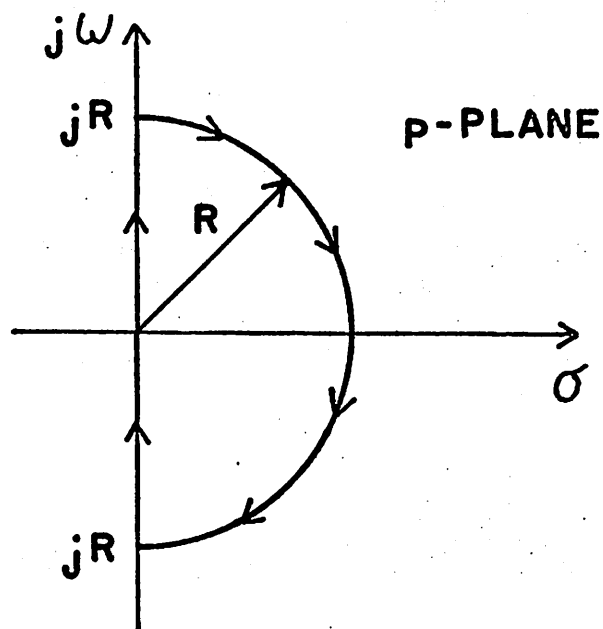
Figure 2.3 The contour of integration used to calculate the gain-squared frequency integral and its variations.
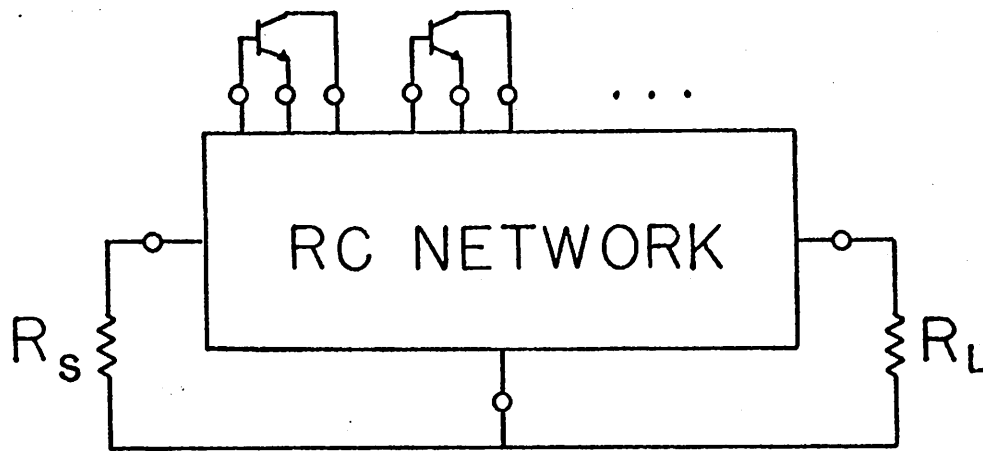
(a)
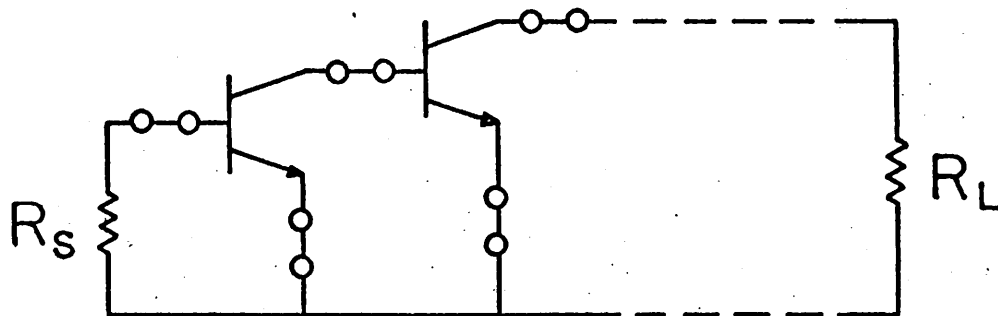
(b)

Figure 2.4 (a) Transistors imbedded in an arbitrary RC network; (b) the
reference amplifier.

3. SINGLE TRANSISTOR AMPLIFIER STAGES

3.1 Introduction

To illustrate the use of the gain-squared frequency integral, the imbedding of a single common-emitter transistor between specified source and load resistances is first examined. The common-emitter connection of a transistor is used since this connection of a transistor is the only one capable of both current and voltage gain. The evaluation procedure of Sec. 2.3 is to be used; hence, according to Fig. 2.4(b), a suitable reference amplifier would be a common-emitter transistor connected between a specified source and load resistance as shown in Fig. 3.1(a).[+] It is desired to determine which transformerless RC networks of Fig. 2.4(a) are capable of improving the broadband performance. To specify a six-terminal RC network, which is the required complexity of the imbedding network of the single-transistor stage, is difficult. The use of RC one-port networks as the sole elements of the imbedding network, as shown in Fig. 3.1(b), leads to an important class of practical, single-transistor stages. As will be seen, the resulting amplifiers are easily designed directly by cut and try methods.

[+]The biasing and coupling circuitry are omitted in Fig. 3.1 for simplicity. They are considered later in the evaluation of single-transistor stages.

Two single-transistor amplifier stages, the series-feedback stage and the shunt-feedback stage, will be shown to be particularly useful as broadband, lowpass, amplifier stages. Specific design examples of these stages are compared for broadband effectiveness and temperature sensitivity. Experimental realizations of the shunt-feedback stage and series-feedback stage are presented.

First, this chapter investigates the practical aspects of biasing and coupling monlithic, integrated, amplifier stages.

3.2 Biasing and coupling of transistor stages

The limited range of possible values of passive components available in monolithic integrated amplifier prevents the application of many of the circuit techniques which are available for the biasing and coupling of successive discrete-component amplifier stages. The limitation of capacitance values to less than 400 pF prohibits the use of capacitors for ac coupling of broadband, lowpass amplifiers if low-frequency response is needed. Solutions to the biasing and coupling of transistor stages need to utilize the unique properties of monolithic integrated circuits: (1) the close matching of active devices and passive components; (2) the economical cost of active devices; (3) the freedom to design active devices for specific applications.[6] Examples of these techniques are presented below.

A cascade of single-transistor stages can be biased by using voltage-reference diodes, as shown in Fig. 3.2. The voltage-reference diode provides the necessary voltage drop between the collector of the transistor

and the base of the succeeding transistor to ensure that each transistor will be biased in a linear region of operation.

The voltage reference diode, whose I, V characteristic is shown in Fig. 3.3, provides an electrical function similar to that of a battery, i. e. a dc voltage source. The voltage-reference diode provides a fixed voltage drop and a small dynamic resistance above some threshold value of voltage V_Z. These diodes can be easily fabricated in a monolithic integrated circuit with reference voltages from approximately 6 V to 100 V. The noise associated with the voltage-reference diode is inversely proportional to the dc bias current and directly proportional to the reference voltage V_Z. Typically, the noise was experimentally found to have a rms value of less than 5 mV for a reference voltage of 6-7 V and a bias current of 0.5 -1 mA. The base-emitter junction diode of a planar double-diffused bipolar transistor has a breakdown or reference voltage typically in the range of 6 V - 12 V; therefore, the base-emitter junction diode can be used as a voltage-reference diode which is easily fabricated in the monolithic circuit.

The cascaded amplifier of series-feedback stages of Fig. 3.2 has been extensively studied.[4,17] The voltage-reference diode and the forward biased, base-emitter diode have approximately equal temperature coefficients of opposite sign; hence, the voltage at the collector of each stage remains approximately constant with temperature. If the positive temperature coefficients of the resistors are also considered, the bias point can be shown to be invariant with temperature (see App. B) for some

bias point. Experimental realizations of this stage are discussed in Sec. 3. 5.

Another technique which is especially useful for achieving an invariant bias point of a single transistor stage is shown in Fig. 3. 4.[6] This bias scheme depends on the close matching of active devices and passive components. If $R_2 = \frac{1}{2}R_1$, the common-emitter amplifier stage T_2 is biased at one-half the supply voltage and the collector current, determined by T_1, is V_{CC}/R_1. The close matching of components ensures that the collector of T_2 remains at one-half the supply voltage with changing temperature.

The design of monolithic integrated circuits includes not only the circuit considerations, but also the active device design. An interesting example of device design to achieve suitable biasing of the active devices is shown in Fig. 3. 5.[18] The transistor T_1 is connected to the base of transistor T_2 whose emitter is grounded; consequently, the collector emitter voltage V_{CE} of T_1 is a very small positive value. To provide linear amplification at this low voltage, transistor T_1 has a larger emitter area (approximately four times larger) than the other transistors. Thus, the gain of transistor T_1 is linear at this low value of V_{CE}. A common-collector output stage and overall shunt-shunt feedback is used in the integrated circuit to obtain an invariant dc bias point of the output transistor. An external capacitor C_B is usually added, as shown in Fig. 3. 5, to decouple the shunt-shunt feedback loop for ac signals. As will be

seen in the course of this report, overall dc feedback is often required for bias point invariance.

The procedures presented in this section will be used in this report for the biasing and coupling of integrated amplifier stages. No one method is suitable for all integrated stages. Rather, the biasing and coupling circuitry of each integrated amplifier must be designed individually. This section has given some basic procedures which have found wide use in the design of integrated circuits.

3.3 Single-transistor amplifier stages

As mentioned previously in Sec. 3.1, the use of RC one-port networks as the sole elements of the imbedding network, as shown in Fig. 3.1(b), is an important class of practical, single-transistor stages. This section uses the evaluation procedure of Sec. 2.3 to determine if any combination of one or more RC one-port networks can improve the broadband performance of the common-emitter transistor stage, i.e. if the value of the change of the gain-squared frequency integral can be made positive.

The reference amplifier used in the evaluation is chosen as the common-emitter transistor connected between a specified source and load resistance, as shown in Fig. 3.1(a). This reference amplifier specifies the reference transfer function $T(p)$. The altered transfer function $T_A(p)$ is calculated, using straight forward analysis techniques, from the amplifier of Fig. 3.1(b) with one or more RC one-port networks as the elements of the imbedding network. The results of the analyses

of all possible amplifiers show that the value of (2.21) for J_Δ is always

negative which indicates that the area of the gain-squared magnitude,

frequency curve is always diminished for any one-port RC imbedding

network. No new amplifier configurations emerge from the analysis;

however, the various amplifier configurations are uniformly compared

to the reference amplifier.

Previous studies[17,19] have shown that the configurations of Fig. 3.6

are useful in obtaining a wideband, lowpass amplifier stage. A further

investigation of these stages shows no significant advantage in broadband

performance can accrue from the use of RC one-ports with complexity in

excess of a single time constant (see App. C).

The amplifiers of Fig. 3.6(a) and 3.6(b) are now quantitatively com-

pared with respect to their broadband effectiveness and temperature sensi-

tivity using the gain-squared frequency integral. The amplifier of Fig. 3.6

(c) can be considered to be the same configuration as the amplifier of Fig.

3.6(b) since the RC one-port in the emitter lead of Fig. 3.6(c) can be

incorporated in the transistor circuit model.[17] The analyses of the ampli-

fiers of Fig. 3.6(a) and 3.6(b) are available in the literature.[17,19]

Each of these amplifiers is designed as an interstage in a cascade of

identical stages to allow the cascading of several stages to achieve the

desired gain. The source and load resistances of a stage are consequently

specified by the preceding and following stages respectively. The design

is done for a MFM response, as mentioned previously, to ensure a

reasonable comparison between the two amplifier stages.

In this section, the transistor employed in the design has the follow-
ing characteristics at $I_C = 5$ mA, $V_{CE} = 8$ V[+]:

$$f_t = 65 \text{ Mc/s} \qquad\qquad r_x = 80 \ \Omega$$

$$\beta_o = 60 \qquad\qquad C_\mu = 20 \text{ pF}$$

For the series-feedback amplifier stage of Fig. 3.6(a), the RC one-port
used in the design is a simple parallel RC network. For a cascade of
series-feedback stages, as shown in Fig. 3.2, the source and load resis-
tances are approximated by the low-frequency interstage impedance. For
a typical design, the input and output impedances of the transistor with
emitter feedback are much larger than the interstage resistance, which is
the parallel connection of R_B and R_C. Hence, the values of the source and
load resistances are approximately given by the parallel combination of R_B
and R_C. From Fig. 3.7(a) the voltage gain function, $A_V(p) = V_L/V_s(p)$,
is given approximately by

$$A_V(p) = \frac{\beta_o R_L}{r_\pi + R_s + r_x + \beta_o R_e} \cdot \frac{p R_e C_e + 1}{a_2 p^2 + a_1 p + 1} \tag{3.1}$$

where p is the complex frequency variable and

$$a_2 = R_e C_e (r_\pi C_\pi + \beta_o R_L C_\mu \left(\frac{R_s + r_x}{R_s + r_x + r_\pi \beta_o R_e} \right) \tag{3.2a}$$

[+]The notation used for the transistor circuit model in this report is that
adopted by the Semiconductor Electronics Education Committee.[20]

$$a_1 = (r_\pi C_\pi + R_e C_e + \beta_o R_L C_\mu) \left(\frac{R_s + r_x}{R_s + r_x + r_\pi + \beta_o R_e} \right) \qquad (3.2b)$$

For a MFM response, the following equality must hold:

$$R_e C_e = \sqrt{2a_2 - a_1^2} \qquad (3.3)$$

To obtain the optimum design, since too many degrees of design freedom are available, an iterative design technique is used to optimize the GBW product. A value of low-frequency gain $A_v(O)$ and the resistor R_e is arbitrarily chosen. Then (3.1) and (3.3) uniquely specify R_L and C_e. The optimum gain-bandwidth product is found by varying the low-frequency gain and R_e.[17] The bias point is chosen such that $1/g_m \ll R_e$. For the transistor given above, the values of the components found for the series-feedback amplifier are shown in Fig. 3.7(a). The values of low-frequency voltage gain and bandwidth for optimum GBW product are 4.6 and 4.8 Mc/s respectively.

For the shunt-feedback amplifier, the imbedding network is shown in Fig. 3.8(a). The source and load resistance for a cascade of stages is approximated by the low-frequency output impedance of the preceding shunt-feedback stage and the input of the following shunt-feedback stage. Hence the source resistance is approximately $R_a + \frac{R_f^2}{\beta_o R_a}$, and the load load resistance is approximately $\frac{R_f}{R_L} \left(\frac{1}{g_m} + \frac{r_x}{\beta_o} \right)$. The latter has a

value of 80Ω for the design considered below and is neglected in the

design. The source resistance has a value of $1\,k\Omega$. The current gain,

$A_I(p) = \dfrac{i_L}{i_s}(p)$, is given by

$$A_I(p) = \frac{\beta_o R_f}{(R_f + R_a)\left(1 + \dfrac{r_x + r_\pi}{R_p}\right) + \beta_o R_a} \quad \frac{pR_a C_a + 1}{a_2 p^2 + a_1 p + 1} \tag{3.4}$$

where

$$R_p = \frac{R_f R_s}{R_s + R_f}$$

$$a_1 = \frac{R_f}{R_1(1 + g_m R_a) + R_f}\left[R_a C_a + R_1 C_\pi + \frac{R_1}{r_\pi}\,\beta_o R_a C_\mu\right] \tag{3.5a}$$

$$a_2 = \frac{R_f}{R_1(1 + g_m R_a) + R_f}(R_a C_a)(R_1 C_\pi) \tag{3.5b}$$

where

$$R_1 = \frac{r_\pi(R_s + r_x)}{r_\pi + R_s + r_x} \tag{3.5c}$$

For a MFM response, the coefficients of (3.4) must satisfy the equality

$$R_a C_a = \sqrt{2a_2 - a_1^2} \tag{3.6}$$

To optimize the gain-bandwidth product, the values of the low-frequency

gain $A_I(0)$ and R_a can be chosen arbitrarily. Then, the low-frequency

value of (3.4) and (3.6) specify the values of R_f and C_a. The optimum

gain-bandwidth product is achieved by varying the values of R_a and

$A_I(0)$.[19] For the transistor used in this section, the optimum values of

the imbedding network are shown in Fig. 3.8(a). The low-frequency gain

and bandwidth are 11.2 and 5 Mc/s.

With the above design information, the procedure given in Sec. 2.3

can also be used to evaluate the broadband performance of the series-

feedback stage and the shunt-feedback stage. The reference amplifiers to

determine the reference transfer functions $T(p)$ are shown in Fig. 3.7(b)

and 3.8(b) for the series-feedback stage and shunt-feedback stages,

respectively. For both stages, the transfer functions of the reference

amplifiers are described by a single dominant pole. For the series-

feedback stage, the gain and bandwidth of the reference amplifier are

25.6 and 575 kc/s, while for the shunt-feedback amplifier the gain and

bandwidth are 37.6 and 1.6 Mc/s.

The altered transfer functions $T_A(p)$ are determined from the

imbedded amplifiers of Fig. 3.7(a) and 3.8(a). The change of the gain-

squared frequency integral due to the addition of the imbedding elements

has been calculated using (2.21). The computational details of the pro-

cedures are given in App. D for the series-feedback stage.

Table 3.1 summarizes the results of the broadband effectiveness

evaluation. The conventional GBW product is also included for

comparison. The change of the gain-squared frequency integral J_Δ is normalized with respect to (2.11) which is computed for the reference amplifiers. The normalization references are 380 Mc/s for the series-feedback stage and 2.3 Gc/s for the shunt-feedback stage. The GBW product is normalized with respect to $g_m/2\pi C_t$, where

$$C_t = C_\pi + C_\mu (1 + g_m R_L) \tag{3.7}$$

The quantity g_m/C_t is a fundamental limiting parameter of the reference amplifier.[21]

The large negative values of J_Δ^N for both amplifier stages indicate that considerable area of the gain-squared, frequency curves of the reference amplifiers is sacrificed to achieve the large bandwidths. The smaller negative values of J_Δ^N of the series-feedback stage indicates that this stage is more effective in achieving broadband performance than the shunt-feedback stage. The normalized GBW products also show that the series-feedback stage has a greater broadband effectiveness than the shunt-feedback stage. However, the smaller normalization values of the series-feedback stage are reflected in the smaller low-frequency gain. The specified source and load resistances are critical in determining the ultimate broadband performance of an amplifier. As will be shown in Sec. 4.4, additional transistors can be introduced to improve the broadband performance.

The use of the gain-squared frequency integral as a scalar measure

of broadband effectiveness gives the same gross results as the GBW product. The GBW product is more useful as a scalar measure since the compromise between low-frequency gain and bandwidth is easily determined. The main advantage of the gain-squared frequency integral as a scalar measure, as mentioned previously, is that the integral is mathematically tractable. The correlation between the two scalar measures indicates that the gain-squared frequency integral could be useful as a gross design tool especially for evaluating the broadband effectiveness of amplifiers whose gain-magnitude is not a monotonically decreasing function of frequency, i.e. for response shapes whose -3 dB bandedge and hence the GBW product are not meaningful.

3.4 The temperature sensitivity of single-transistor amplifier stages

An evaluation of the temperature sensitivity of the two stages considered in Sec. 3.3 is next made using the change in the gain-squared frequency integral. This evaluation is made in the same manner as the evaluation of broadband capability. The reference transfer functions $T(p)$, however, are calculated for the series-feedback and shunt-feedback stages of Fig. 3.7(a) and 3.8(a) operating at an ambient temperature of 25° C. The altered transfer functions $T_A(p)$ for the respective amplifiers are calculated for the same amplifiers operating at a different ambient temperature. The scalar measure of (2.20) does not determine the nature of the response change: the details of the change of the amplifier characteristics must be determined by inspecting the

altered transfer function $T_A(p)$.

The ambient temperature change is chosen to be from 25° C to 100° C. For the following analysis, all resistors are assumed to be diffused resistors with the exception of the source and load resistors which are assumed to be discrete components with negligible temperature coefficients. The resistors of the shunt-feedback stage R_a and R_f are fabricated from a base diffusion. The value of base resistors increases 12 percent as the temperature increases from 25° C to 100° C.[7] The resistor R_e of the series-feedback stage is fabricated from a low resistivity emitter diffusion whose resistivity has only a small temperature dependence and its change is neglected.

The results of App. B indicate that the bias points of these stages remain constant with temperature. Hence, the parameters of the transistor circuit model can be assumed to have the following variations with temperature:

$$\beta_o(T_2) = 1.6 \ \beta_o(T_1)$$

$$g_m(T_2) = g_m(T_1) \frac{T_1}{T_2}$$

(3.8)

$$r_\pi(T_2) = \frac{\beta_o(T_2)}{g_m(T_2)} = 1.6 \frac{T_2}{T_1} \ r_\pi(T_1)$$

$$C_\pi = \frac{g_m(T_2)}{\omega_t} - C_\mu = \frac{T_1}{T_2} \frac{g_m(T_1)}{\omega_t} - C_\mu$$

where $T_1 = 300^O$ K and $T_2 = 375^O$ K. The capacitance C_μ is approximately constant over this temperature range as is the parameter f_t.[8,9]

The variation of the gain-squared frequency integral with temperature will be assumed small so that (2.20) is applicable for the computation of J_b. With this first-order assumption, the sensitivity to each transistor parameter or passive component can be computed separately and the results added algebraically to determine the net sensitivity of the amplifier. The procedure identifies the most sensitive parameters and indicates any possibility of achieving cancelling temperature sensitivities.

The temperature sensitivities, which have been calculated from (2.20), are shown in Fig. 3.9 for an ambient temperature change from 25° C to 100° C. The results are normalized with respect to the gain-squared frequency integral of the stages operating at 25° C. The temperature sensitivity of the series-feedback stage is much less than the shunt-feedback stage. The lower sensitivity of the series-feedback stage is attributed to the assumed zero temperature dependence of the emitter resistor R_e.

The greater sensitivity of the shunt-feedback can be attributed to the sensitivity of J with respect to the resistors R_a and R_f, and β_o. The resistors R_a and R_f of the shunt-feedback stage have large values which necessitates their fabrication from the higher resistivity, temperature dependent, base diffusion. The mid-frequency gain $A_I(0)$ is more sensitive with respect to β_o than the series-feedback stage. The sensitivity of the low-frequency gain could be improved if the value of R_f were

reduced such that the low-frequency gain(3.4) is given approximately by

$$A_I(0) \approx \frac{R_f}{R_a} \qquad\qquad (3.9)$$

Since the resistors R_a and R_f ideally have the same temperature dependence the gain would be constant with temperature; however, the broad-band effectivenss would be reduced.[19]

The details of the changes in amplifier performance can be determined by examining the altered transfer functions which are given by (3.1) and (3.4) with the values of the coefficients at 100° C. The values of the low-frequency gain increase 4 percent or to 5.1 for the series-feedback stage and 10 percent or to 12.2 for the shunt-feedback stage. The value of the bandwidth of the series-feedback decreases 6 percent to 4.5 Mc/s while the value of the bandwidth of the shunt-feedback stage decreases 20 percent to 4 Mc/s.

For a cascade of these stages, the source and load resistances of a stage, i.e. the interstage resistances, must also be assumed to be diffused resistors. An inspection of the transfer function of the shunt-feedback stage, given by (3.4), indicates that a small change of the source resistance of the shunt-feedback stage has a small effect on the transfer function. However, the transfer function of the series-feedback stage, given by (3.1), depends on the load resistance R_L; i.e. the low-frequency gain is approximately

$$A_V(0) = \frac{R_L}{R_c} \tag{3.10}$$

Hence, changes of the low-frequency gain are proportional to changes of R_L. The values of the coefficients (3.2), a_1 and a_2, also depend on R_L. If the sensitivity of R_L is included in the sensitivity analysis above, the net sensitivity of the series-feedback stage nearly doubles; however, the sensitivity is still less than the shunt-feedback stage.

3.5 Experimental realizations of single-transistor amplifier stage

Experimental studies of the single-transistor amplifier stages have also been made. The stages are designed according to the procedure given in Sec. 3.3. The biasing of the stages is done using voltage-reference diodes as discussed in Sec. 3.2.

The series-feedback stage has been realized as both a discrete-component amplifier[4] and as a monolithic, integrated amplifier. A photomicrograph of the plan view of the integrated realization and its discrete-component counterpart are shown in Fig. 3.10(a) and 3.10(b) respectively. The components of a single integrated amplifier stage are chosen such that several stages may be directly cascaded. The details of the fabrication of the circuit are discussed in Sec. 4.3.

The shunt-feedback stage has been realized as a discrete-component amplifier using diffused components which are not electrically isolated, as shown in Fig. 3.11. Hence, the parasitic capacitances of the isolation

junctions are absent from the diagram of Fig. 3.11. Also, the components are not thermally coupled since they are on separate substrates.

The dc bias constancy of these experimental stages was studied to confirm the predictions of App. B. For an emitter current of 5 mA, the monolithic, integrated, series-feedback stage was found to have less than a 1 percent variation of emitter current for a temperature change from 25° C to 100° C. The discrete-component, shunt-feedback stage had a 5 percent variation of emitter current for the same temperature variation since the elements were not at a uniform temperature. The 1 percent to 5 percent variation of the bias points is quite good with respect to the variation of the transistor parameters. The value of the base-emitter voltage, V_{BE}, decreases 20 percent and β_o increases 60 percent over this temperature range. The agreement with the theoretical predictions of App. B is quite good.

3.6 Conclusions

This chapter has investigated the use of the gain-squared frequency integral for the evaluation of the performance of single-transistor amplifier stages. For the evaluation of broadband effectiveness, the gain-squared frequency integral was found to give a scalar measure which agreed with the GBW product; however, the simplicity of the physical interpretation of the GBW product is more useful in the design of lowpass broadband amplifiers. The gain-squared frequency integral was especially useful in the evaluation of the temperature sensitivity. The

results show that this scalar measure of sensitivity correlated well with the temperature sensitivity interpreted in terms of the variation of low-frequency gain and bandwidth.

	Shunt-feedback Stage	Series-feedback Stage
$A(0)$	11.1	4.6
ω_o	5 Mc/s	4.8 Mc/s
J^N_Δ	-0.75	-0.72
GBW^N_Q	0.89	0.34

Table 3.1 The broadband effectiveness of the shunt-feedback stage and the series-feedback stage.

(a)

RC I-PORT
NETWORKS
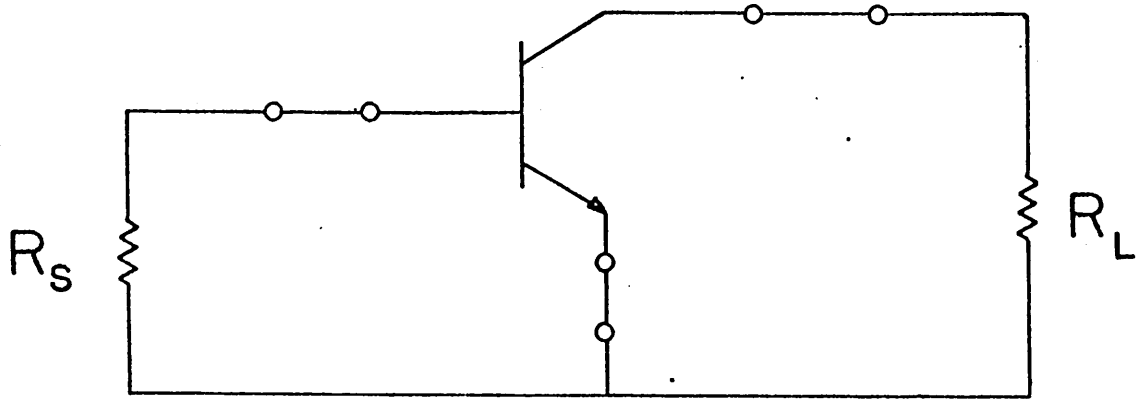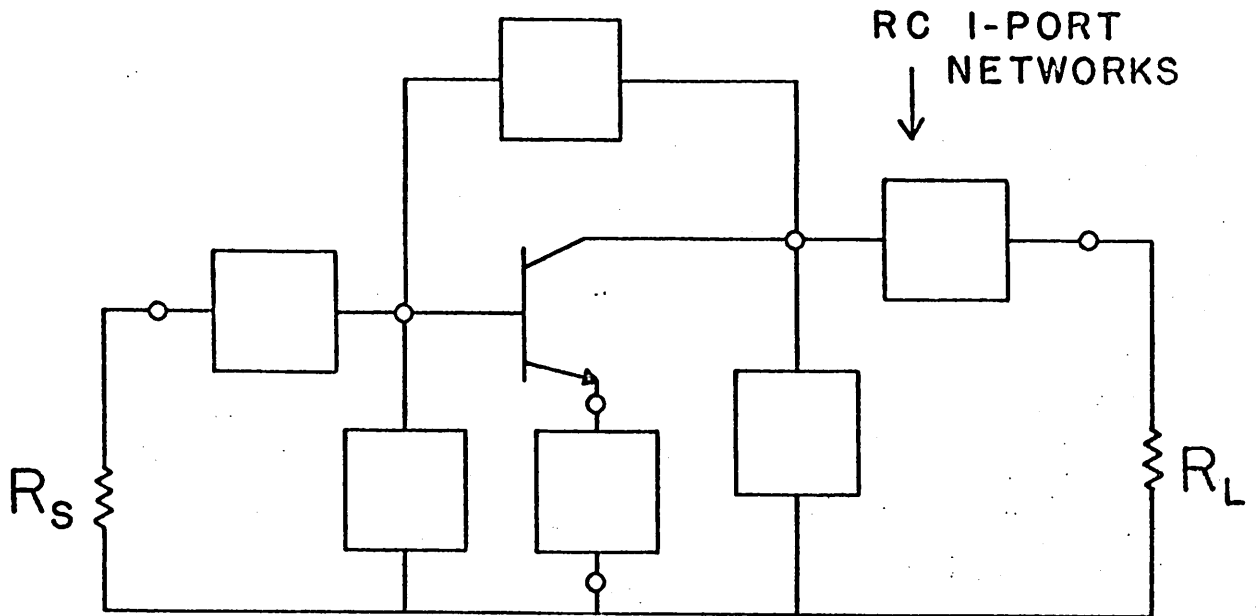
(b)

Figure 3.1 (a) Reference amplifier for a single common-emitter
transistor; (b) an imbedding network consisting of all
possible RC one-port networks.
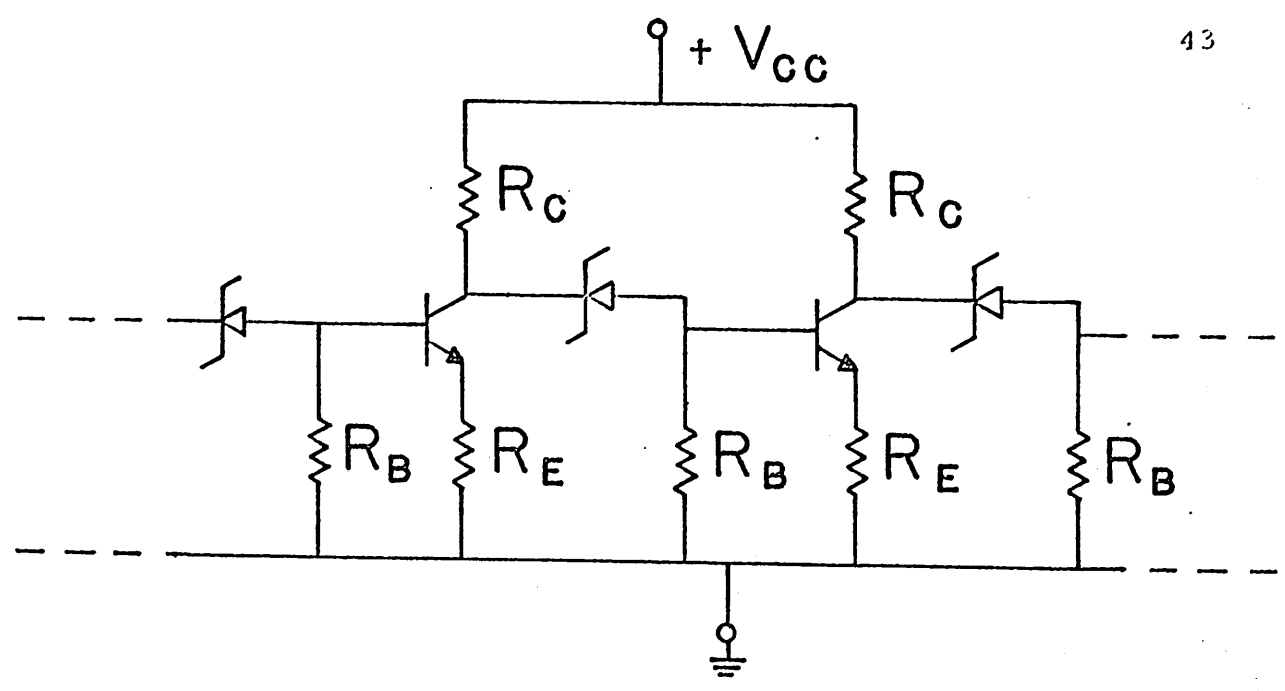
Figure 3. 2 A cascade amplifier using voltage reference diodes for ac coupling of successive stages.
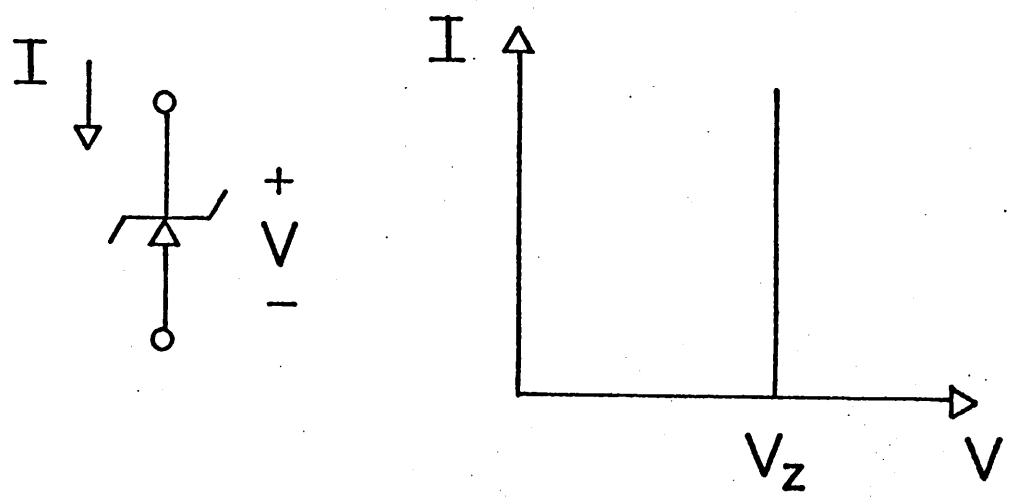
Figure 3. 3 The dc I, V characteristic of a voltage reference diode.
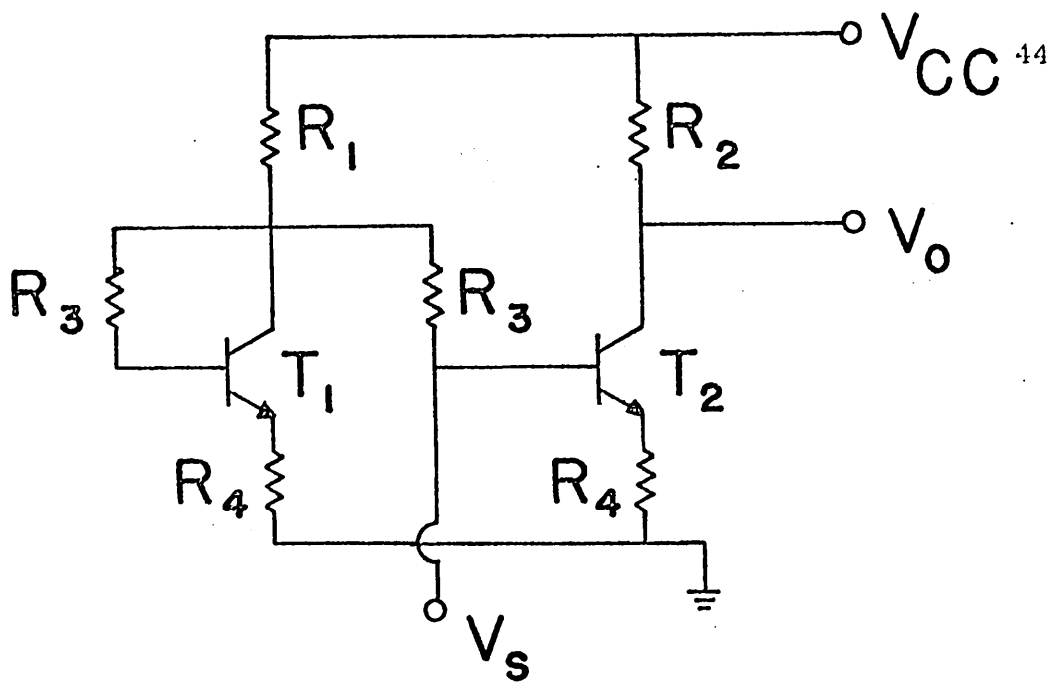
Figure 3.4 A biasing circuit suitable for integrated amplifiers.
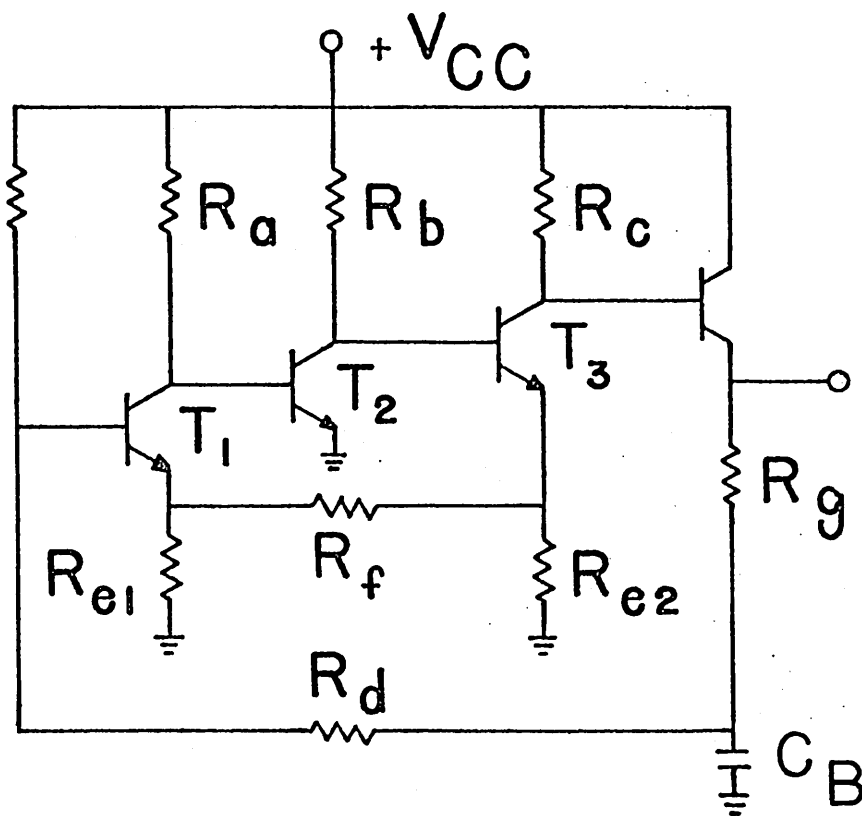
Figure 3.5 A direct-coupled amplifier.
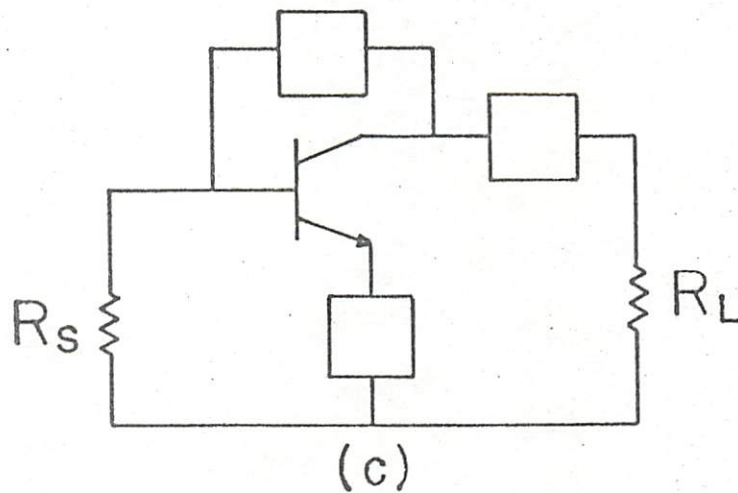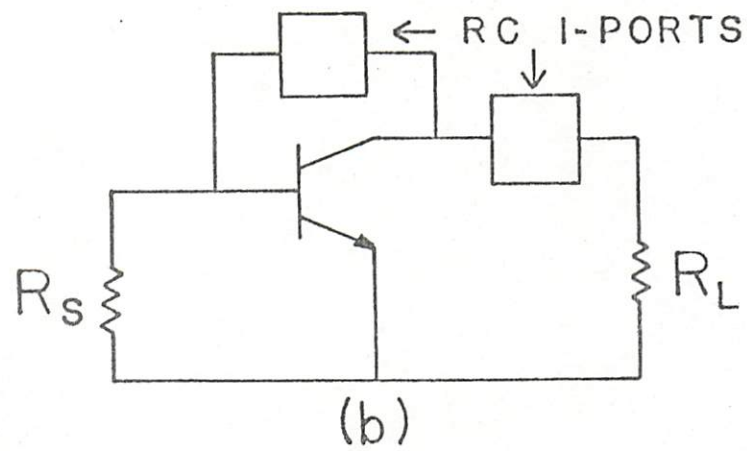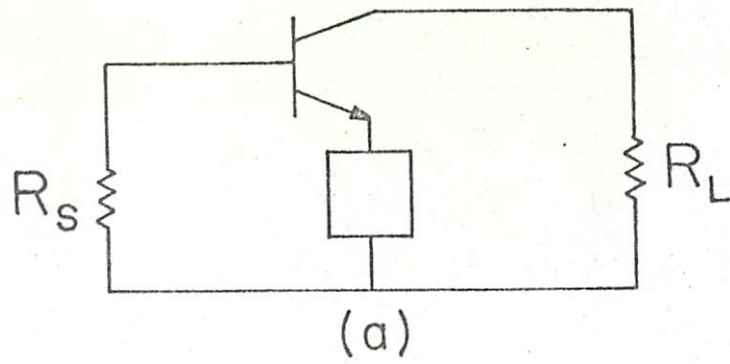
Figure 3.6 Single transistor broadband amplifiers employing one-port RC networks.

$R_s = 280\,\Omega$

$+$

V_s

$-$

$R_e = 50\,\Omega$ $C_e = 500_pF$

$+$

V_L $R_L = 280\,\Omega$

$-$

(a)

$280\,\Omega$

$+$

V_s

$-$

$280\,\Omega$

$+$

V_L

$-$

(b)
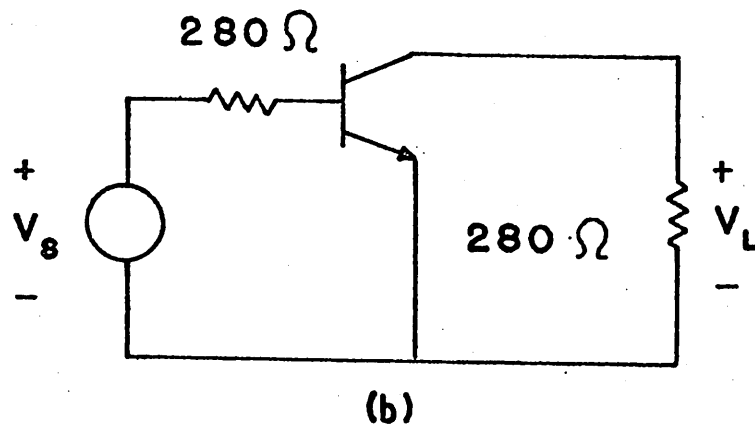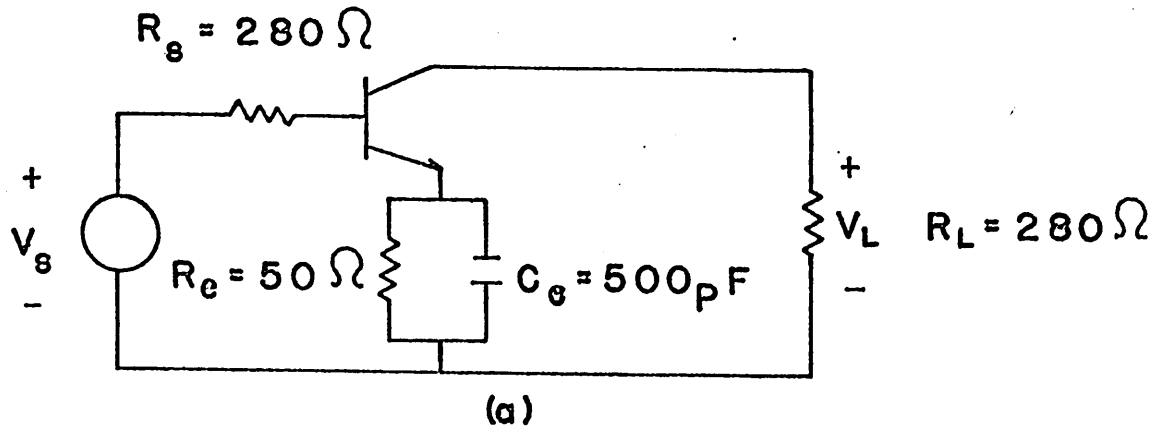
Figure 3.7 (a) The shunt-feedback amplifier stage; (b) the reference
amplifier for the series-feedback amplifier stage.

$R_f = 3.4 \, K\Omega$

$R_a = 200 \, \Omega$

$C_a = 347 \, pF$

i_s

$1K\Omega$

i_L

(a)

i_s

$1K\Omega$

i_L

(b)
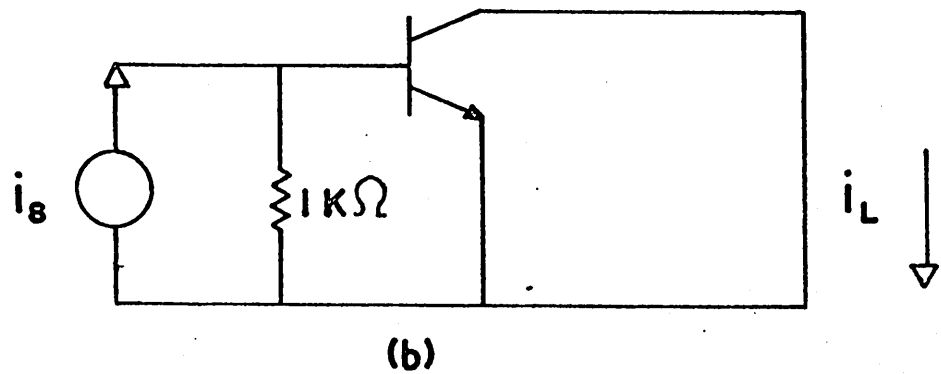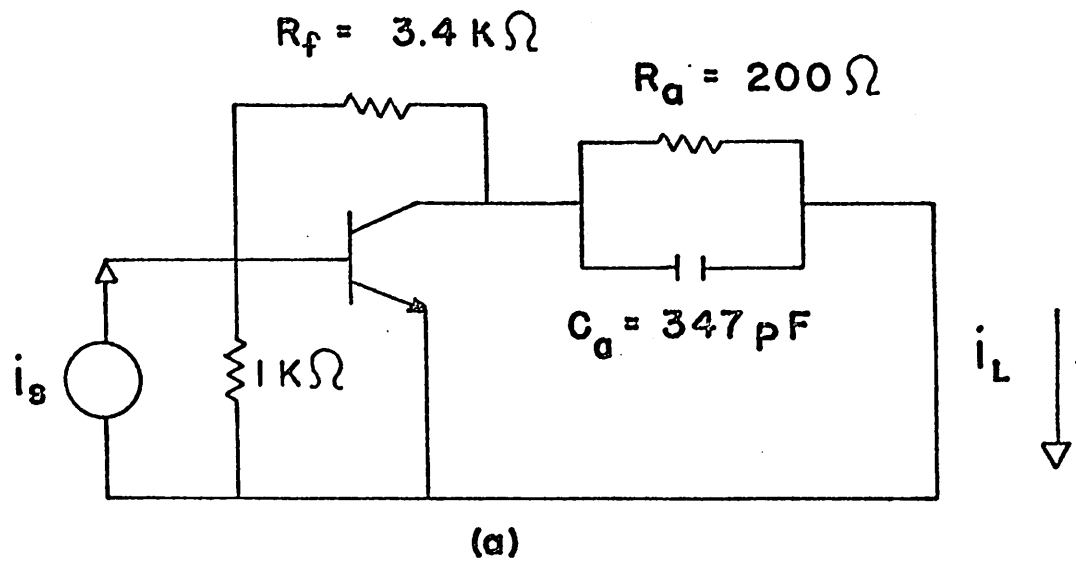
Figure 3.8 (a) The shunt-feedback amplifier stage; (b) the reference amplifier of the shunt-feedback amplifier stage.
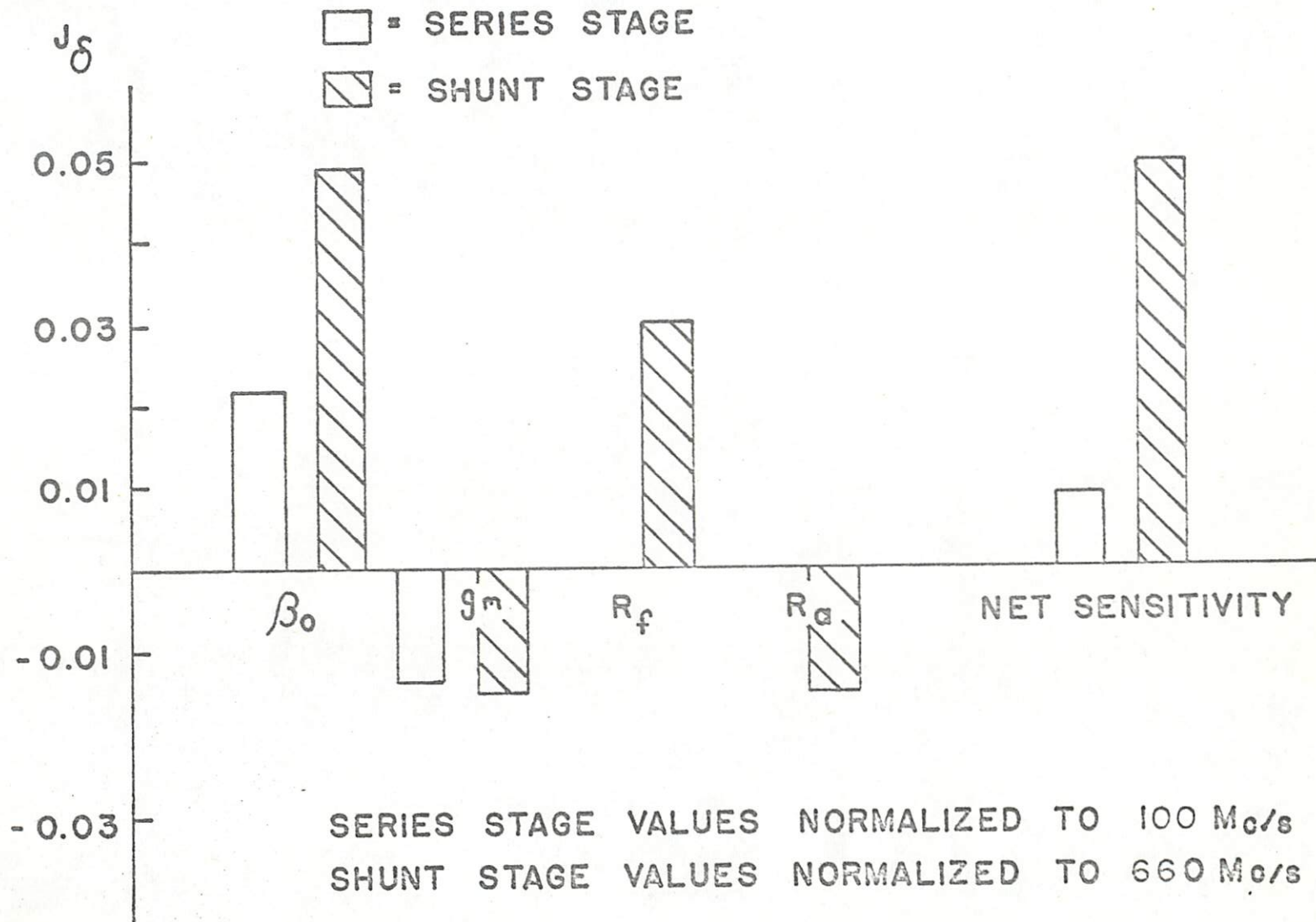
Figure 3. 9 The temperature sensitivities of the shunt-feedback stage and the series-feedback stage.

(a)

(b)
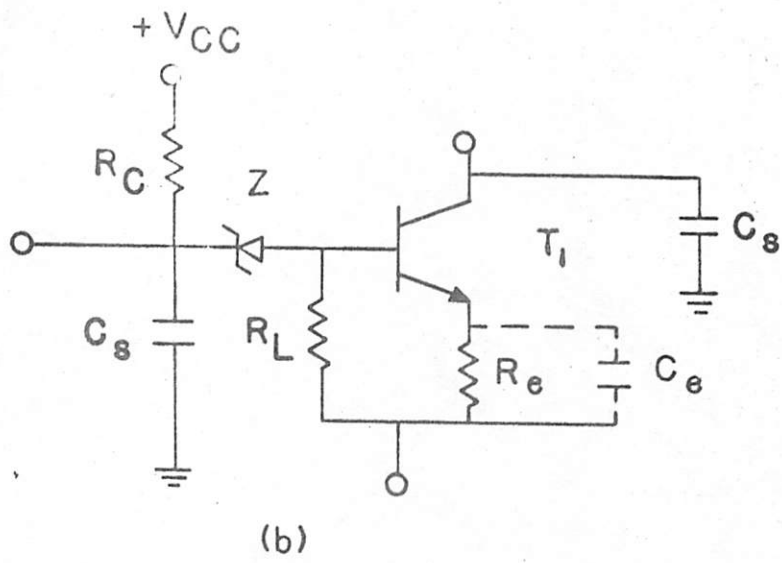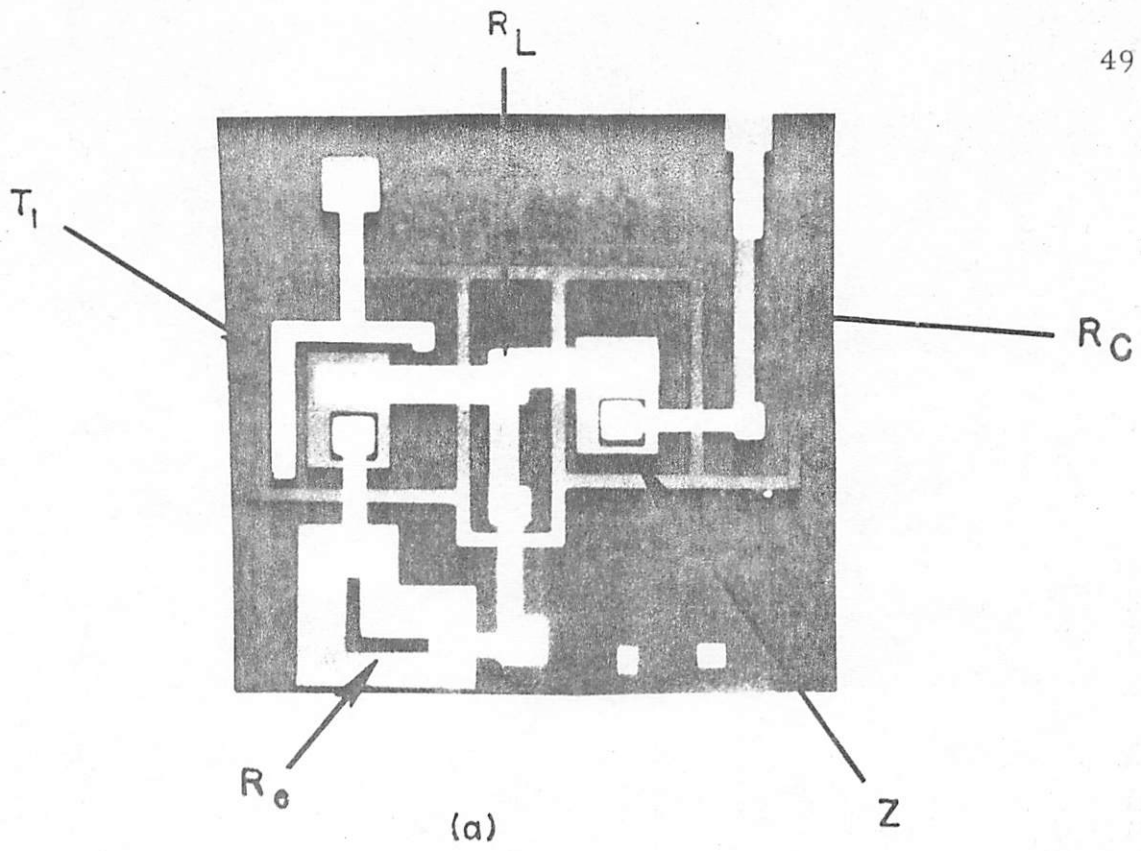
Figure 3.10 (a) Plan view of the integrated realization of the series-feedback stage; (b) the discrete-component representation of the integrated realization of the series-feedback stage.
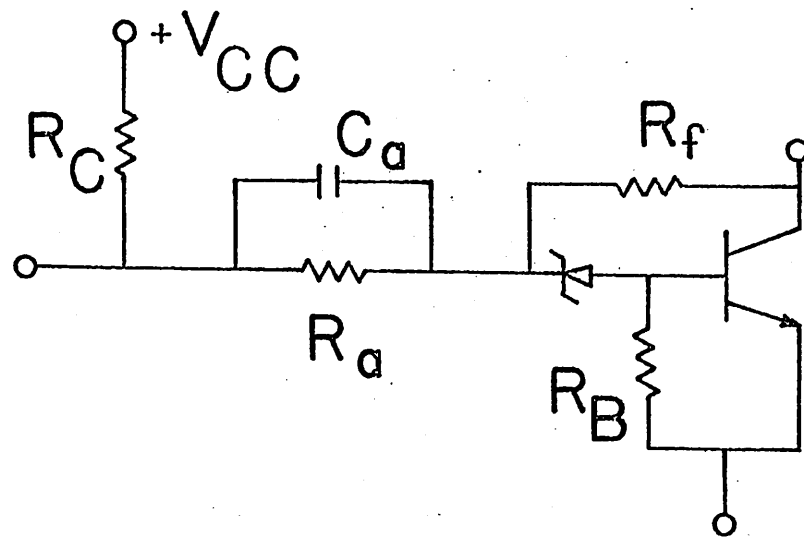
Figure 3.11 The discrete-component realization of the shunt-feedback
stage.

4. TWO-TRANSISTOR AMPLIFIER STAGES

4.1 Introduction

The study of single-transistor stages has developed an understanding of the gain-squared frequency integral and demonstrated its use to compare different single-stage amplifiers. The use of a single transistor for wideband amplification does not provide enough gain for most applications. Consequently, several single-stage amplifiers are cascaded to achieve the necessary gain. The capacitive interaction between successive stages is not accounted for in the designs previously considered. In this chapter, the restricted, but important class of two-transistor amplifier stages are designed to include the effect of this interaction on the magnitude-frequency response.

The problem of optimally imbedding a transistor pair in an RC network as shown in Fig. 2.4(a) is more difficult than the problem of optimally imbedding a single transistor. The diagram of a two-transistor pair is shown in Fig. 4.1. Each transistor can be any of three dc connections, common-base, common-collector and common-emitter; hence, nine dc configurations for the two transistors, connected between the source and load resistances, exist. Even if a particular dc connection is chosen a-priori, any number of RC imbedding networks are possible. The use of one-port RC networks in all possible locations, let alone a

nine-terminal RC network, yields too many imbedding networks to analyze each in detail as was done for the single transistor stage. Experience and intuition are necessary to reduce the number of possible amplifier configurations.

The dc connection of two common-emitter transistors is the most useful connection for obtaining the maximum low-frequency gain for most source and load specifications. Two common-emitter pairs, one using local feedback around each transistor and the other using overall feedback around both transistors, are compared for broadband effectiveness and temperature sensitivity. These two pairs are similar in topology. As will be seen, the results of this comparison give valuable information for the design of broadband, lowpass, integrated amplifiers.

Pair configurations which use the other possible dc connections are evaluated for their broadband effectiveness. Three of these composite-stages are found particularly useful as monolithic integrated amplifiers.

4.2 Common-emitter transistor pairs

The amplifier stages using common-emitter transistor pairs useful for obtaining large bandwidth and insensitivity are shown in Fig. 4.2 and 4.3. The bias and coupling circuitry are omitted in Fig. 4.2 and 4.3; the design of this circuitry is presented later in this chapter. The amplifier stages of Fig. 4.2(a) and 4.3(a), the shunt-series cascade and the series-shunt cascade respectively, use only local feedback around each transistor, while the amplifier stages of Fig. 4.2(b) and 4.3(b), the shunt-series

feedback pair and series-shunt feedback pair, use overall feedback. As will be seen in the course of this report, the choice of topology is often dictated by the requirements of biasing and coupling the transistors. Therefore, the objective of this section is to determine the relative advantages in the broadband performance and temperature sensitivity of amplifiers which use either local or overall feedback.

The shunt-series cascade and the shunt-series feedback pair are used as the vehicles for the comparison of local and overall feedback. Both amplifiers have low-input impedances and, consequently are useful as current amplifiers. Even though the amplifiers employ topologically different feedback loops, the feedback current into the base of the input stage is identical if the gain across the emitter of the output transistor of the shunt-series cascade approaches it theoretical limit of unity. Therefore, if the two amplifiers are designed for the same value of gain and source and load resistance, the low frequency current gain, as is brought out shortly, is approximately given by

$$A_I(0) \approx \frac{R_f}{R_e} \qquad (4.1)$$

The broadband performance will also be identical. The gain-squared frequency integral is used to evaluate the deviation of these stages from this ideal behavior to ascertain if any advantage is obtained from overall feedback for a monolithic integrated circuit. (App. E indicates that the

series-shunt cascade and the series-shunt feedback pair also have identical broadband performance.)

The shunt-series cascade, shown in Fig. 4.2(a), is designed using existing design procedures.[3] If the ohmic base resistance is small compared with r_{π_2} and $\beta_{o_2} R_e$ of the series-feedback stage, the capacitive interaction between the two single-transistor stages can be modeled by loading the shunt-feedback stage with a parallel RC network.[3] This approximation leads to an easily designed common-emitter pair whose current gain, $A_I(p) = \dfrac{i_L}{i_s}(p)$, is given approximately by

$$(4.2)$$

$$A_I(p) = \frac{R_f}{R_e + \dfrac{1}{g_{m_2}}} \frac{1}{\left[R_f(C_f + C_L)\dfrac{p^2}{\omega_t} + R_f C_f p + 1\right]\left[\dfrac{p}{\omega_t}(R_e + \dfrac{r_{x2}}{g_{m_2}}) + 1\right]}$$

under the assumptions that

$$R_f \gg r_{\pi 1} \qquad\qquad (4.3a)$$

$$\frac{\beta_o(\dfrac{1}{g_{m2}} + \beta_o R_e)}{R_f + \beta_o(\dfrac{1}{g_{m2}} + \beta_o R_e)} \gg 1 \qquad\qquad (4.3b)$$

$$r_{x_2} \gg r_{\pi_2} + \beta_o R_e \qquad\qquad (4.3c)$$

where

$$\frac{1}{R_c C_c} = \omega_t \tag{4.4a}$$

and

$$C_L \approx C_c + C_\mu (1 + g_m R_L) \tag{4.4b}$$

The pole, $\omega_t \dfrac{R_c + \dfrac{1}{g_{m2}}}{r_{x_2}}$, is usually non-dominant and the gain function

can be approximated by

$$A_I(p) = \frac{R_f}{R_c + \dfrac{1}{g_{m_2}}} \quad \frac{1}{R_f(C_f + C_L)\dfrac{p^2}{\omega_t} + R_f C_f p + 1} \tag{4.5}$$

The design is for a MFM response; thus,

$$R_f C_f = \sqrt{2R_f(C_f + C_L)\frac{1}{\omega_t}} \tag{4.6}$$

The design of the shunt-series feedback pair is also done using existing design techniques.[22] The current gain,

$$A_I(p) + \frac{i_L}{i_s}(p)$$

is given approximately by

$$A_I(p) = \frac{R_f + R_c}{R_c} \quad \frac{1}{\frac{1}{\mu_o p_1 p_2} p^2 + \left[R_f C_f + \frac{1}{\mu_o \lambda_o} \left(\frac{1}{p_1} + \frac{1}{p_2} \right) \right] p + 1} \tag{4.7}$$

where

$$\mu_o \lambda_o = \beta_{o1} \left(\frac{R_p}{R_p + r_{\pi 1} + r_{x1}} \right) \beta_{o2} \left(\frac{R_I}{R_I + r_{\pi 2}(1 + g_{m2}R_c)} \right) \frac{R_c + R_f}{R_f} >> 1 \tag{4.8a}$$

$$\frac{1}{p_1} = r_\pi C_{\pi 1} \tag{4.8b}$$

$$\frac{1}{p_2} = \frac{R_I}{R_I + r_{\pi 2}(1 + g_{m2}R_e)} r_\pi (r + g_{m2}R_c) \frac{C_{\pi 2}}{1 + g_{m2}R_e} + C_\mu \left(1 + \frac{g_{m2}R_L}{1 + g_{m2}R_c} \right) \tag{4.8c}$$

$$R_p = \frac{R_f R_s}{R_f + R_s} \tag{4.8d}$$

The assumptions of (4.3) are also used to obtain (4.7). To obtain a MFM, it is necessary that

$$p_1 + p_2 + \mu_o \lambda_o p_1 p_2 R_f C_f = \sqrt{2 p_1 p_2 (1 + \mu_o \lambda_o)} \tag{4.9}$$

In the design of each stage, there are five resistors R_s, R_L, R_I, R_c and R_f and two capacitors C_c and C_f, whose values must be chosen. The source and load resistors R_s and R_L are usually specified. The resistor R_1 is usually fixed by the value of supply voltage V_{CC} and the desired bias current of T_1. The low-frequency gain $A_1(0)$, the MFM condition and (4.4a) constrain the remaining four components. For the design of the shunt-series cascade and the shunt-series feedback pair, a low-frequency current gain of 20 is desired. The resistor R_f is chosen to optimize the bandwidth for this gain.[22] Then, R_c is specified by the low-frequency gain, C_c is specified by (4.4a), and C_f is specified by the MFM condition.

For the design of a monolithic integrated amplifier, an exact one-to-one correspondence between the integrated amplifier and its discrete-component counterpart does not adequately predict the phase and frequency performance. The circuit models of the integrated resistors and transistors (see Figs. 1.1 and 1.2) have a capacitance to ground associated with the isolation junction. This parasitic capacitance can be quite large. For the integrated realization of Sec. 4.3, the capacitance of the isolation junction is approximately 0.25 pF/mil^2.[8] The effect of this parasitic capacitance is to decrease the bandwidth of the amplifier.[10] The experimental results of Sec. 4.3 indicate that for the amplifiers considered, the parasitic capacitances of the resistor R_I and the transistor T_1 are most important in determining the frequency behavior. Fig. 4.4, a discrete-

component representation of the integrated realization, includes the effect of the isolation junction as a discrete-component 100 pF capacitor from the collector of the first transistor to ground.

Figs. 4.4(a) and 4.4(b) indicate the values obtained for the realization of a typical monolithic integrated circuit, taken from Sec. 4.3, for the shunt-series cascade and shunt-series feedback pair respectively. The transistors have the following measured parameters which approximate the elements of a hybrid-pi circuit model:[20]

$$\beta_{o1} = 70 \qquad\qquad \beta_{o2} = 50$$

$$C_{\mu 1} = 3 \text{ pF} \qquad\qquad C_{\mu 2} = 3 \text{ pF}$$

$$f_{t1} = 160 \text{ Mc/s} \qquad\qquad f_{t2} = 160 \text{ Mc/s}$$

$$I_{C1} = 7.7 \text{ mA} \qquad\qquad I_{C2} = 7.5 \text{ mA}$$

$$V_{CE1} = 8 \text{ V} \qquad\qquad V_{CE2} = 9 \text{ V}$$

The load and source resistance are external to the integrated circuit and must be capacitively coupled to the input and output terminals of the amplifier.

The shunt-series cascade uses two voltage reference diodes to bias and couple the transistors as shown in Fig. 4.4(a). Ideally, the sum of the voltage reference diode and the base-emitter junction of each transistor are identical. Consequently, the voltage across the emitter resistor R_c controls the bias points of the transistor. The bias points are

then

$$I_{C1} \approx \frac{V_{CC} - V_{BE} - V_Z}{R_C} \qquad (4.10a)$$

and

$$I_{C2} \approx \frac{R_f}{R_e} \frac{V_{BE}}{R_{B1}} \qquad (4.10b)$$

Fig. 4.7(b) shows the location of R_C and R_{B1}.

The same bias scheme cannot be used for the shunt-series feedback pair. If the resistor R_f is connected directly, the output stage saturates. A capacitor in the feedback path and a bias resistor are added externally, as shown in Fig. 4.4(b), to bias this stage. A voltage reference diode is still used to couple the transistors. The bias and coupling circuitry used here is necessary in order that the same integrated realization can be used to verify the results of the comparison experimentally. An interesting use of the shunt-series feedback pair is as a differential amplifier.[23] An additional low-frequency, feedback loop is introduced to provide an invariant bias point.

The broadband performance and temperature sensitivities of the shunt-series cascade and shunt-series feedback pair are evaluated in a similar manner to the single-transistor stages using the gain-squared frequency integral. The reference amplifier for the broadband performance

comparison is shown in Fig. 4.5. The computational details of the change in the gain-squared frequency integral are given in App. D for the shunt-series cascade. The normalized change in the gain-squared frequency integral is -0.980 for the shunt-series cascade and -0.981 for the shunt-series feedback pair with respect to the gain-squared frequency integral of the reference amplifier of 2.9×10^3 Gc/s.

Figure 4.5b shows the gain-magnitude, frequency curve (A) of the shunt-series cascade. Three additional curves are also given in Fig. 4.5b. These curves can be used to interpret the difference in the J_Δ values which were calculated for the shunt-series cascade and shunt-series feedback pair. The difference between the curves A and B or C and D can be seen to be only slight. The difference in the corresponding J_Δ values of these curves is approximately 0.1 percent. However, the curve C (or D) has a value of low-frequency gain which is 5 dB or 17 percent greater than curve A (or B). This difference is reflected by a difference of 1 percent in the corresponding J_Δ values. The difference in the J_Δ values does not reflect the improvement in broadband effectiveness as well as the GBW product. However, a difference of 0.1 percent is seen not to represent a significant difference in the broadband effectiveness of the shunt-series cascade and shunt-series feedback pair.

The low-frequency current gain and bandwidth of the shunt-series cascade, calculated from (4.2), are 28.2 and 11.3 Mc/s. For the shunt-series feedback pair, the corresponding values, calculated from (4.5), are 30.2 and 10.7 Mc/s. These values also give an identical gain-bandwidth product of 330 Mc/s for both stages.

The temperature sensitivities of the shunt-series cascade and the shunt-series feedback pair, summarized in Fig. 4.6, are also calculated using the variation in the gain-squared frequency integral. For the temperature sensitivities the variation is expected to be small; hence, (2.20) is applicable for the numerical calculations of the temperature sensitivities. The numerical calculations of Fig. 4.6 take account of an increase in the ambient temperature from 25°C to 100°C. At 100°C the measured parameters from Sec. 4.3 of the transistors and passive components are the following values:

$$\beta_{o1} = 110 \qquad \beta_{o2} = 80$$

$$I_{C1} = 6 \text{ mA} \qquad I_{C2} = 5.1 \text{ mA}$$

$$R_f = 1.6 \text{ k}\Omega \qquad R_e = 51 \ \Omega$$

$$R_C = 2.5 \text{ k}\Omega \qquad R_{B1} = 4.4 \text{ k}\Omega$$

$$R_{B2} = 2.2 \text{ k}\Omega$$

As mentioned previously, the variations of the capacitances and f_t of the transistors are negligible over this temperature range.

The change of the gain-squared frequency integral with temperature is shown in Fig. 4.6. A typical calculation of the temperature sensitivity is given in App. F. The parameter R_I includes the changes of the resistors R_C, R_{B1} and R_{B2}. The changes of the transistor parameters are the same as (3.7). The change of emitter current has the following effects on the transistor parameters:

$$g_m(T_2) = g_m(T_1) \frac{I_C(T_2)}{I_C(T_1)}$$

$$r_\pi(T_2) = r_\pi(T_1) \frac{I_C(T_1)}{I_C(T_2)} \qquad (4.11)$$

and

$$C_\pi(T_2) = \frac{g_m(T_1)}{\omega_t} \frac{I_C(T_2)}{I_C(T_1)}$$

The difference in the net sensitivity, as indicated in Fig. 4.6, is

only slight. App. G indicates the method of interpreting the change of the gain-squared frequency integral for the shunt-series cascade in terms of low-frequency gain and bandwidth of the amplifier. The results are summarized in Table 4.6. As shown in App. G, the poles of the transfer function are on radials less than 45°; hence the response is no longer a MFM response. However, the magnitude is still a monitonically decreasing function of frequency. The major difference between the amplifiers is that the change of low-frequency gain is of the opposite sign for the two amplifiers. The difference can be attributed to the dependence of the low-frequency gain of the shunt-series cascade, $R_f (R_e + 1/g_m)$, on $1/g_m$ which increases approximately 80 percent. This increase of $1/g_m$ causes the low-frequency gain of the cascade to decrease. The gain of the shunt-series feedback pair is approximately R_f/R_e. Since R_f has a greater temperature variation than R_e, the low-frequency gain of the cascade increases.

4.3 Monolithic integrated realizations of two-transistor amplifier stages

To confirm the predicted behavior of the two-transistor amplifiers discussed in the previous section, an integrated circuit was fabricated. The plan view of the integrated circuit is shown in Fig. 4.7(a) along with a discrete-component representation in Fig. 4.7(b). This section discusses the fabrication procedure, the range of values obtained in the integrated circuit, and the temperature behavior of the amplifier.

Since the performance of the shunt-series cascade and the shunt-

series feedback pair is similar, the integrated realization is designed to realize either configuration. The resistor R_f is connected to the circuit externally to achieve either amplifier as shown in Fig. 4.4. The voltage-reference diodes Z_1 and Z_2 provide the necessary dc voltage drops to allow the direct coupling of the resistor R_f for the shunt-series cascade. The voltage reference diodes also provide nearly constant dc operating points as discussed previously. Separate dc bias must be provided for the shunt-series pair. A resistor and capacitor are added externally to ensure the same dc operating points as the shunt-series cascade.

The circuits are fabricated on one ohm-cm, n-type, epitaxial silicon with a thickness of 12 μ on a five ohm-cm, p-type substrate. The fabrication procedure, summarized in Table 4.2, consists of two p-type diffusions and one n-type diffusion. The first p-type diffusion is designed to diffuse through the eptaxial material and provide isolated n-type regions. The second p-type diffusion and n-type diffusion are used to make double-diffused bipolar transistors, the voltage reference-diodes, and the resistors. All the resistors, except the emitter resistor R_e, are fabricated from the p-type, base diffusion. The resistor R_e is fabricated from the n-type, emitter diffusion. The variations in the processing steps are also noted in Table 4.2.

Table 4.3 gives the values of the individual components for the circuit tested and the variations obtained during different fabrication

runs. The units for any single run were found to be quite close in their performance. A typical variation of 10 percent in low-frequency gain and bandwidth among different units on the same run was found. The wide variation of the sheet resistance of the base diffusion causes a wide variation of the low-frequency gain since the gain, (4.2) or (4.5), is directly proportional to the value of the base diffused resistor R_f.

The magnitude-frequency response curves for an experimental realization of the shunt-series cascade and shunt-series feedback pair are shown in Fig. 4.8 and 4.9 respectively. The response of both amplifiers has a peak in the magnitude-frequency curve as shown by the dashed curves in Fig. 4.8 and Fig. 4.9. The peaked response is attributed to a value of the capacitor C_f smaller than its design value. The pole locations of the shunt-series cascade, computed from (4.2), are given by

$$-\sigma_a \pm j\omega_a = -\frac{1}{2}\frac{C_f}{C_f + C_L}\left[1 \pm j\sqrt{4(1 + \frac{C_L}{C_f})\frac{\omega_t}{R_f C_f} - 1}\right] \quad (4.12)$$

Normally the condition

$$C_f << C_L \qquad\qquad (4.13)$$

is satisfied. Then, (4.12) is given approximately by

$$- \sigma_a \pm j\omega_a = -\frac{1}{2}\frac{C_f}{C_L} \pm j\frac{1}{2}\frac{C_f}{C_L}\sqrt{\frac{4\omega_t}{R_f C_f^2} - 1} \qquad (4.14)$$

If a small variation of the capacitance is considered, the change of pole location is given by

$$-\Delta\sigma_a \pm j\Delta\omega_a = -\frac{1}{2}\frac{\Delta C_f}{C_L}(1 \mp j) \qquad (4.15)$$

where the condition that $\sigma_a = \omega_a$ for the nominal design has been used to simplify (4.15). If C_f is smaller than its nominal value, i.e. $\Delta C_f < 0$, then the changes of the real and imaginary parts of the poles are

$$\left|\Delta\sigma_a\right| < 0 \qquad (4.16a)$$

$$\left|\Delta\omega_a\right| > 0 \qquad (4.16b)$$

The poles now lie on radials greater than 45° and a peaked response results. An external capacitance of 10 pF is added in parallel with R_f to obtain the flat response as shown. The peaked response of the shunt-series feedback pair can be explained similarly. The gain and bandwidth are 26 and 11.5 Mc/s for the shunt-series cascade and 29 and 10.5 Mc/s for the shunt-series feedback pair. The predicted values are listed in Table 4.1. The experimental values of the low-freqeuncy gain are slightly smaller because the ohmic base resistance is neglected in the theoretical analysis. This resistance is large for these integrated circuit transistors.[21] If a base resistance of 150 ohms is included in

the calculation of the gain, the calculated gain agrees with the predicted gain.

The response curves of the amplifiers at 100° C, including C_f, are also shown in Fig. 4.8 and 4.9. The gain of the shunt-series cascade has a maximum variation of -0.5 dB from 0° C to 100° C from low frequency to the -3 dB bandedge of the amplifier operating at 100° C. The shunt-series feedback pair had a maximum variation of -1 dB over the same temperature range from low frequency to the -3 dB bandedge of the amplifier operating at 100° C. The values of the gain and bandwidth at 100° C are listed in Table 4.4 along with the predicted values from Sec. 4.2. The gain variation of the experimental shunt-series cascade is greater than predicted. The ohmic base resistance again accounts for the difference. The gain, including r_x is approximately

$$A_I(0) = \frac{R_f}{R_e + \dfrac{1}{g_{m2}} + \dfrac{r_x}{\beta_{o2}}} \tag{4.17}$$

If the value of 150 ohms is used for r_x, the predicted value of gain at 100° C becomes 27 which agrees with 2 percent of the measured value of 26.4.

The bandwidth variation is 20 percent compared with a predicted variation of 2 percent. The external capacitor used was a ceramic disk capacitor with a negative temperature coefficient. Eqn. (4.15) indicates that a decrease of C_f reduces the real part of the poles of the amplifier

and increases the imaginary part. The positive temperature coefficient of R_f compensates the increase of the imaginary part due to C_f. Since the response at 100° C is not peaked, the net effect is apparently a decrease of the imaginary part equal to or greater than the decrease of the real part. These effects account for the large bandwidth variation.

The experimental behavior of the shunt-series feedback pair is opposite to the increase in gain predicted by the model. Experimentally the gain had a variation of -1 dB over the temperature range from 25° C to 100° C. The biasing scheme of Fig. 4.3(b) was unable to maintain a stable bias point for the output transistor. The dc collector current of the output transistor decreases as the temperature increases. This decrease of dc collector current causes the short-circuit current gain to be much less than that predicted.[24] The decreased collector current can also cause f_t to decrease[24] which, along with the variation of C_f, can account for the bandwidth variation. This stage can be expected to perform as predicted if a suitable bias scheme is used.[23]

4.4 Other two-transistor amplifier stages

Eight transformerless dc connections of two transistors, other than the common-emitter cascade, are possible. Two of these connections are simply a common-base cascade and a common-collector cascade which have only little use as broadband amplifiers. The other six configurations are shown in Fig. 4.10. The input biasing circuitry is not shown in Fig. 4.10. The configurations are to be denoted by E-C for a

common-emitter transistor driving a common-collector transistor as in Fig. 4. 10(a) and similarly for the other configurations. This section evaluates the use of the configurations as composite lowpass, broadband, amplifier stages. These composite stages are particularly suited for integrated circuit applications because of the ease of obtaining additional transistors in an integrated circuit. The intent of this section is to determine if the broadband performance of any of the composite stages is better than a single common-emitter stage.

Broadband performance can be evaluated using either the change of the gain-squared frequency integral or the conventional gain-bandwidth product. The procedure for using the gain-squared frequency integral is similar to the procedure described in Sec. 3. 3. The imbedding network of the reference amplifier, shown in Fig. 4. 4(a) is generalized to include the use of additional transistors. The normalized change of gain-squared frequency integral is given by (D. 3) of App. D. as

$$J_{\Delta}^{N} = \frac{T_A(p_a) - T(p_a)}{T(p_a)} \tag{4.18}$$

where $T(p)$ is the transfer function of the reference amplifier shown in Fig. 3. 1(a), $T_A(p_a)$ is the transfer function of one of the composite stages, and p_a is the pole of $T(-p)$. The evaluation procedure, then, is simply to compute the transfer functions of the composite stages and to compute J_{Δ}^{N} by (4. 18). The GBW product can also be used to evaluate

the broadband performance of the composite stages. The -3 dB bandedge ω_o is computed from the transfer function $T_A(p)$ and multiplied by $T_A(0)$. Generally, it will be convenient to normalize the GBW product of the composite stage by the GBW product of the reference common-emitter stage. Both of these measures of broadband performance are used to evaluate the potential use of the composite stages as broadband, lowpass amplifiers.

The analyses of these configurations are done using an integrated circuit transistor with the following characteristics:

$$\beta_o = 50 \qquad\qquad \omega_t = 10^9 \text{ rad/sec}$$

$$r_x = 100 \, \Omega \qquad\qquad C_\mu = 3 \text{ pF}$$

$$g_m = 0.2 \text{ mho}$$

Each of the amplifiers of Fig. 4.10(a), (b), (c), and (d) contain one common-emitter transistor. The transfer function, i.e. the current or voltage transfer function, is chosen as the one which preserves the low-frequency current or voltage gain of the common-emitter transistor. For example, the common-collector transistor of the E-C stage of Fig. 4.10(a) is capable of current gain, but not voltage gain; therefore, the low-frequency voltage gain of the E-C stage cannot be greater than the voltage gain of the common-emitter stage, but the current gain can be greater than the current gain of the common-emitter stage. Thus, the voltage-gain of the E-C stage is used. The choice of transfer function is

made similarly for the C-E, E-B, and B-E stages. By preserving the low-frequency gain of the reference common-emitter stage, the change of the gain-squared frequency integral and the normalized GBW product reflects entirely the change in the bandwidth of the composite amplifier. Thus, the broadband performance of these composite stages can be easily evaluated. For the C-B and B-C stages of Fig. 4.10(e) and (f), the voltage transfer function is used to evaluate the broadband performance of the C-B stage and current transfer function is used to evaluate the B-C stage. This choice gives the maximum low frequency voltage gain of the input transistor of the C-B stage and the maximum low-frequency current gain of the input transistor of the B-C stage.

The low-frequency gain of the composite stages is designed to be equal to the low-frequency gain of the reference common-emitter stage when possible. The resistor R_I of the composite stage is chosen to satisfy the low-frequency gain requirement. The value of R_I is 350 Ω for the E-C stage, 50 Ω for the C-E stage and 16 k Ω for the B-E stage. The resistor R_I of the C-B stage is chosen to be much larger than $1/g_m$ and is neglected in the analysis. For the B-C stage of Fig. 4.10(f), R_I is chosen as 2.9 k Ω, which is the low-frequency input impedance of the output common-collector stage. A large value of R_I would increase the low-frequency gain, but reduce the bandwidth because of the loading of the common-collector stage. The choice made is a reasonable design choice. The source and load resistors are arbitrarily chosen as the typical

values of $R_s = 10$ k Ω and $R_L = 50$ Ω for the current amplifiers and $R_s = 50$ and $R_L = 300$ for the voltage amplifiers. The computation of the transfer functions can be handled by straightforward analysis techniques.[25]

The results of the investigation are given in Table 4.5. The GBW products which are normalized with respect to the GBW product of the reference amplifier, show that the E-B stage, commonly called the cascode stage, the C-B stage, commonly called the paraphase circuit and the C-E stage are most efficient of the composite stages in achieving a better broadband performance than a common-emitter stage. The change of the gain-squared frequency integral for the C-B stage is negative because the -B stage cannot achieve the same low-frequency gain as its reference common-emitter amplifier. The integral J is a measure of the area of the gain-squared frequency curve and emphasizes the change of the gain of the stage. The bandwidth of the C-B stage is two times greater than the reference amplifier. This stage would be particularly suited for a broadband, integrated amplifier stage which does not require the use of additional RC components to achieve wideband performance.

Of the remaining composite stages (three) Table 4.5 shows that the E-C and B-E stages have little effect on the broadband performance of the common-emitter reference stage. As indicated in Chapter 5, these stages are best used in achieving a low-output impedance or low-input impedance for an amplifier.

The improved broadband performance of the E-B, C-B and C-E

stages can be used to advantage in achieving broadband performance. RC one-port networks can be added as additional components of these composite stages as previously done in Sec. 3.1. In fact, the broadbanding techniques of Sec. 3.3 can be directly applied to the C-E stage and the E-B stage.

As an example of the use of composite stages, a method of improving the broadband effectiveness of the emitter-feedback stage, investigated in Sec. 3.3, is presented. If the time constant, $R_e C_e$, is constrained to to equal to $\dfrac{1}{\omega_t}$, the calculations are greatly simplified. The voltage-transfer function[26] of the emitter-feedback stage, shown in Fig. 4.11(a) is given by

$$T(p) = \frac{\beta_o R_L}{R_s + r_x + r_\pi + \beta_o R_e} \; \frac{1}{(p/p_a + 1)} \qquad (4.20)$$

where

$$\frac{-1}{p_a} = R_{\pi o} \frac{C_\pi}{1 + g_m R_e} + C_\mu \left(1 + \frac{g_m R_L}{1 + g_m R_e} + \frac{R_L}{R_{\pi o}}\right) \qquad (4.21)$$

and

$$R_{\pi o} = \frac{(R_s + r_x)(r_\pi + \beta_o R_e)}{R_s + r_x + r_\pi + \beta_o R_e} \qquad (4.22)$$

The source and load resistors are again specified as 50 Ω and 300 Ω respectively. The transistor is specified by the parameters which were

given earlier in this section. R_c is arbitrarily chosen as 15 Ω. The values of low-frequency gain and bandwidth, calculated from (4.20), are 13 and 7.3×10^7 rad/sec. The broadband effectiveness can be compared to the common-emitter reference amplifier as previously; the results are

$$GBW^N = 0.92$$

$$J_\Delta^N = -0.42$$

Now, consider the E-C stage with series feedback added as shown in Fig. 4.11(b). The base lead of the common-base transistor should be returned to the emitter of the common-emitter transistor if Fig. 4.11(a) is to be a composite stage. However, since the current in this base lead is only $\dfrac{1}{\beta_o}$ of the load current and the current through the feedback network, the grounding of the base lead of the common-base does not effect the performance. As will be seen in Sec. 5.4, the connection of Fig. 4.11(b) leads to an easy bias scheme.

For the same values as above, the voltage transfer function is

$$T(p) = \frac{\alpha_o \beta_o R_L}{R_s + r_x + \beta_o R_e} \frac{1}{(p/p_a + 1)} \tag{4.24}$$

where

$$- \frac{1}{P_a} = R_{\pi o} \frac{C_\pi}{1 + g_m R_e} + C_\mu \left(1 + \frac{1}{1 + g_m R_e} + \frac{1}{g_m R_{\pi o}} \right) \qquad (4.25)$$

and $R_{\pi o}$ is given by (4.22). The value of low-frequency gain and band-width are now 13 and 1.4×10^8 rad/sec. Compared to the common-emitter reference stage, the scalar measures of the broadband effective-ness are

$$GBW^N = 1.8 \qquad (4.26a)$$

$$J_\Delta^N = -0.31 \qquad (4.26b)$$

The GBW^N and J_Δ^N indicate that the use of the composite E-B stage greatly improves the broadband performance of the stage. The band-width of the composite series-feedback stage is two and one-half times the bandwidth of the series-feedback stage. Physically, the common-base transistor reduces the load of the common-emitter transistor from $R_L = 300$ ohms to $R_L = 5$ ohms. This decrease of load reduces the "Miller effect capacitance," $\frac{g_m R_L}{1 + g_m R_e} C_\mu$, by a factor of 60 leading to a greater bandwidth as seen from (4.21) and (4.25).

Similarly, local shunt feedback applied to the common-emitter transistor of these composite stages could result in an improvement of the broadband performance of the stages.

	T = 25° C		T = 100° C	
	Gain	ω_o	Gain	ω_o
Shunt-series Cascade	28.3	11.3 Mc/s	28.0	10.8 Mc/s
Shunt-series Pair	30.2	10.7 Mc/s	31.6	9.3 Mc/s

Table 4.1 The variation with temperature of the low-frequency gain and bandwidth of the shunt-series cascade and shunt-series feedback pair.

Process	Temperature °C	Time and Atmosphere	Sheet Resistance (ohms/square)	Junction Depth (Micron)
1. Initial oxidation	1175	10 min wet O_2 5 min dry N_2		0.4 (Oxide)
2. Isolation predeposit	985	60 min dry N_2 and BI_3	24-26	
3. Isolation drive-in	1175	17 hr. dry N_2 10 min wet O_2 5 min dry N_2		12
4. Base predeposit	950	30 min dry N_2 and BI_3	45-60	
5. Base drive-in	1150	10 min wet O_2 110 min dry N_2	120-200	3.0-3.2
6. Emitter predeposit	950	60 min dry N_2 and P_3N_5	6-8	
7. Emitter drive-in	1100	10 min wet O_2 10 min dry N_2	2.5-3.5	1.5-2.0
8. Aluminum sinter	525	30 min dry N_2		

Table 4.2 Summary of processing steps.

Parameter	Design Value	Value of Experimental Circuit	Range
R_f	1 k Ω	1.46 k Ω	.9 - 1.5 k Ω
R_e	50 Ω	48 Ω	45 - 55 Ω
R_C	1.5 k Ω	2.2 k Ω	-
R_{B1}	3 k Ω	7 k Ω	-
R_{B2}	1.5 k Ω	2 k Ω	-
β_{o1}	100	70	50 - 150
β_{o2}	100	50	50 - 150
f_t	200 Mc/s	160 Mc/s	-
V_z	7 V	7.2 V	6 - 8 V

Table 4.3 The values of the parameters of the integrated realizations.

	Predicted		Measured	
	Gain	ω_o	Gain	ω_o
Cascade	28	10.8 Mc/s	24.6	9.3 Mc/s
Pair	30.8	9.3 Mc/s	26	7.5 Mc/s

Table 4.4 Measured and predicted characteristics of the amplfiers at 100° C.

	Gain	GBW	
Reference common-emitter Stage	$a_I = 48.5$	$GBW^N = 8.45 \times 10^8$	$J_N = 4.1 \times 10^{10}$
	$a_V = 37.5$	$GBW^N = 10.2 \times 10^8$	$J_N = 3.9 \times 10^{10}$
E - C	$a_V = 35.8$	$GBW_N = 0.95$	$J_\delta^N = 0.07$
C - E	$a_V = 37$	$GBW_N = 1.1$	$J_\delta^N = 0.02$
B - E	$a_I = 46.5$	$GBW_N = 0.97$	$J_\delta^N = 0.02$
E - B	$a_I = 47.5$	$GBW_N = 1.1$	$J_\delta^N = 0.06$
C - B	$a_V = 20$	$GBW_N = 1.06$	$J_\delta^N = -0.29$
B - C	$a_I = 25$	$GBW_N = 0.25$	$J_\delta^N = -0.62$

Table 4.5 The broadband performance of the composite amplifier stages.
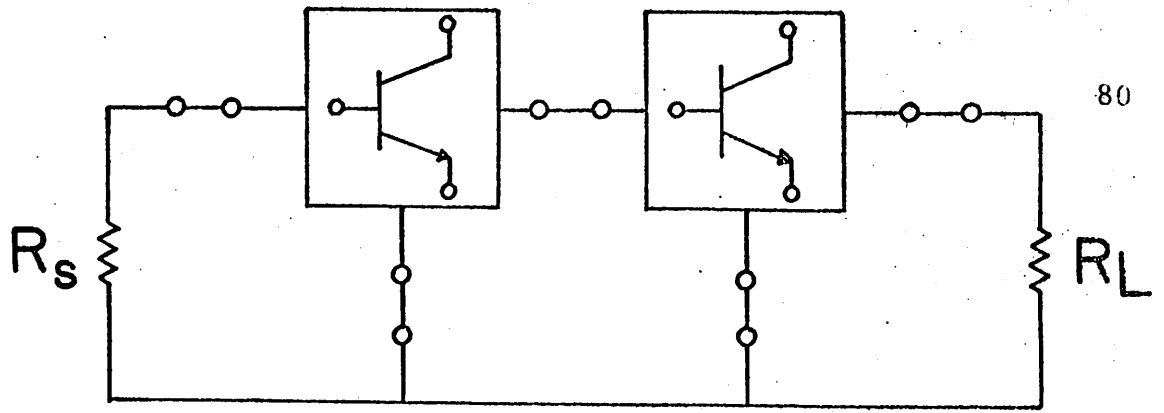
Fig. 4.1 A representation of a two-transistor amplifier stage.
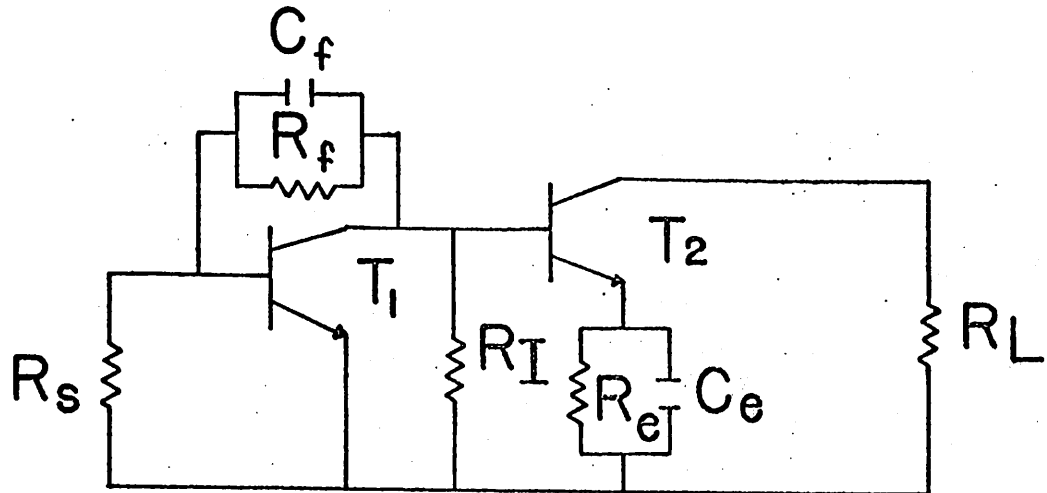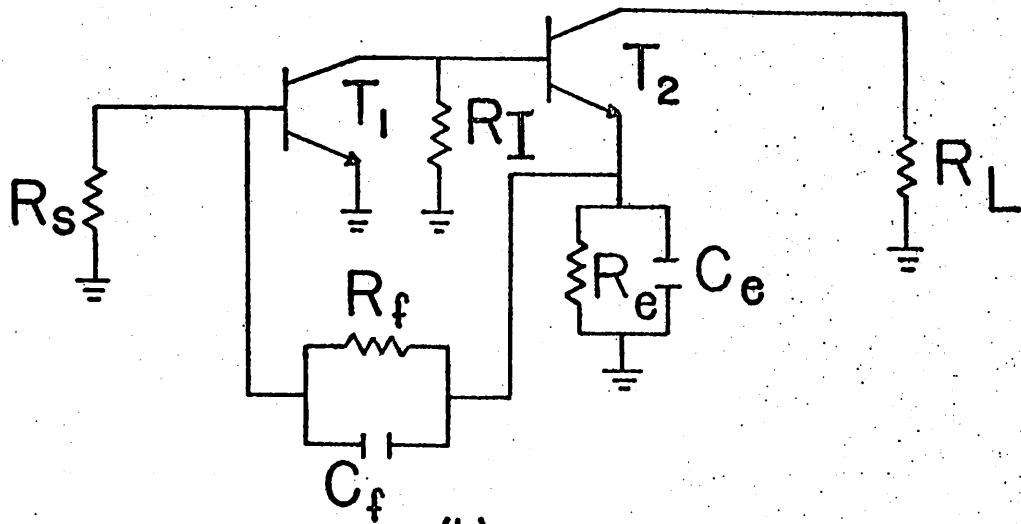
Figure 4.2 (a) Shunt-series cascade; (b) shunt-series feedback pair.
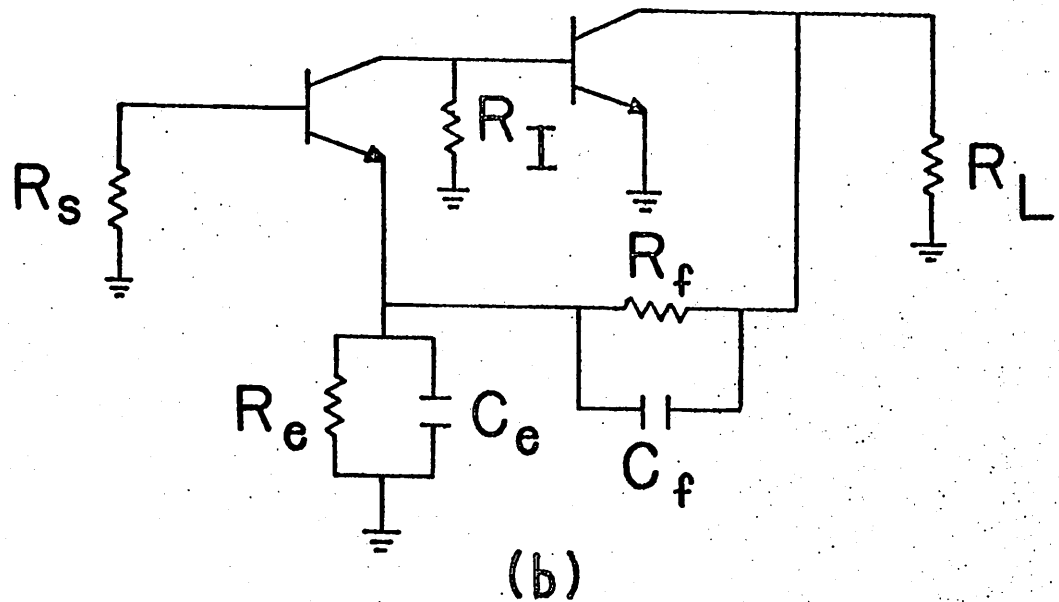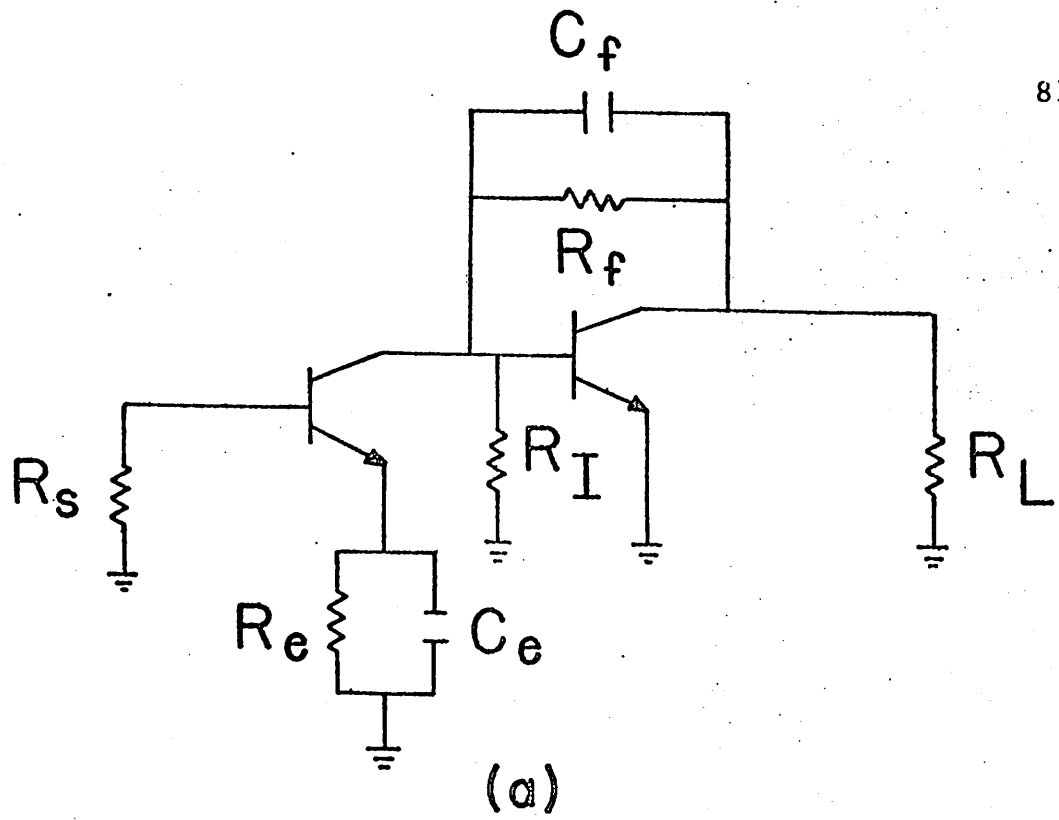
Figure 4. 3 (a) Series-shunt cascade; (b) series-shunt feedback pair.
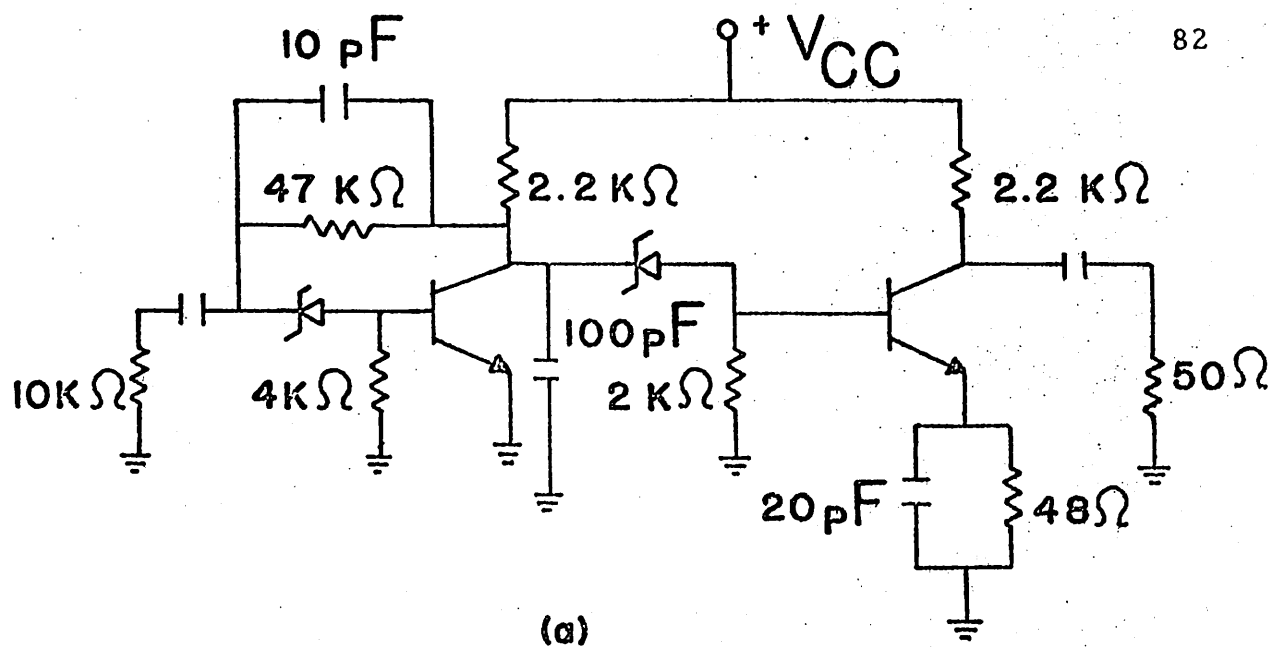
(a)
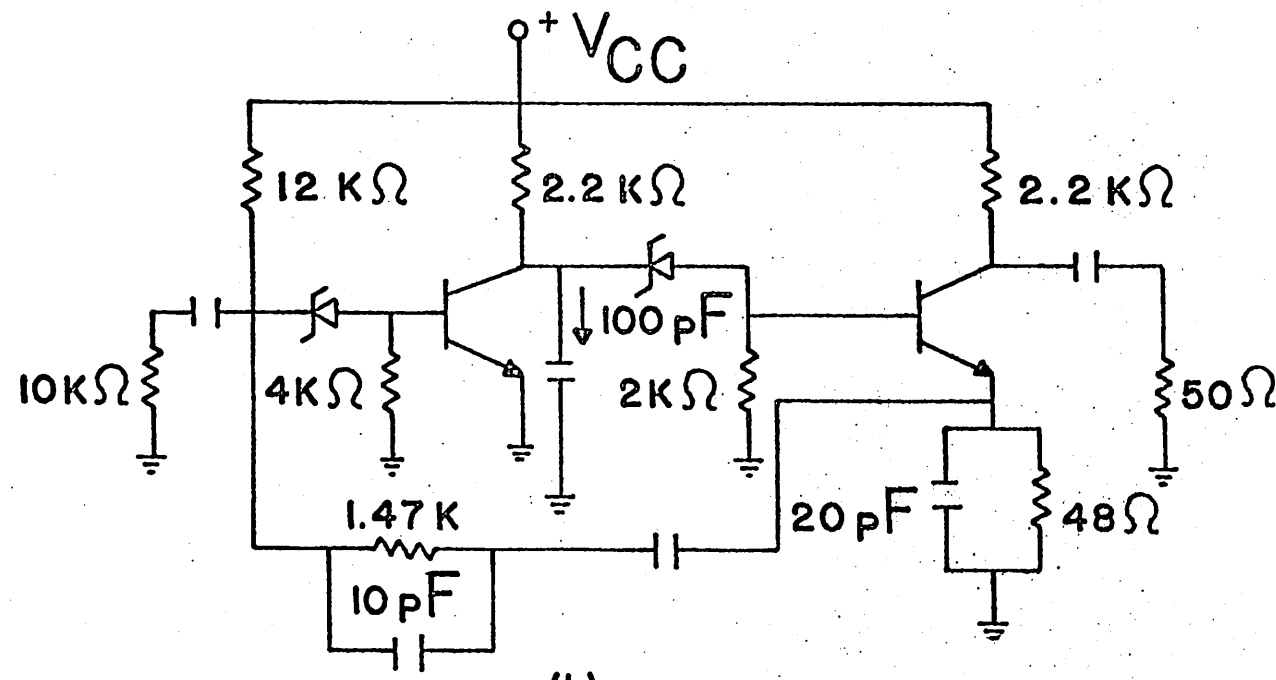
(b)

Figure 4.4 Discrete-component representations of (a) the shunt-series cascade and (b) the shunt-series feedback pair.
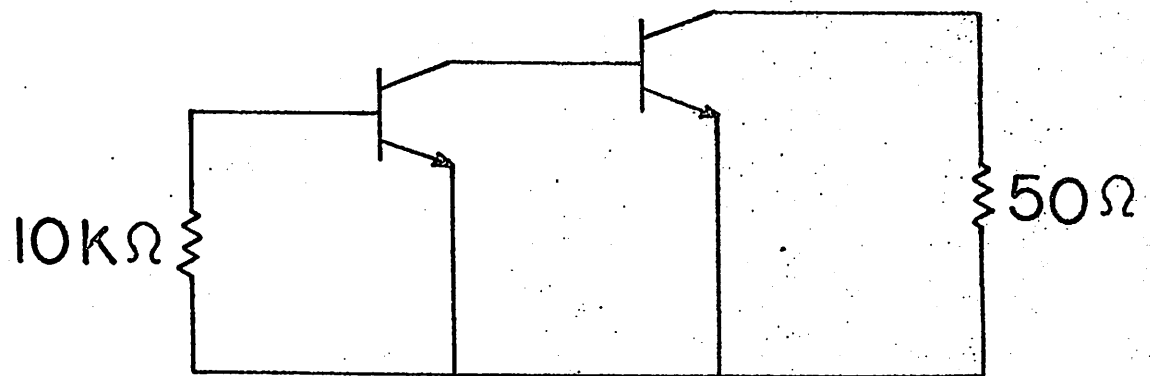
Figure 4. 5 The reference amplifier for the shunt-series cascade and the shunt-series feedback pair.
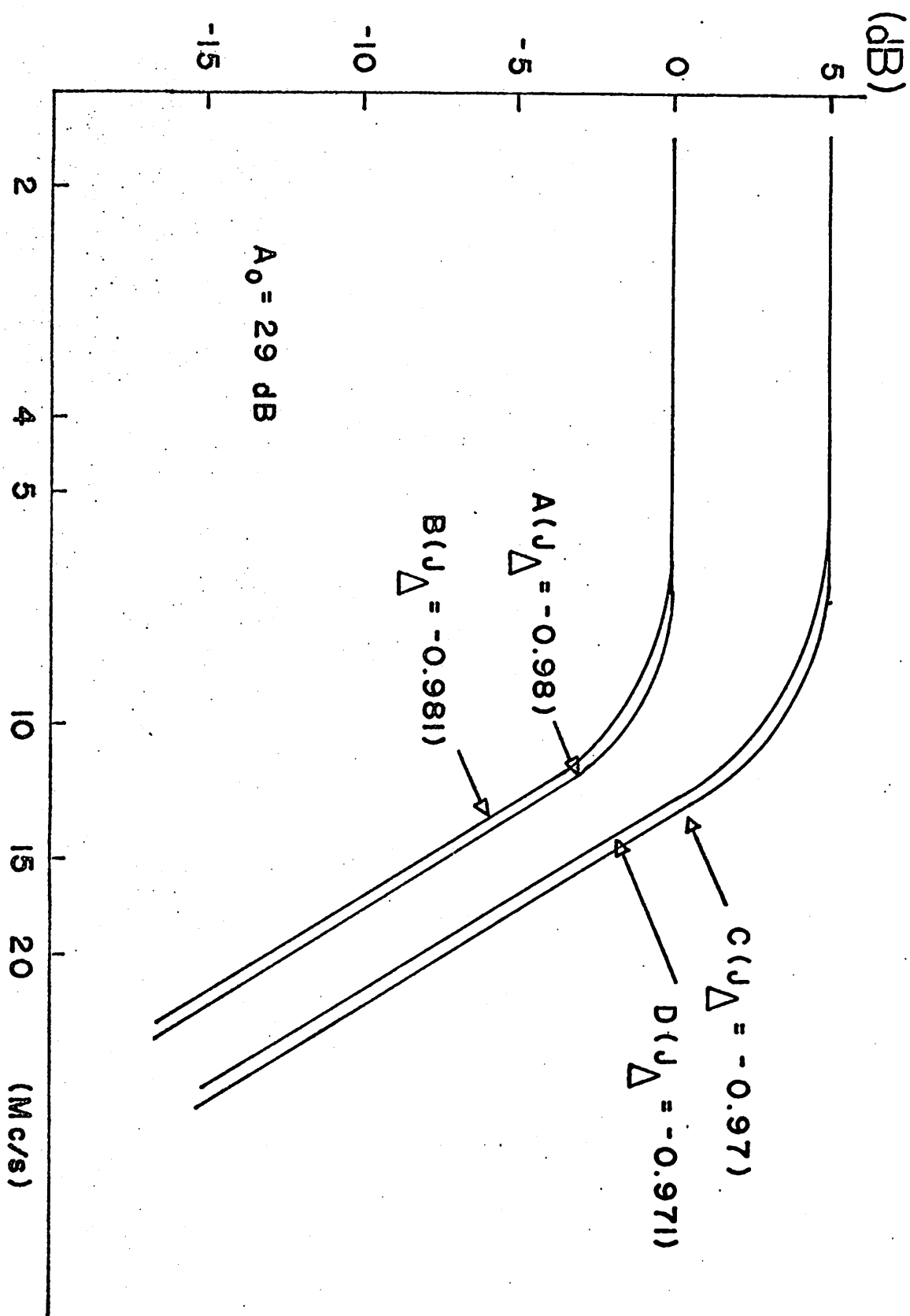
Figure 4.55 Gain-magnitude, frequency curves.
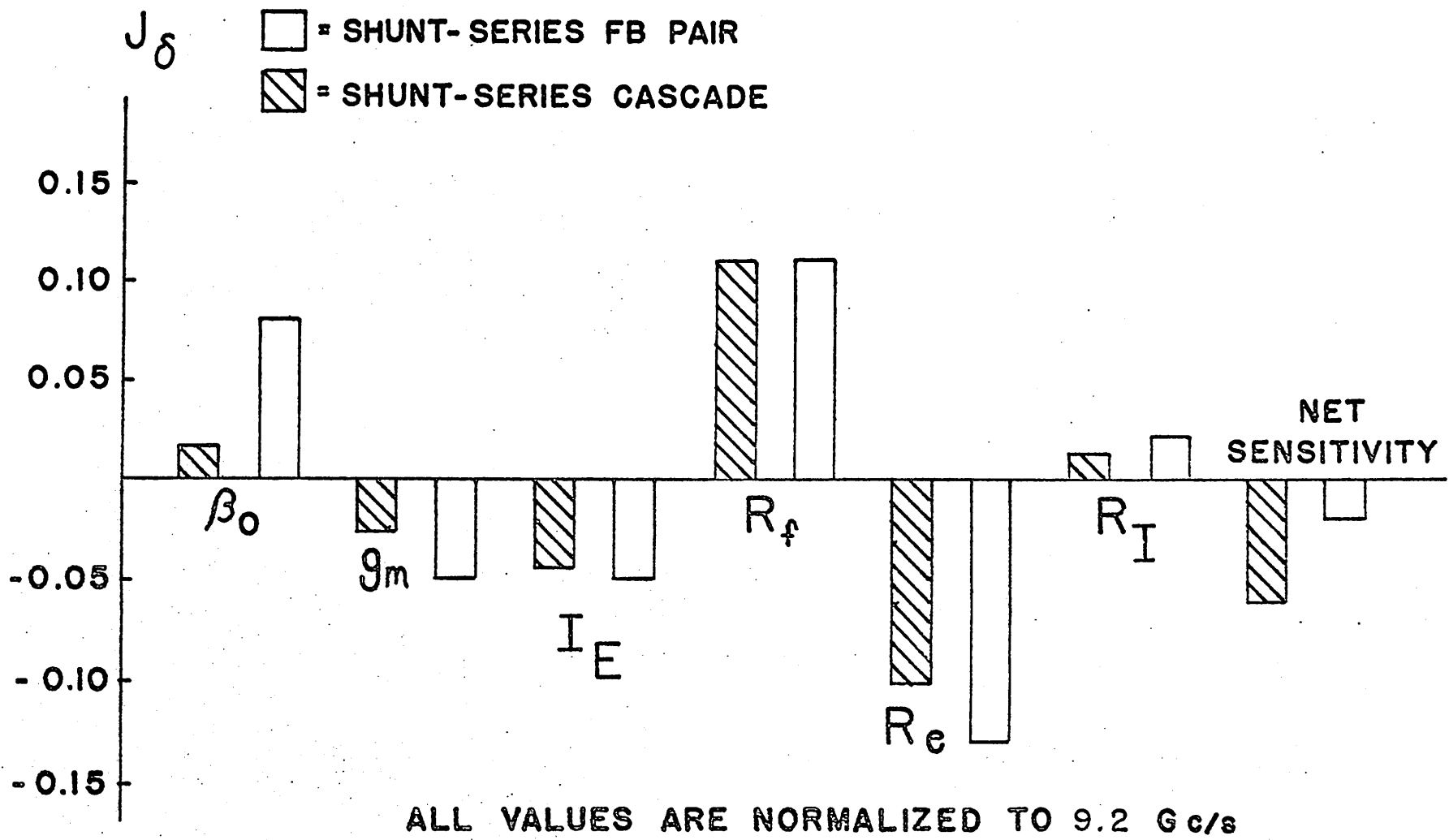
Figure 4.6 The temperature sensitivities of the shunt-series cascade and feedback pair.
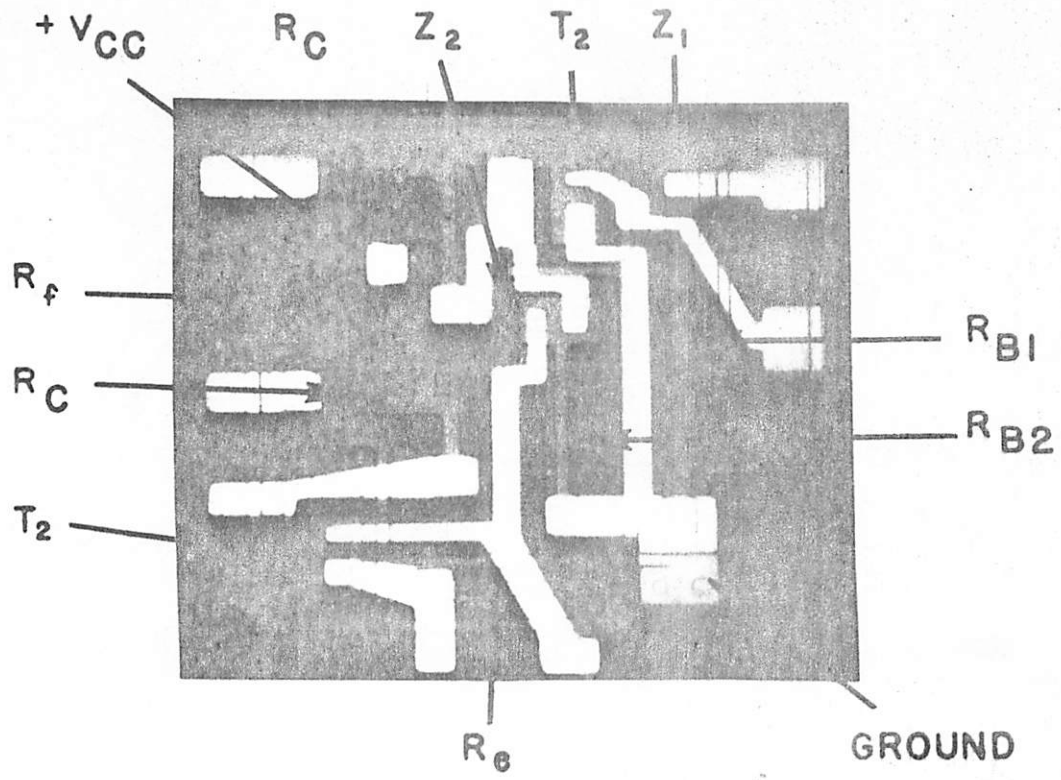
(a)
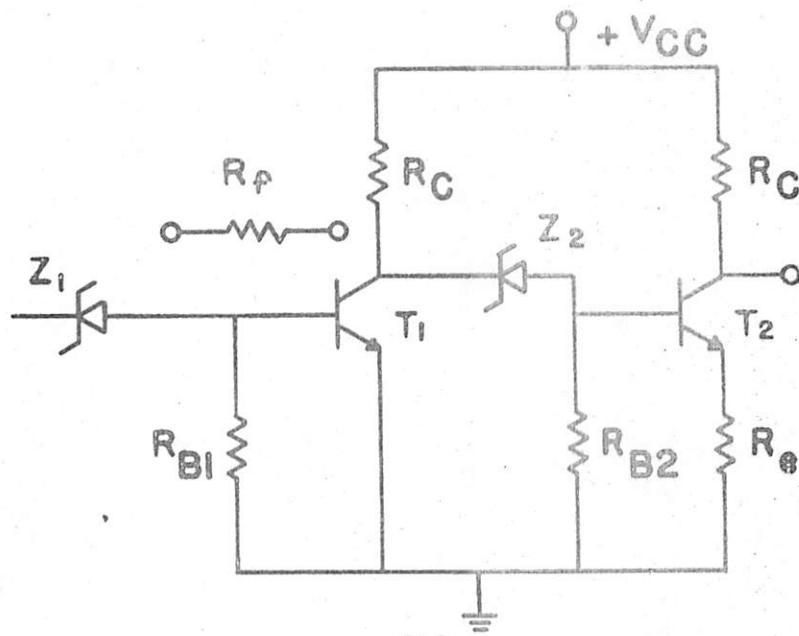
(b)

Figure 4.7 (a) The plan view of the integrated realization of the shunt-series cascade and feedback pair; (b) a discrete-component representation of the integrated realization.
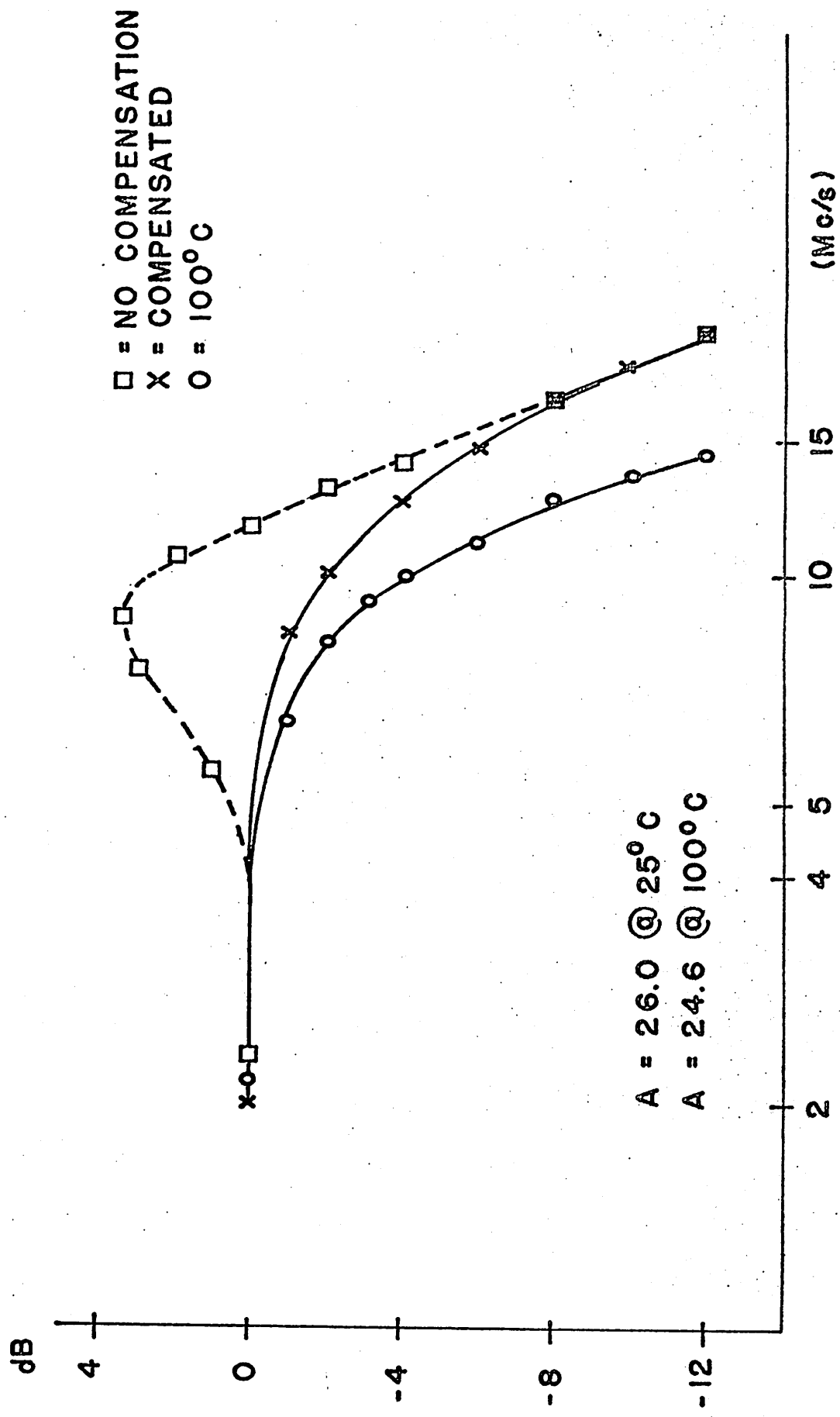
Figure 4.8 The experimental magnitude-frequency response of the shunt-series cascade.

dB

4 —

0 —

-4 —

-8 —

-12 —

□ = NO COMPENSATION
X = COMPENSATED
O = 100° C

(Mc/s)

A = 29 @ 25°C
A = 26 @ 100°C
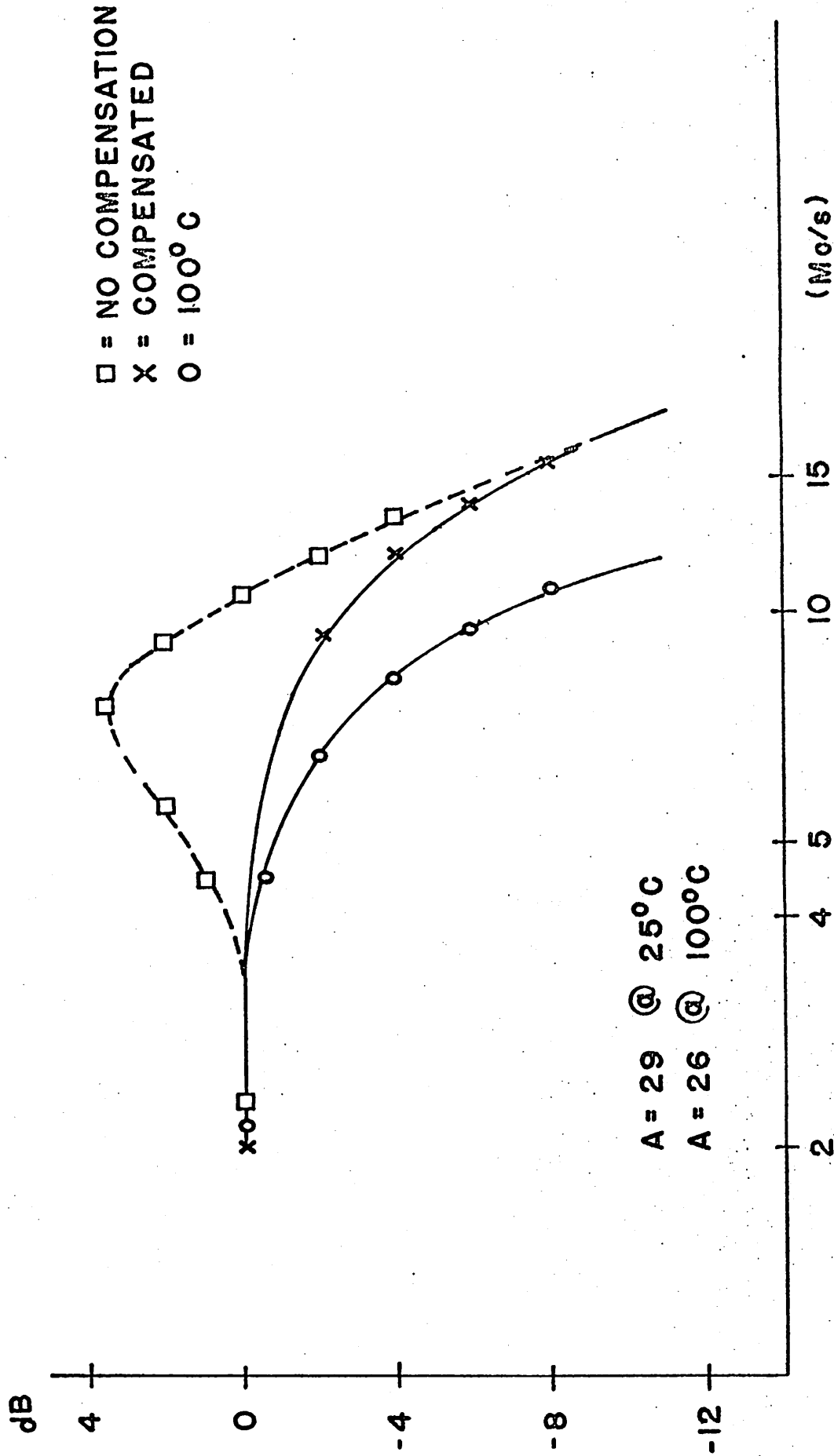
Figure 4.9 The experimental magnitude-frequency response of the shunt-series feedback pair.

(a) E - C

(b) C - E

(c) B - E

(d) E - B

(e) C - B

(f) B - C
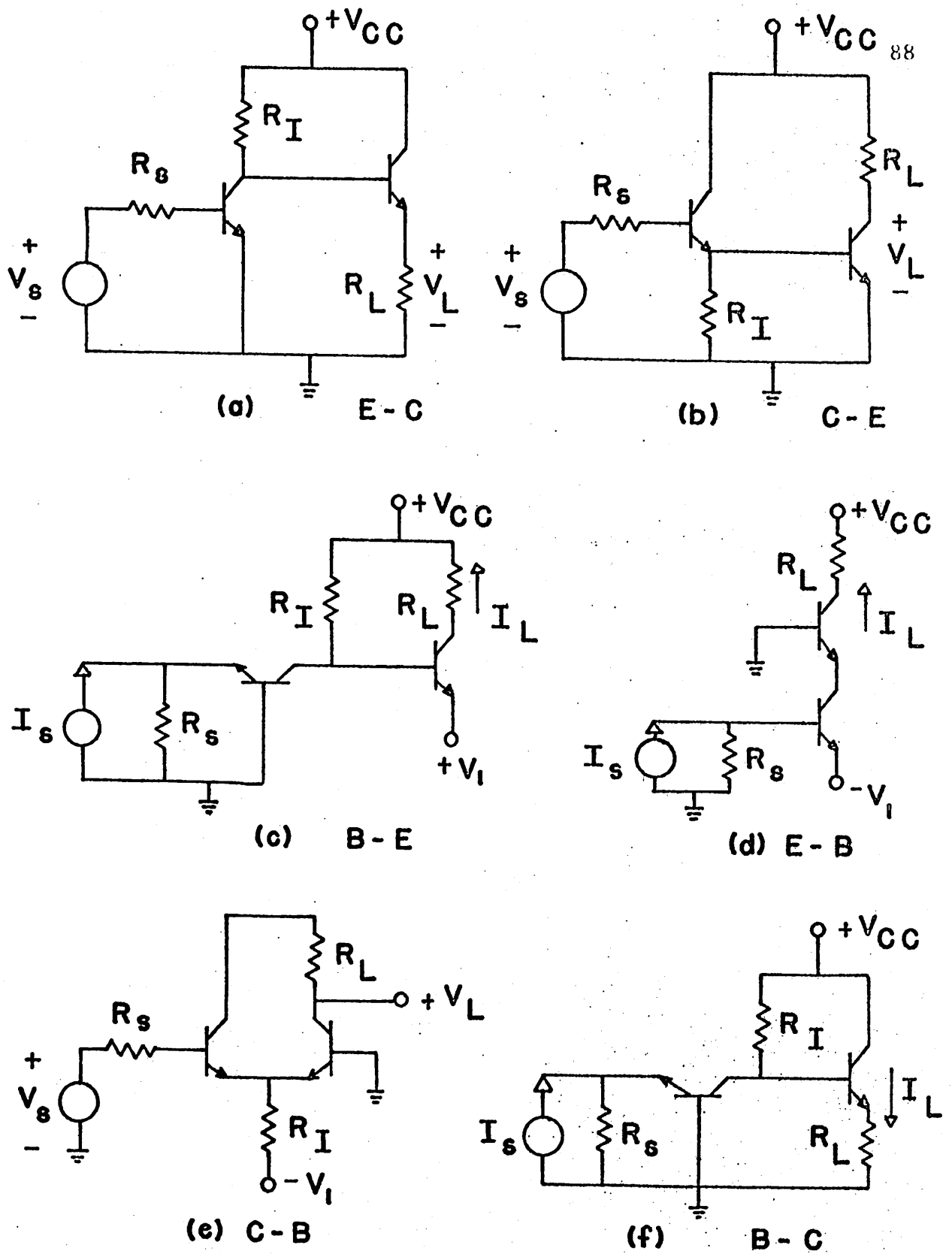
Figure 4.10 Two-transistor amplifiers.
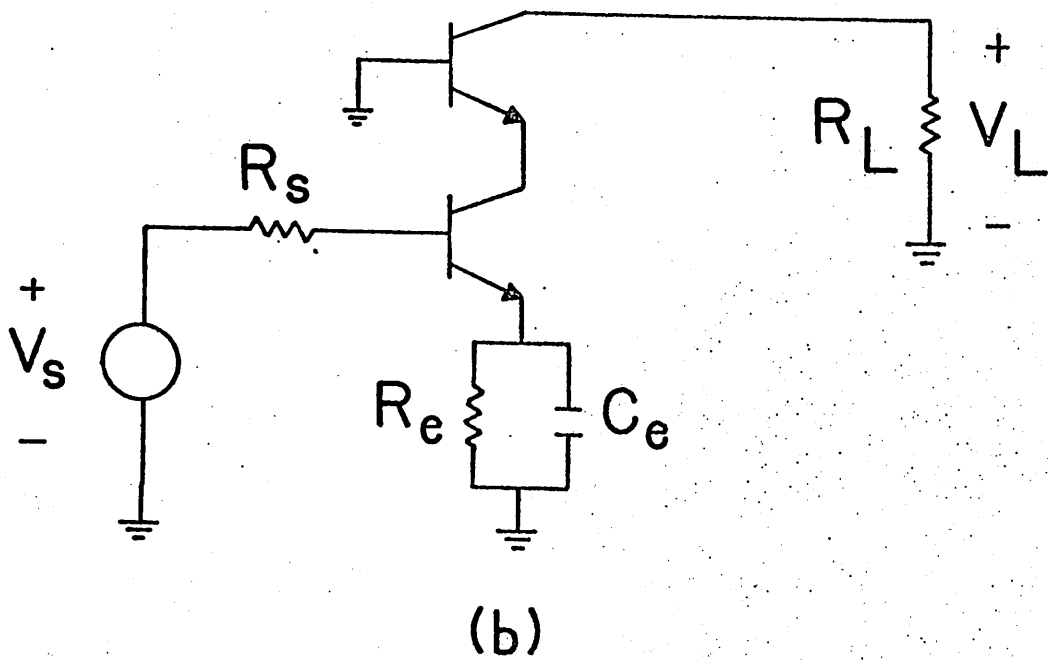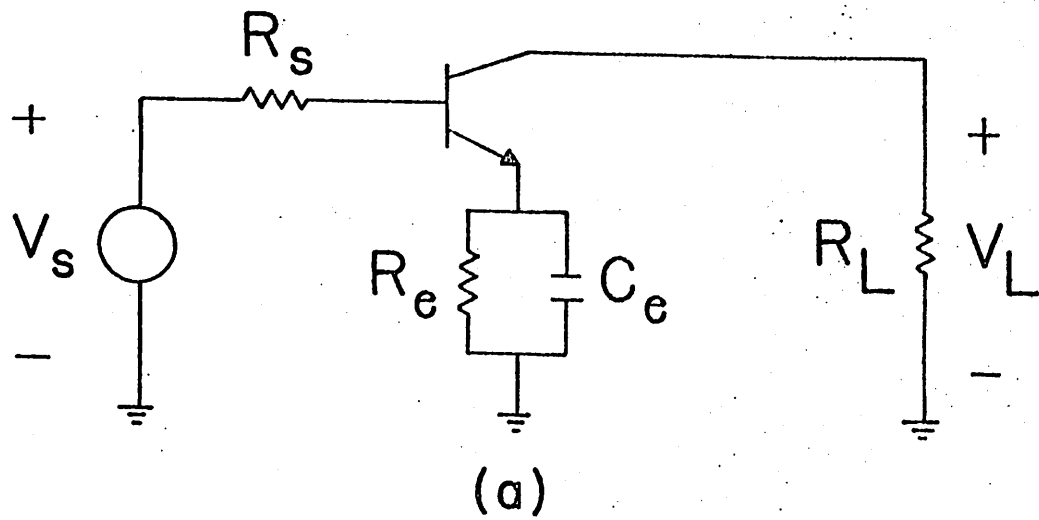
Figure 4.11 (a) A series-feedback, common-emitter stage; (b) an E-C composite stage with series feedback.

5. MULTI-STAGE TRANSISTOR AMPLIFIER

5.1 Introduction

The design of a monolithic, integrated, broadband amplifier can be considered to consist of four steps: the design of the broadband, lowpass amplifier stage; the design of any necessary input or output transistor stages; the design of the biasing and coupling circuitry of the amplifier; the design of the topology of the integrated circuit. The results of this report indicate that these four steps are interrelated. Two scalar measures, the GBW product and the gain-squared frequency integral, have been used to study the relationship of these four steps.

As a measure of broadband effectiveness of the broadband, low-pass amplifier stage, both the GBW product and gain-squared frequency integral were used. The evaluations, using the two single parameter measures, indicate that either is useful in determining the relative broadband performance of different amplifier configurations. The GBW product is usually preferred since the compromise between low-frequency gain and bandwidth is more easily determined.[+] The results obtained from the two measures showed generally a good agreement.

[+]The gain-squared frequency integral, as its name implies, is proportional to the square of the low-frequency gain.

The gain-squared frequency integral also provides a method of obtaining a single-parameter measure of the temperature sensitivity of a broadband, lowpass, amplifier stage. No mathematically tractable measure of temperature sensitivity is obtainable from the GBW product. The experimental studies of the shunt-series cascade and shunt-series feedback pair showed that the gain-squared frequency integral could successfully predict the behavior of these stages with temperature.

The results of the report indicate that feedback is sufficient to desensitize the low-frequency gain of monolithic, integrated amplifiers to changes of temperature. Then, the value of the low-frequency gain can be designed to be approximately the ratio of diffused resistance values. As will be seen, the most insensitivity is obtained when the critical resistors are fabricated from the same diffusion. Generally, the base diffusion is used instead of the emitter diffusion because of its higher resistivity and lower parasitic capacitance. Then, the temperature variation of the low-frequency gain depends upon the matching of the temperature coefficients of the diffused resistors.

The variation of the bandwidth of the feedback amplifiers was shown to be primarily dependent on the temperature coefficients of the diffused resistors. Typically, the bandwidth was found to decrease 10 percent over the temperature range $25^{\circ}C$ to $100^{\circ}C$. For many applications, this variation of the bandwidth will not inhibit the usefulness of the amplifier. Procedures have been developed which control the sensitivity of the poles.[27, 28] The method introduces additional degrees of freedom in the form of additional feedback paths and

forward transmission paths. These degrees of freedom are used to control the sensitivity of the poles to the variations of the active and passive components. The resulting amplifier is more complex in topology than the ones considered and warrants use only if the invariance of the value of the bandwidth of the amplifier is of primary importance.

The gain-squared frequency integral is especially useful for determining the effect on broadband performance of adding additional components, such as input and output stages, to a given amplifier stage. The results of Sec. 4.4 can be used to predict the effect of adding an output or input stage to the basic amplifier stage. For example, the E-C stage was seen to have little effect on the broadband performance of the common-emitter stage, i. e. the low-frequency gain and bandwidth of the E-C were nearly identical to the values of the common-emitter stage. Hence, for the example of Sec. 4.4, the common-collector output stage has no effect on the reference amplifier. As will be demonstrated, similar results apply to more complex amplifiers.

The choice of overall or local feedback can be dictated by the requirements of biasing and coupling the transistors. In particular, the comparison of the shunt-series cascade and the shunt-series feedback pair has shown that the broadband performance and temperature sensitivity of these two stages is not significantly different. The integrated shunt-series cascade, however, is more easily biased than the shunt-series feedback pair. Hence, the preference for local or

overall feedback can be determined by the configuration which yields the most satisfactory biasing of the transistors.

The bias points of the transistors must be temperature invariant to ensure a desensitized response. The temperature sensitivity of the response was shown to depend on the temperature variation of the bias points of the transistors. Although the drift of the bias points could theoretically be used to obtain a lower desensitivity, in practice the design for an invariant bias point is sufficiently difficult in itself.

A one-to-one correspondence between a monolithic, integrated, broadband amplifier and its discrete-component counterpart does not describe the frequency behavior of the integrated amplifier. The difference was found to be the isolation junction capacitance which is necessarily present in a monolithic, integrated amplifier. If this capacitance is modeled by one or more capacitors in the discrete-component amplifier, the frequency performance would be accurately described.

This chapter considers the application of the above design techniques to the design of integrated, multi-stage amplifiers. The detailed evaluation of a multi-stage amplifier, as was done for the simple amplifier stage, is computationally difficult; however, this evaluation need not be done since the study of one and two-transistor amplifier stages has given the necessary insight to make engineering decisions to ensure that the multi-stage amplifier has a broadband, lowpass, temperature-insensitive response.

First, two industrial examples which were developed by Motorola and RCA are used to illustrate the applicability of the design techniques

of the previous chapters. An additional design example is presented
which shows a design method which is suitable for obtaining a broad-
band, temperature-insensitive multi-stage transistor amplifier.

5.2 Integrated feedback triples

Figure 5.1 shows two basic feedback triples which are useful
for obtaining large bandwidth. Feedback amplifiers with more than
three common-emitter transistors are not considered since the high-
frequency phase shift of the transistors normally precludes stable,
wideband operation.

The series-series feedback triple of Fig. 5.1(b) is better suited
for integrated realization than the shunt-shunt feedback triple of
Fig. 5.1(a).[18, 25] The effect of capacitance at the input or output of
the amplifier, always present in integrated circuits, is to increase
the high-frequency phase shift of the loop transmission function of the
shunt-shunt triple; thus, the stability margin of the stage is decreased.
For the series-series feedback triple, Solomon and Wilson[26] indicate
that since the output capacitance is not included in the feedback loop,
it has no effect on the stability margin, and the input capacitance pro-
duces a transmission zero of the loop transmission function which can
be used to improve the stability margin. Further, they indicate that the
series-series feedback triple is more easily biased as an integrated
amplifier than the shunt-shunt feedback triple.

The cascade amplifier of Fig. 5.2, a series-shunt feedback pair
in cascade with an emitter feedback stage, has similar characteristics
to the series-series feedback triple. The topological difference is the

same as the difference between the shunt-series cascade and the shunt-series feedback pair discussed in Sec. 4.2. For the latter, the change of the terminal of the feedback resistor from the emitter to the base of the output transistor was shown to have a negligible effect on the broadband performance and temperature sensitivity. This equivalence allows the series-series triple to be designed as a two stage amplifier. The output emitter-feedback stage loads the series-shunt feedback pair. This load can be approximated by a parallel RC network if 4.3(c) is satisfied. Hence, the frequency behavior is determined by the loaded series-shunt feedback pair.

The analysis of the temperature sensitivity of such a multi-transistor stage can be done using the gain-squared frequency integral. Such an analysis is computationally difficult and is practical only if a computer is used to do the computations. However, the analysis of the temperature sensitivities of Sec. 3.4 and 4.2 can be used to determine the factors which are critical to the design of desensitized, broadband, integrated amplifiers. First, the temperature sensitivities [18, 25] of the series-series triple are given.

The low-frequency voltage gain of the series-series feedback triple is approximately given by

$$A_V(0) = \frac{R_f}{R_{e1}} \frac{R_L}{R_{e2}} \tag{5.1}$$

if R_{e1} and R_{e2} are much smaller than R_f. Thus, the low-frequency gain is given by the ratio of resistors. The integrated realization uses the base diffusion of the transistors to realize all of the resistors

R_f, R_L, R_{c1} and R_{e2}. Ideally, these resistors which have been fabricated simultaneously, have the same temperature dependence and the low-frequency gain is constant with temperature change. The temperature coefficient of the diffused resistor is determined by the sheet resistance.[30] The reported gain variation for a low-frequency gain of 40 dB is reported to be 0.6 percent for a temperature range from $-55^{\circ}C$ to $100^{\circ}C$.[18] The data indicates that the temperature coefficients of the base-diffused resistors are matched to better than ±1 percent, i.e.

$$\frac{T.C._1 - T.C._2}{T.C._1} \leq .01 \tag{5.2}$$

where T.C. is the temperature coefficient of a diffused resistor.

5.3 A cascade of C-B composite stages

An interesting example, which uses the unique properties of integrated circuits, is the cascade amplifier shown in Fig. 5.3.[31] Fig. 5.3 is a discrete-component representation of an integrated, monolithic, cascade of C-B composite stages, which is commercially available. A common-collector transistor is used between the successive C-B stages of the cascade. The function of the common-collector transistor is to provide a high impedance for the preceding C-B stage and a low impedance for the following C-B stage. The C-B stage also provides a dc level shift. The expression for low-frequency gain of a single C-B stage is

$$A_V(0) = \frac{\beta_o R_L}{R_s + 2(r_\pi + r_x)} \tag{5.3}$$

This expression shows that the low output impedance of the common-collector transistor, i. e. the source resistance R_s of the C-B stage, ensures that the low-frequency voltage gain of each C-B stage is high. The high input impedance of the common-collector transistors ensures that load resistance R_L is approximately the collector bias resistor of the common-base transistor of the C-B stage. This load resistance cannot be arbitrarily large since a large value of R_L will cause a small value of the low-frequency gain and bandwidth of the common-collector output transistor.

The low-frequency voltage gain and bandwidth of the cascade of C-B stages are specified as 75 dB and 5 Mc/s.[31] The reported variation of the gain of the cascade -7 percent from -25°C to 100°C. If r_x and R_s are small compared with r_π, the low-frequency gain is approximately

$$A_V(0) = g_m R_L = \frac{qI_C}{kT} R_L \qquad (5.4)$$

Eqn. 5.4 indicates the low-frequency gain decreases as the temperature increases if the bias points are constant with temperature. Hence, the variation of the gain is due primarily to the temperature dependence of the transistors.

5.4 A design example

A typical design example is presented to illustrate the possible methods of using the techniques of the previous sections. The design specifications will be considered to be the following: (1) the source resistance is a terminated 50 Ω coaxial line; the value of the

low-frequency voltage gain should be approximately 20; the value of the -3 dB bandwidth should be greater than 30 Mc/s; the output resistance should be less than 50 Ω .

The E-C composite stage was shown in Sec. 4.4 to have good broadband effectiveness when compared to the common-emitter transistor stage. For this reason, the possibility of using this composite stage will be considered. A simple parallel RC network was introduced in the emitter of the E-C stage in Sec. 4.4 and the low-frequency voltage gain (4.24) is

$$A_V(0) = \frac{\alpha_o \beta_o R_L}{R_s + r_x + r_\pi + \beta_o R_e} \tag{5.5}$$

If the condition

$$\beta_o R_e >> R_s + r_x + r_\pi \tag{5.6}$$

is satisfied, the gain (5.5) is

$$A_V(0) = \alpha_o \frac{R_L}{R_e} \tag{5.7}$$

Eqn. (5.7) indicates that the low-frequency gain can be desensitized to changes of the ambient temperature if R_L and R_e are realized from the same diffusion. The variation of α_o may usually be neglected. Consider the transistor to have the following characteristics:

$$\beta_o = 50 \qquad\qquad C_\mu = 3 \text{ pF}$$
$$r_x = 100 \ \Omega \qquad\qquad \omega_t = 10^9 \text{ rad/sec}$$
$$g_m = 0.2 \text{ mho}$$

If R_c is chosen as 50 Ω , (5.6) is satisfied. For a voltage gain of 20, R_L is specified by (5.7) as 1 kΩ. The bandwidth is then given by (4.25) and is approximately 50 Mc/s. This design will then supply the necessary gain and bandwidth.

The low output resistance can be achieved by using a common-collector output stage. For the values of Fig. 5.4, the low-frequency gain is approximately unity and the output resistance is approximately 20 Ω. The one remaining problem is then the biasing of the amplifier. Fig. 5.4 shows the amplifier with the bias circuitry included. The bias point is controlled by using the circuit of Fig. 3.5.[6] The common-base transistor is biased by returning the base lead to the tapped resistor as shown. As discussed in Sec. 4.4, the current in the base lead is not critical in determining the response of the overall amplifier.

The amplifier will deviate from the predicted performance because of second order effects not included in the above analysis. The collector depletion capacitance of the common base stage contributes a pole of the overall gain function approximately equal to $-1/R_L C_\mu$. The value of this pole is approximately 50 Mc/s. Hence, there will be bandwidth shrinkage; the value will be approximately 32 Mc/s which still satisfies the design goal.

This simple, C-B composite stage could be cascaded with similar stages. Since the low-frequency gain and bandwidth of each C-B stage is insensitive to temperature changes and the bias point of the stage is temperature-invariant, a simple dc voltage level shift, such as a voltage-reference diode would provide, would permit the cascading of these stages. Overall feedback would not be necessary to achieve

an insensitive, broadband amplifier since each stage is temperature insensitive.

5.5   Conclusions

This report has been concerned with the design of integrated, broadband, lowpass amplifiers. Several conclusions can be made from the results of the report which apply equally to any design situation.

The use of scalar measures to evaluate the broadband effectiveness was shown to be a practical method of comparing different amplifier configurations. Of the two scalar measures which were used in this report, the GBW product and the gain-squared frequency integral, the GBW product is usually preferred since the compromise between the low-frequency gain the bandwidth of an amplifier stage is more easily determined; however, the two scalar measures showed a generally good agreement. The gain-squared frequency integral was especially useful to determine the effect on broadband performance of adding additional components, e.g., the input and output stages.

The gain-squared frequency integral provides a mathematically tractable scalar measure which was of particular use in evaluating the temperature sensitivity of an amplifier stage. The results of evaluating the temperature sensitivity of integrated amplifier stages, showed that the use of existing discrete-component feedback amplifier designs can provide a temperature-insensitive, low-frequency gain. The variation of the bandwidth with temperature is dependent on the temperature coefficient of the diffused resistors. For many applications,

the variation, which was typically less than 10 percent, does not inhibit the usefulness of the amplifier stage.

The bias points of the transistors must be temperature invariant to insure a temperature insensitive response. As was shown, the choice of overall or local feedback can be dictated by this requirement. The difference in the broadband effectiveness and temperature sensitivity between local and overall feedback stages was shown to be insignificant. Hence, the design of a suitable bias and coupling circuit for the integrated amplifier can often dictate the topology of the feedback loops.

The ease of obtaining additional transistors in an integrated circuit make the use of the composite-transistor stages particularly suited for broadband, lowpass, integrated amplifiers. A simple design example of a E-C composite stage, the cascode stage, showed that a broadband, lowpass, insensitive, amplifier stage could be achieved which gave better broadband performance than a similar single-transistor stage. These composite stages provide the attractive possibility of obtaining wideband performance from amplifier stages which use relatively simple broadbanding techniques.

The design techniques, which were presented in this report, were shown to have practical importance in the design of multi-stage transistor amplifiers. Three examples showed that the results, which were obtained from the study of simple amplifier stages, could be successfully applied to the design of multi-stage transistor amplifiers to achieve a broadband, temperature-insensitive response.
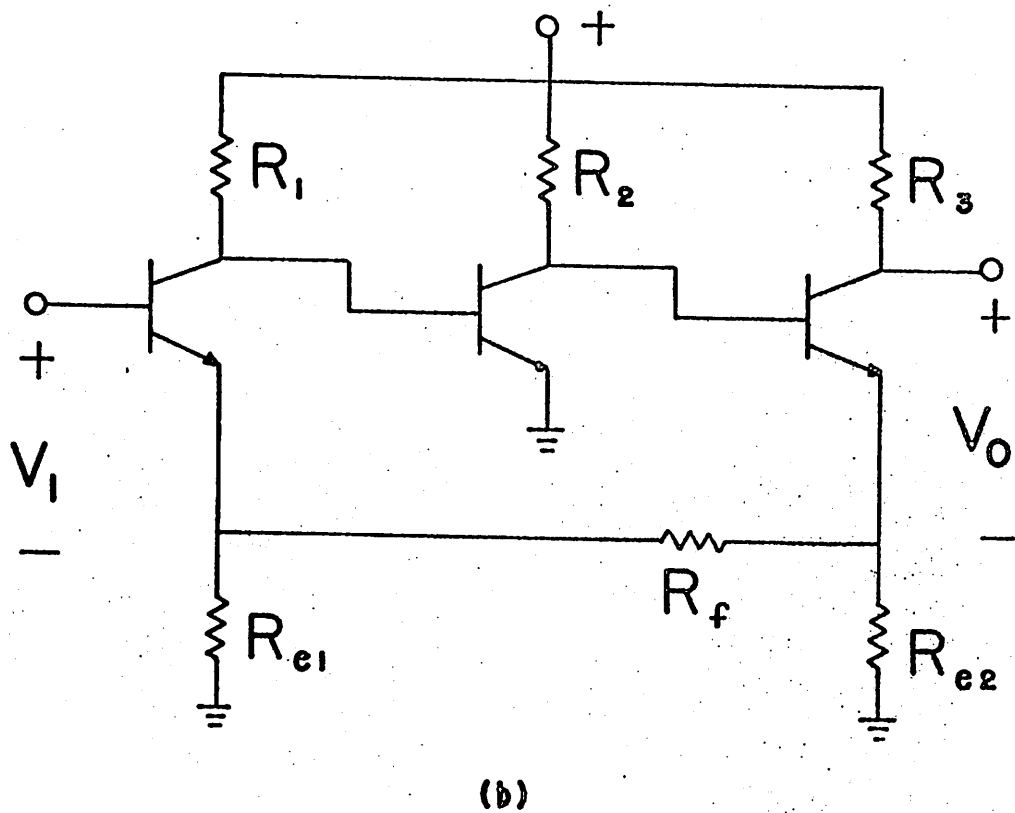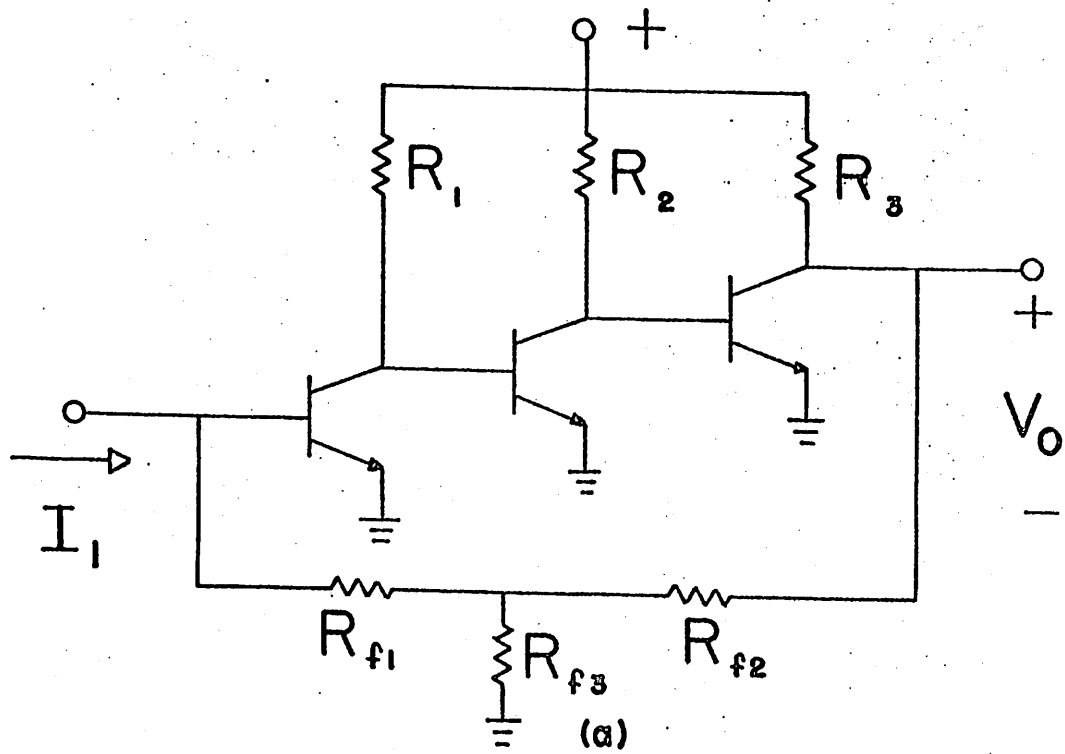
Figure 5.1 (a) Shunt-shunt feedback triple; (b) series-series feedback triple.
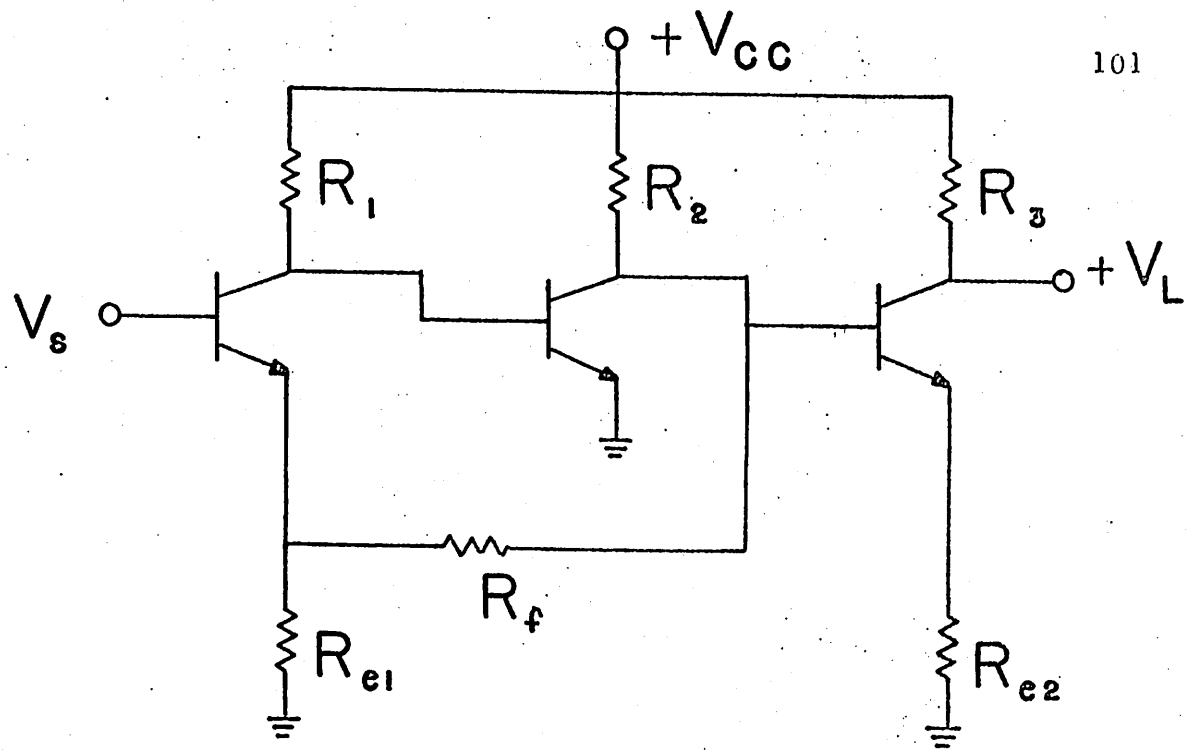
Figure 5.2 An equivalent representation of the series-series triple.
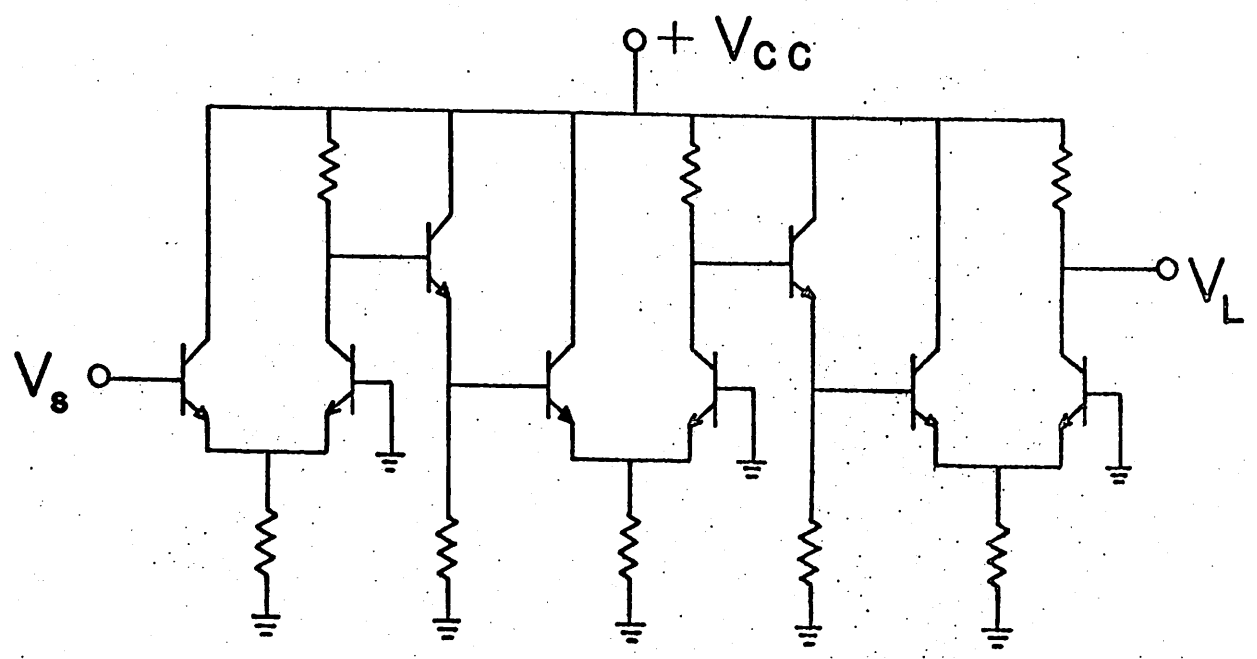
Figure 5.3 A cascade of composite C-B stages.
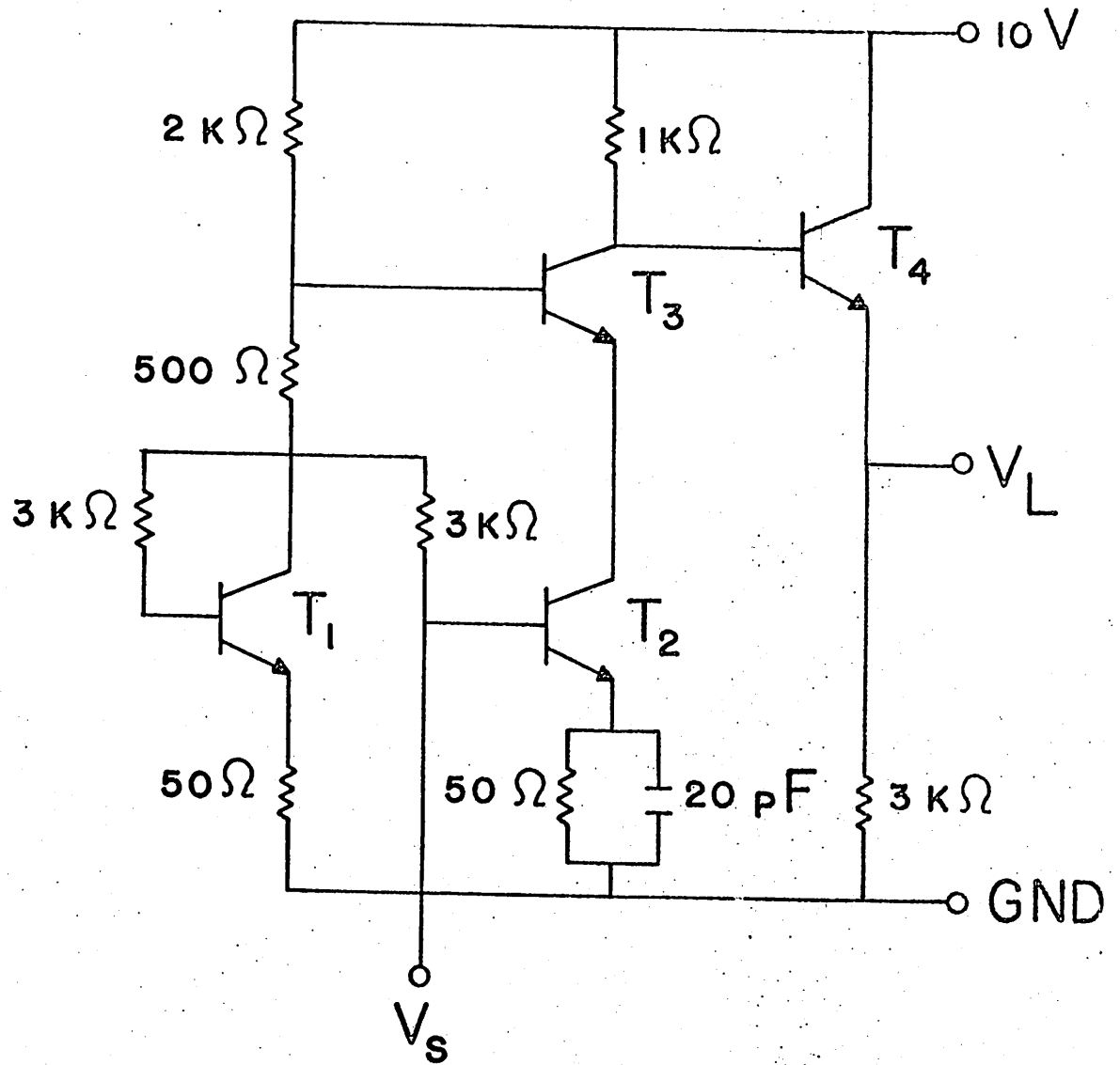
Figure 5.4 A simple E-C composite broadband amplifier stage.

APPENDIX A

THE FINITE GAIN-SQUARED FREQUENCY INTEGRAL

The gain-squared frequency integral can be modified to evaluate

only a finite frequency interval by the use of weighting functions $W(j\omega)$

as indicated in (A. 1). [32]

$$J = \frac{1}{2} \int_{-\infty}^{\infty} W(j\omega) \; T(j\omega) \; T(-j\omega) \; d\omega \qquad \text{(A. 1)}$$

One appropriate weighting function is

$$W(j\omega) = \sqrt{1 - (\frac{\omega}{\omega_o})^2} - j\omega \qquad \text{(A. 2)}$$

$W(j\omega)$ is a multi-valued function of ω. For the integrand to be positive

real

$$\sqrt{1 - (\frac{\omega}{\omega_o})^2} = \begin{cases} -j \left| \sqrt{1 - (\frac{\omega}{\omega_o})^2} \right| & \omega < -\omega_o \\ \sqrt{1 - (\frac{\omega}{\omega_o})^2} & -\omega_o \le \omega \le \omega_o \\ +j \left| \sqrt{1 - (\frac{\omega}{\omega_o})^2} \right| & \omega > \omega_o \end{cases} \qquad \text{(A. 3)}$$

Hence, the quantity $\sqrt{1 - (\frac{\omega}{\omega_o})^2}$ is an odd function for $|\omega| > \omega_o$ and an even

function for $|\omega| < \omega_o$. The odd component of the integrand of (A. 1) must

vanish. Then (A. 1) is simply

$$J = \frac{1}{2} \int_{-\omega_0}^{\omega_0} \sqrt{1 - \left(\frac{\omega}{\omega_0}\right)^2} \; T(j\omega) \; T(-j\omega) \; d\omega \qquad \text{(A. 4)}$$

If the same contour of integration is used as in Chapter 2, (A. 4) can be evaluated by the Cauchy integral formula as

$$J = -\pi \sum_{k=1}^{m} \left\{ \sqrt{1 + \left(\frac{p_k}{\omega_0}\right)^2} - \frac{p_k}{\omega_0} \right\} T(p_k) \; \text{Res} \left[T(p), \; r_k \right] \qquad \text{(A. 5)}$$

The terms of (A. 5) are defined as in Chapter 2. A similar procedure can be used to calculate the variation of the finite gain-squared frequency integral. The finite gain-squared frequency integral can be used as a scalar measure to evaluate the performance of broadband, lowpass amplifiers (see Sec. 2. 1).

APPENDIX B

THE dc BIAS POINT CONSTANCY OF A CASCADED AMPLIFIER USING VOLTAGE-REFERENCE DIODES

The dc bias point constancy of an interstage of an infinite cascade of identical stages can be computed by considering the cascaded amplifier of Fig. B.1. The equations describing the dc bias point are

$$V_{CC} = R_C I_E + (R_C + R_L) I_L + V_Z \qquad \text{(B.1)}$$

$$R_L I_L = V_{BE} + I_E R_E \qquad \text{(B.2)}$$

If the supply voltage is constant, the variation of (B.1) and (B.2) gives

$$R_C \Delta I_E + (R_C + R_L) \Delta I_L + \Delta V_Z + \Delta(I_E + I_L) + \Delta R_L I_L = 0 \qquad \text{(B.3)}$$

and

$$R_L \Delta I_L + I_L \Delta R_L = \Delta V_{BE} + R_E \Delta I_E + \Delta R_E I_E \qquad \text{(B.4)}$$

The resistors R_L and R_C are fabricated from the same base diffusion and ideally have identical temperature coefficients. Hence, Eqns. (B.2) and (B.3) and (B.4) can be combined using the fact that $\dfrac{\Delta R_C}{R_C} = \dfrac{\Delta R_L}{R_L}$ to give

$$\Delta I_E = \frac{-1}{R_k}\left[\Delta V_Z + \Delta V_{BE}(1 + \frac{R_C}{R_L})\right] - \frac{I_E}{R_k}\left[\Delta R_C + \Delta R_E(1 + \frac{R_C}{R_L})\right] \quad (B.5)$$

where

$$R_k = R_C(1 + \frac{R_E}{R_L}) + R_E \quad (B.6)$$

To realize the small resistance value of R_E the emitter diffusion is used thus dictating that

$$\left|\frac{\Delta R_E}{R_E}\right| << \left|\frac{\Delta R_C}{R_C}\right| \quad (B.7)$$

Then, (B.5) can be written as

$$\Delta I_E = \frac{-1}{R_k}\left[\Delta V_Z + \Delta V_{BE}(1 + \frac{R_C}{R_L})\right] - \frac{I_E}{R_k}\Delta R_C \quad (B.8)$$

The changes with temperature of ΔV_Z and ΔV_{BE} are opposite in sign.[33] For a low voltage-reference diode, the temperature coefficient of the base emitter junction makes the first term of (B.8) positive (the temperature coefficient of a forward biased diode is negative). The second term of (B.8) always gives a negative contribution to the change in emitter current since the temperature coefficient of base diffused resistors is positive. The second term is a linear function of I_E; consequently, the net change in emitter current can be made zero by selecting the optimum bias current I_E.

For a finite cascade of identical stages it is necessary to stabilize the current of the first stage. Overall dc feedback, such as shown in Fig. 3.5 for a three stage amplifier, could provide the necessary constant bias point for the first stage.

The shunt-feedback stage can use a similar bias and coupling scheme as the series-feedback scheme. The coupling scheme using the voltage reference diode in a cascade of identical stages is shown in Fig. B. 2. For all stages fabricated on the same wafer, the corresponding components are identical. Each collector is at the same dc voltage, namely $V_Z +$ V_{BE}. Thus, no dc current flows through the resistor R_f and (B. 1) – (B. 8) hold with $R_E = 0$; the change in emitter current is then

$$\Delta I_E = \frac{-1}{R_C} \left[(\Delta V_Z + \Delta V_{BE} (1 + \frac{R_C}{R_B}) \right] - \frac{\Delta R_E}{R_E} I_E \qquad \text{(B. 9)}$$

Eqn. (B. 9) is of the same form as (B. 8); consequently, the bias current I_E can again be constant with temperature.
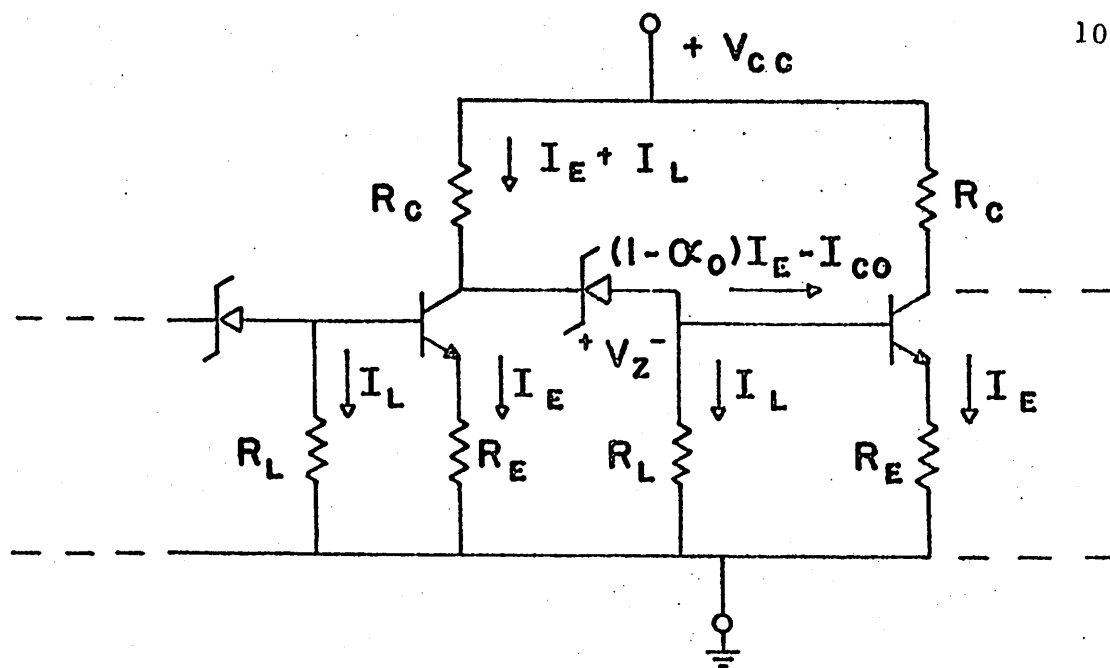
Figure B. 1 A cascade of emitter-feedback stages.
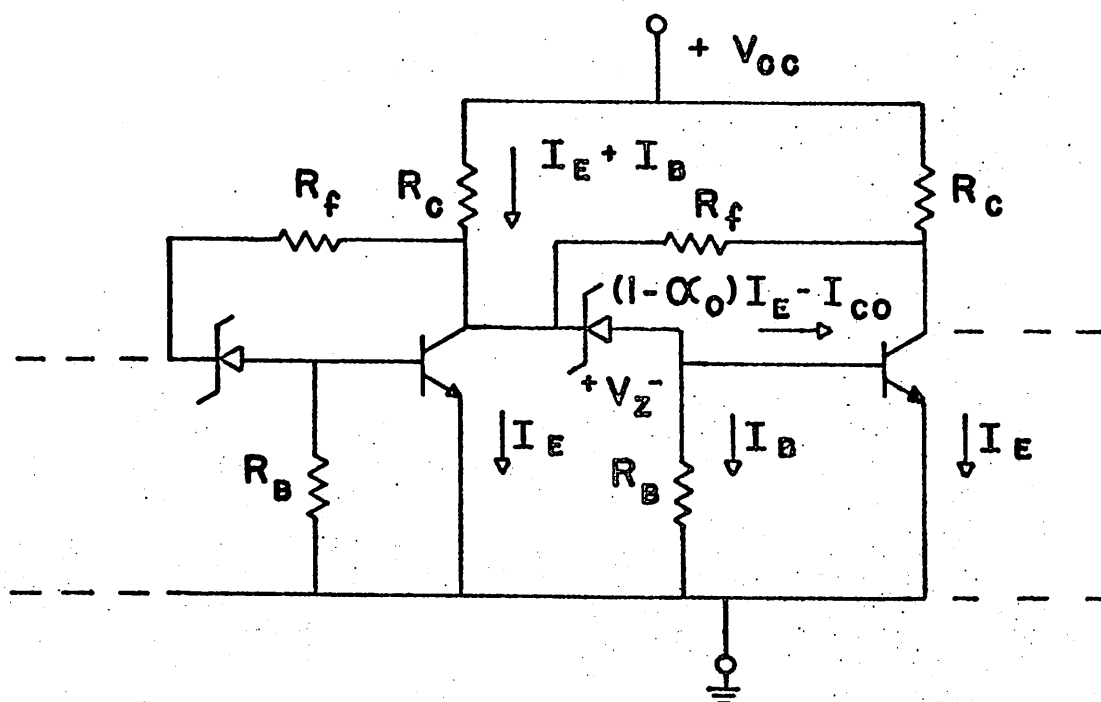
Figure B. 2 A cascade of shunt-feedback stages.

APPENDIX C

THE REQUIRED COMPLEXITY OF RC ONE-PORT NETWORKS

The imbedding of a single transistor in RC one-port networks of greater complexity than a single time constant results in no significant advantage in the gain-squared frequency integral. This result is easily verified by considering a simple example. If the amplifier of Fig. 3.2(a) is used, (2.16) gives

$$J_\Delta = -\pi \frac{\beta_o^2 R_L^2}{(R_s' + r_\pi)^2} \omega_a \frac{\beta_o Z_a(\omega_a)}{2(R_s' + \beta_o Z_a(\omega_a))} \tag{C.1}$$

where

$$Z_a(p) = \sum_{k=1}^{n} \frac{R_k}{1 + pR_k C_k} \tag{C.2}$$

and $R_s' = R_s + r_x$. ω_a is the dominant pole of the reference transfer function $T(p)$. Eqn. (C.1) is obtained assuming

$$\beta_o >> 1$$

The change of the gain-squared frequency integral (C.1) depends only upon the value of $Z_a(p)$ evaluated at $p = \omega_a$; consequently, any $Z_a(\omega_a)$ of arbitrary complexity gives the same resulting change of the gain-squared

frequency integral. Additional complexity affects only the response shape. The simplest MFM response requires only a single time constant for Z_a;[4] hence, no advantage accrues from greater complexity in this case.

If the integral J_Δ is computed for the other configuration of Fig. 3.2, the value of J_Δ depends only on the values of the impedances of the imbedding network evaluated at ω_a. Consequently, increased complexity of the impedances contributes only to the shape of the response and does not affect the broadband effectiveness of the amplifier

APPENDIX D

THE USE OF THE GAIN-SQUARED FREQUENCY INTEGRAL FOR THE EVALUATION OF BROADBAND PERFORMANCE

This appendix gives an example of the procedure, outlined in Sec. 2. 3, of evaluating the broadband performance of an RC imbedding network. The series-feedback amplifier of Fig. 3. 7(a) is used to indicate the evaluation procedure. The reference transfer function, calculated for the values of the reference amplifier of Fig. 3. 7(b) is

$$T(p) = -\frac{25.6}{p/3.6 \times 10^6 + 1} \tag{D.1}$$

Since the transfer function of the reference amplifier is described by a dominant pole, the pole of $T(-p)$ is simply $p_a = 3.6 \times 10^6$ rad/sec. The altered transfer function $T_A(p)$ is simply (3. 1).

$$T_A(p) = 4.6 \frac{p(2.5 \times 10^{-8}) + 1}{(1.1 \times 10^{-14})p^2 + (1.8 \times 10^{-6})p + 1} \tag{D.2}$$

The change in the gain-squared frequency integral can be evaluated by using (2. 16). It is convenient to normalize (2. 21) by the gain-squared frequency integral (2. 11) of the reference amplifier, giving for this example

$$J_\Delta^N = \frac{T_\Delta(p_a)}{T(p_a)} \tag{D.3}$$

and T_Λ is found by subtracting (D. 1) from (D. 2). The second term of (2. 21) has been ignored since (2. 22) is satisfied for this case. Eqn. (D. 3) can then be calculated from the values of (D. 1) and (D. 2) for $p = p_a$. The normalized change in the gain-squared frequency integral is found to be

$$J_\Delta^N = -0.72 \qquad (D. 4)$$

As a second example of the evaluation of the broadband performance, the shunt-series cascade is used. The appropriate transfer function, calculated from the reference amplifier shown in Fig. 4. 5, is

$$T(p) = \frac{2.68 \times 10^3}{(p/.066 + 1)(p/0.94 + 1)} \qquad (D. 5)$$

where the frequency variable is normalized to 1.42×10^8 rad/sec. The altered transfer function is given by (5. 1) and is

$$T_A(p) = \frac{28.3}{1 + 2.68p + 4.05p^2} \qquad (D. 6)$$

The integral (2. 21) is used to evaluate the broadband performance and is normalized by the gain-squared frequency integral (2. 11) of the reference amplifier

$$J = \frac{\pi}{2} a_o^2 \frac{P_1 P_2}{P_1 + P_2} \qquad (D. 7)$$

where a_o is the low-frequency gain and p_1 and p_2 are the poles of $T(-p)$.

Thus, if (2.21) is normalized by (D.7), the result is

$$J_\Delta^N = \frac{2}{a_o} \frac{p_1 + p_2}{p_2 - p_1} \left[T_\Delta (p_1) - T_\Delta (p_2) \right] \qquad (D.8)$$

If (D.8) is evaluated the normalized change in the gain-squared frequency integral is

$$J_\Delta^N = -0.98 \qquad (D.9)$$

APPENDIX E

THE EQUIVALENCE OF THE SERIES-SHUNT CASCADE
AND THE SERIES-SHUNT FEEDBACK PAIR

The series-shunt cascade and the shunt-series cascade can be shown to have similar broadband performance. The low-frequency voltage gain of the series-shunt cascade of Fig. 4.3(a) can be shown to be given by

$$\frac{V_L}{V_s}(0) = \left(\frac{1}{R_e + \frac{1}{g_{m1}} + \frac{r_{x1} + R_s}{\beta_{o1}}} \right) \left(\frac{\beta_{o2} R_L}{(\frac{R_L}{R_f} + 1)(\frac{r_{x2} + r_{\pi2}}{R_p} + 1) + \beta_{o2}\frac{R_L}{R_f}} \right)$$

$$\text{(E. 1)}$$

where

$$R_p = \frac{R_I(r_{x2} + r_{\pi2})}{R_I + r_{x2} + r_{\pi2}} \qquad \text{(E. 2)}$$

The shunt-series feedback pair of Fig. 4.3(b) has a low-frequency voltage gain given by

$$\text{(E. 3)}$$

$$\frac{V_L}{V_s}(0) = \frac{\beta_{o2} R_L}{\left(R_e + \frac{1}{g_{m1}} + \frac{r_{x1} + R_s}{\beta_{o1}} \right) \left(1 + \frac{r_{x2} + r_{\pi2}}{R_I} \right) \left(1 + \frac{R_L}{R_e + R_e} \right) + \frac{\beta_{o2} R_L R_e}{R_e + R_f}}$$

For a typical design of these amplifier stages, it is reasonable to assume that

$$R_e >> \frac{1}{g_{m1}} , \quad \frac{r_{x2} + R_s}{\beta_{o2}} \tag{E.4a}$$

$$r_{x2} + r_{\pi2} >> R_p, R_f \tag{E.4b}$$

$$\beta_o >> 1 \tag{E.4c}$$

Then, the low-frequency gain (E. 1) is given by

$$\frac{V_L}{V_s}(0) = \frac{R_f}{R_e} \frac{1}{(1 + \frac{R_f}{R_L})} \tag{E.5}$$

and (E. 3) is given by

$$\frac{V_L}{V_s}(0) = \frac{R_f + R_e}{R_e} \frac{1}{(1 + \frac{R_f + R_e}{R_L})} \tag{E.6}$$

The low-frequency voltage gains are identical if $R_f >> R_e$. Even though the equivalence of the low-frequency gains of the series-shunt cascade and the series-shunt feedback pair are only a necessary condition for the equivalence of the stages, the results of Sec. 4.2 would indicate that the frequency behavior of these stages is also ideally identical.

APPENDIX F

THE USE OF THE GAIN-SQUARED FREQUENCY INTEGRAL FOR THE COMPUTATION OF TEMPERATURE SENSITIVITY

The method of using the gain-squared frequency integral to calculate the temperature sensitivity is demonstrated in this section.

The shunt-series cascade is used as an example. The reference transfer function is given by (4.1) with the components at 25° C.

$$T(p) = \frac{28.3}{1 + p + 0.5p^2} \tag{F.1}$$

where the frequency variable is normalized to 6.7×10^7 rad/sec. The reference transfer function has normalized complex poles, $-p_1$ and $-\bar{p}_1$, and has a reference gain-squared frequency integral, calculated from (2.11)

$$J = -\pi \, |p_1|^2 \, \frac{\mathrm{Im}T(p_1)}{\mathrm{Im}p_1} \tag{F.2}$$

where $\mathrm{Im}T(p_1)$ is the imaginary part of $T(j\omega)$ evaluated at $j\omega = p_1$. If (2.20) is used to calculate the change of gain-squared frequency integral, the result is

$$J_8^N = 2\left[\frac{\mathrm{Im}T_A(p_1)}{\mathrm{Im}T(p_1)} - 1\right] \tag{F.3}$$

The altered transfer function is obtained by calculating the value of (4.2) at 100° C. For the change of the value of the resistor R_f, given in Sec. 4.2, the altered transfer function, calculated from (4.2) is

$$T_A(p) = \frac{31}{1 + 1.09p + .545p^2} \qquad (F.4)$$

The result of substituting these values in (F.3) is

$$J_\delta^N = 0.11 \qquad (F.5)$$

The procedure is repeated for the other sensitive parameters, and the results added to obtain the net temperature sensitivity.

APPENDIX G

AN INTERPRETATION OF THE CHANGE IN
GAIN-SQUARED FREQUENCY INTEGRAL

To interpret the normalized change of the gain-squared frequency integral, (2.11) is calculated for a two-pole function

$$T(p) = \frac{a_o}{1 + a_1 p + a_2 p^2} \tag{G.1}$$

giving

$$J = \frac{\pi}{4} a_o^2 \frac{\sigma_a^2 + \omega_a^2}{\sigma_a} \tag{G.2}$$

where the poles of $T(p)$ are assumed at $-\sigma_a \pm j\omega_a$. The altered transfer function is given by

$$T_A(p) = \frac{\hat{a}_o}{1 + \hat{a}_2 p + \hat{a}_2 p^2} \tag{G.3}$$

From (2.20) the normalized change in the gain-squared frequency integral can be expressed as

$$J_\delta^N = \frac{J_A}{J} - 1 = \frac{\hat{a}_o^2}{a_o^2} \frac{\hat{\sigma}_a^2 + \hat{\omega}_a^2}{\sigma_a^2 + \omega_a^2} \frac{\sigma_a}{\sigma_a} \tag{G.4}$$

For a two pole, maximally flat magnitude function $\sigma_a = \omega_a$; hence (G. 4) can

be expressed as

$$J_\delta^N + 1 = \frac{\hat{a}_o^2}{a_o^2} \quad \frac{\hat{\sigma}_a^2 + \hat{\omega}_a^2}{2\sigma_a^2} \tag{G. 5}$$

The -3 dB bandedge of a two-pole function is simply shown to be

$$\omega_o = \left[-(\sigma_a^2 - \omega_a^2) + \sqrt{2\sigma_a^4 + 2\omega_a^4} \right]^{1/2} \tag{G. 6}$$

The change in bandwidth can then be calculated using (G. 5) once the

midband gain is determined for the perturbed amplifier.

The shunt-series cascade was found to have a net sensitivity of

-0.06. An inspection of (4. 2) shows that the real part of the pole is not

effected by temperature change. Hence (F. 5) can be written as

$$J_\delta^N + 1 = \frac{\hat{a}_o^2}{a_o^2} \quad \frac{1}{2} \quad (1 + \frac{\hat{\omega}_a^2}{\sigma_a^2}) \tag{G. 7}$$

Eqn. (4. 2) shows the low-frequency gain is 28. Then, (G. 7) can be

calculated giving

$$\frac{\hat{\omega}_a^2}{\sigma_a^2} = 0.86 \tag{G. 8}$$

Since $\omega_a < \omega_a$, the poles will lie on radials less than $45^{\circ}C$. Then, (G. 6) can be used to calculate the new bandwidth giving

$$\hat{\omega}_o = \sqrt{2} \; \sigma_a \, (0.9) \qquad\qquad (G. 9)$$

But $\sqrt{2} \; \sigma_a$ is the bandwidth of the amplifier at 25° C. Therefore,

$$\hat{\omega}_o = 0.9 \, \omega_o \qquad\qquad (G. 10)$$

REFERENCES

1. H. W. Bode, Network Analysis and Feedback Amplifier Design, D. Van Nostrand and Company, Princeton, New Jersey, 1945.

2. M. S. Ghausi and D. O. Pederson, "A new design approach to feedback amplifiers," IRE Trans. CT, No. 9, pp. 274-283, Sept. 1961.

3. E. M. Cherry and D. E. Hooper, "The design of wide-band transistor feedback amplifiers," Proc. IEE, Vol. 110, No. 2, pp. 375-389, Feb. 1963.

4. A. J. Brodersen and R. S. Pepper, "Integrated low pass wideband amplifiers," ERL Report No. 60-460, Electronics Research Laboratory, University of California, Berkeley, Oct. 12, 1962.

5. R. M. Warner and J. M. Fordemwalt, Integrated Circuits, McGraw-Hill, Inc., N. Y., 1965, pp. 252-264.

6. R. J. Widlar, "Some circuit design techniques for linear integrated circuits," IEEE Trans. CT, CT-12, No. 4, pp. 586-590, Dec. 1965.

7. Research Triangle Inst., "Integrated silicon device technology," Vol. I (Resistance), Report ASD-TDR-63-361 (Wright-Patterson AFB), pp. 2-26 - 2-49, June 1963.

8. Research Triangle Inst., "Integrated silicon device technology," Vol. II (Capacitance), Report ASD-T DR-63-361 (Wright-Patterson AFB), pp. 2-1 - 3-25, Oct. 1963.

9. Research Triangle Inst., "Integrated silicon device technology," Vol. XI (Bipolar transistors), Report ASD-TDR-63-316, pp. 252 - 266, April 1966.

10. D. O. Pederson, Electronic Circuits, McGraw-Hill Inc., New York, 1965, pp. 139-142.

11. R. M. Warner and J. M. Fordemwalt, op. cit., pp. 252-264.

12. L. Weinberg, Network Analysis and Synthesis, McGraw-Hill, Inc., 1962, pp. 491-493.

13. D. O. Pederson, op. cit., pp. 171-173.

14. D. C. Youla, "A new theory of broadband matching," Tran. PGCT, Vol. CT-11, No. 1, pp. 30-49, March 1964.

15. C. Y. Chan and E. S. Kuh, "A general matching theory and application to tunnel diode amplifiers," ERL Report No. 65-23, Electronics Research Laboratory, University of California, Berkeley, Aug. 17, 1965.

16. H. W. Bode, op. cit., Ch. XIII.

17. D. O. Pederson and R. S. Pepper, "An evaluation of transistor low pass broadbanding techniques," IRE Wescon Con. Record, Part 2, p. 113, August 1959.

18. J. E. Solomon and G. R. Wilson, "A monolithic feedback triple with a 3-GHz gain bandwidth product," ISSCC Digest of Tech. Papers, pp. 40-41, Feb. 1966.

19. M. S. Ghausi and D. O. Pederson, "A new feedback broadbanding technique for transistor amplifier," Proc. Nat'l. Elect. Conf., pp. 127-140, Oct. 1962.

20. C. L. Searle, A. R. Boothroyd, E. J. Angelo, Jr., P. E. Gray, and D. O. Pederson, Elementary Circuit Properties of Transistors, SEEC Vol. 5, John Wiley and Sons, Inc., 1964.

21. D. O. Pederson, op. cit., pp. 122-129.

22. M. S. Ghausi, "Optimum design of the shunt-series feedback pair with a maximally flat magnitude response," IRE Trans. CT, CT-8, No. 4, pp. 448-453, Dec. 1961.

23. G. W. Haines, "An integrated stabilized gain block," IEEE Int'l. Con. Record, Vol. 14, Pt. 7, pp. 296-307, Mar. 1966.

24. Research Triangle Inst., "Integrated silicon device technology," Vol. XI (Bipolar transistors). Report ASD-TDR-63-316, April 1966, pp. 157, 198.

25. D. O. Pederson, op. cit., pp. 708-710.

26. D. O. Pederson, ibid, pp. 174-177.

27. A. A. Gaash, D. O. Pederson, and R. S. Pepper, "Design of integrable desensitized frequency selective amplifiers," ISSCC Digest of Tech. Papers, pp. 34-35, Feb. 1966.

28. S. S. Hakim, "Synthesis of RC active filters with prescribed pole sensitivity," Proc. IEE, Vol. 112, No. 12, pp. 2235-2242, Dec. 1965.

29. J. E. Solomon and G. R. Wilson, "A highly desensitized, wideband monolithic amplifier," IEEE J. on Solid State Circuits, Vol. 1, No. 1, Sept. 1966. (to appear)

30. R. M. Wardner and J. M. Fordemwalt, op. cit. pp. 263-264.

31. RCA Linear Integrated Circuits, CA3011, CA3012 data sheet.

32. H. W. Bode, op. cit., pp. 297-298.

33. R. M. Warner and J. M. Fordemwalt, op. cit. pp. 66-67.